THE USE OF MULTIPLE BIOMARKERS IN MARINE POLLUTION MONITORING: A CASE STUDY IN VICTORIA HARBOUR, HONG KONG

LEUNG KAR LONG

MPhil

The Hong Kong Polytechnic University

2022

The Hong Kong Polytechnic University
Department of Applied Biology and Chemical Technology

The use of multiple biomarkers in marine pollution monitoring: a case study in Victoria Harbour, Hong Kong

Leung Kar Long

A thesis submitted in partial fulfilment of the requirements for the degree of

Master of Philosophy

August 2022

CERTIFICATE OF ORIGINALITY

I hereby declare that this thesis is my own work and that, to the best of my knowledge and belief, it reproduces no material previously published or written, nor material that has been accepted for the award of any other degree or diploma, except where due acknowledgement has been made in the text.

_____ (Signed)

Leung Kar Long (Name of student)

Abstract

The rapid growth of human population, industrialisation and urbanisation in coastal areas have resulted in different extents of marine pollution worldwide. For instance, heavy metals and persistent organic pollutants (POPs) are chemical pollutants that have received great attention owing to their persistency and bioaccumulation nature. In the case of Hong Kong waters, the presence of heavy metals such as cadmium (Cd), chromium (Cr), copper (Cu), lead (Pb) and zinc (Zn), and POPs such as polycyclic aromatic hydrocarbons (PAHs), polychlorinated biphenyls (PCBs) and organochlorine pesticides (OCPs), have been reported since the 1980s. Chemical analyses and monitoring of heavy metals and POPs are routinely carried out in seawater and sediments in Hong Kong and elsewhere, but it should be noted that such results of environmental concentrations do not provide any information about bioavailability of these pollutants. To address this concern, the biomonitoring approach has been proposed, in which one could select a model animal and analyse the bioaccumulated level of a target pollutant to indicate its bioavailable fraction. A range of cellular biomarkers have also been developed to indicate the biological responses of the model animal to the target pollutant. This information of biological impact is essential for the ecological risk assessment of the pollutant. However, pollutants usually occur as a mixture in the environment, and it remains a challenge on how to select the optimal combination of biomarkers for pollution monitoring in this cocktail situation.

Victoria Harbour, Hong Kong, was investigated here as a case study to tackle this challenge by identifying the optimal subset of biomarkers in the green-lipped mussel *Perna viridis* that can explain the maximal variability of mixed pollutants using multivariate statistical techniques. We adopted a transplantation approach in the fieldwork, where all mussels were collected from a reference site and redeployed at the same site and four other polluted sites within Victoria Harbour. There were two rounds of mussel transplantation that lasted five weeks each in the dry season and wet season of 2019 (5 sites × 2 seasons). Mussels were then retrieved and processed (n = 10 per site, each n pooled from 10 mussels), from which haemolymph was freshly extracted to assess lysosomal destabilisation (LysD) and micronucleus frequency (MN), while hepatopancreas was used to determine seven other biomarkers, namely superoxide dismutase (SOD), catalase (CAT), glutathione (GSH), acetylcholinesterase (AChE), lipid peroxidation (LPx), the nucleic acid ratio of RNA to DNA (R:D) and the total energy reserve (Et). The remaining soft tissue was used to analyse Cd, Cr, Cu, Pb, Zn and 16 forms of low-

molecular-weight (LMW) and high-molecular-weight (HMW) PAHs, as well as 28 congeners of PCBs and 21 types of OCPs, following established methods. Since PCBs and OCPs were not detectable in all samples, seven variables of detected pollutants (Cd, Cr, Cu, Pb, Zn, LMW PAHs and HMW PAHs) and nine variables of biomarkers in *P. viridis* (SOD, CAT, GSH, AChE, LysD, MN, LPx, R:D and Et) obtained from five sites in two seasons were analysed with the multivariate statistical software PRIMER 7.

Significantly the lowest levels of Cu, LMW PAHs and HMW PAHs were found in *P. viridis* at the reference site regardless of the season. The reference-site mussels also showed the lowest concentrations of Cd and Zn in the dry season and Cr in the wet season, but relatively high levels of Pb. The results of principal component analysis (PCA) identified LMW PAHs and HMW PAHs as two key variables to drive the reference-site samples to cluster away from the within-harbour samples, based on PC1 and PC2 (cumulative variation: 58–62%). This spatial clustering was more pronounced in the dry season than wet season, as revealed by the results of non-metric multi-dimensional scaling (nMDS; 2D stress: 0.16–0.19) and the similarity profile analysis (SIMPROF; $p < 0.05$). As for the biomarkers, *P. viridis* at the reference site showed significantly the highest levels of SOD and AChE and lowest extents of LysD, MN and Et in the dry season, but the highest values of CAT, AChE and R:D and lowest levels of GSH and LysD in the wet season, compared to the within-harbour sites. The results of PCA, using PC1 and PC2, revealed that the different biological responses of mussels between the reference site and within-harbour sites were mainly due to CAT, LysD and MN in the dry season, and GSH and LysD in the wet season (cumulative variation: 49–50%). The similarity and dissimilarity among samples based on the nine variables of biomarkers were elucidated using nMDS (2D stress: 0.19) and SIMPROF ($p < 0.05$), in which most of the reference-site samples formed their own cluster regardless of the season.

To link these biological changes to the tissue burden of heavy metals and PAHs in *P. viridis*, the routine for linking of biota to environment (BIOENV) was employed to derive the single best biomarker that provided the highest correlation with the similarity matrix of pollutants per season, where LysD and R:D were identified in the dry season ($\rho = 0.20$) and wet season ($\rho = 0.14$), respectively ($p < 0.001$). Moreover, the optimal subset predictors for the pollutants were derived to be LysD, R:D, GSH and AChE in the dry season ($\rho = 0.33$), and LysD, R:D, CAT and Et in the wet season ($\rho = 0.25$; $p < 0.01$). Based on these BIOENV results, LysD and R:D

appeared to be the two most responsive biomarkers to the cocktail situation of heavy metals and PAHs, among the nine tested biomarkers in *P. viridis*. LysD is a cytohistological biomarker of effect, which quantifies the swelling or bursting of lysosomes induced by sequestration and overload of xenobiotics. R:D is a biomarker of growth at the molecular level, of which a higher value indicates a greater growth potential, given that the quantity of DNA is relatively stable but that of RNA increases along with protein synthesis. In conclusion, we recommend LysD and R:D in *P. viridis* to be two core biomarkers for marine pollution montoring in Hong Kong waters, and our findings are applicable to other Indo-Pacific areas where *P. viridis* is abundant. The non-specific nature of LysD and R:D makes them suitable as a screening tool to pinpoint the pollution hotspots, which can then be assessed with other more specific biomarkers and sophisticated chemical analyses to characterise the pollutants and their biological impacts.

Acknowledgements

The present study was funded by the Environment and Conservation Fund (ECF) by ECF committee under the Environment and Conservation Fund Ordinance (Cap. 450) by the Hong Kong Special Administrative Region (Project No. 2017-66). I would like to express my sincerest gratitude to Dr James Fang for accepting me as a research student for allowing me to acquire in-depth scientific knowledge and develop research skills. My sincere thanks particularly goes to Dr Hang-Kin Kong, Dr Sirius Tse and Mr Pat Lo for teaching me the background knowledge in proteomics, providing me invaluable hands-on training and guidance in terms of the laboratory work, instrumental operation and data analysis. I would also like to thank Miss Joyce Wong, Dr Alston Lee, Dr Chi-On Chan for providing technical supports and guidance in chemical analysis. My thankfulness must also be offered to Mr Matthew Leung, Mr John Kwok and his friends for providing locations for mussels deployment and technical supports in field sampling and sample preparation, and to Mr Kwok-Hung Pang for offering transportation service for my field works. Also, I would like to thank Dr Priscilla Leung and Dr Jack Ip for teaching me the skills for dissecting mussels. I would like to acknowledge the University Research Facility in Life Sciences (ULS) and the University Research Facility in Chemical and Environmental Analysis (UCEA) in our university for providing a variety of cutting-edge laboratory instruments for use.

Table of Contents

List of Figures

Figure 4.2. Two-dimensional plots of the principal component analysis (PCA) for biomarkers in *Perna viridis* among five sites in the **(a)** dry season and **(b)** wet season, 50 samples per season.

Figure 4.3. Hierarchical cluster analysis (CLUSTER) for biomarkers in *Perna viridis* among five sites in the **(a)** dry season and **(b)** wet season, 50 samples per season, based on Euclidean distance of the nine variables reported in Figure 4.1.

List of Tables

Chapter 1: General Introduction

The exponential growth of human population, industrialisation and urbanisation since the industrial revolution in the 18th century has been associated with production of countless chemicals and their discharge into the ocean worldwide. This rapid development has raised the concern of marine pollution, which has been defined by the United Nations (1982) as "*the introduction by man, directly or indirectly, of substances or energy into the marine environment, including estuaries, which results or is likely to result in such deleterious effects as harm to living resources and marine life, hazards to human health, hindrance to marine activities, including fishing and other legitimate uses of the sea, impairment of quality for use of seawater and reduction of amenities*." Potential sources of chemical pollution in marine environments include sewage discharge, surface runoff, dredging, dumping, atmospheric deposition and accidental spillage, among others.

Heavy metals and persistent organic pollutants (POPs) are chemical pollutants that have received great attention owing to their persistency and bioaccumulation nature. To name a few, heavy metals such as cadmium (Cd), chromium (Cr), copper (Cu), lead (Pb) and zinc (Zn), and POPs such as polycyclic aromatic hydrocarbons (PAHs), polychlorinated biphenyls (PCBs), organochlorine pesticides (OCPs) and polybrominated diphenyl ethers (PBDEs), have been reported in marine sediment and biota worldwide (e.g., Barletta *et al*., 2019; Fuoco & Giannarelli, 2019; Kumar *et al*., 2019; Karaouzas *et al*., 2021; Zhang *et al*., 2020). These pollutants are generally considered toxic, carcinogenic or mutagenic that can disrupt the immune system, endocrine system, reproductive system, cardiovascular system and nervous system of marine organisms (Alharbi *et al*., 2018; Briffa *et al*., 2020). Indeed, pollutants of different sources often exist as a cocktail and interact with each other in the environment, processes which might further modify the toxicity to marine life.

1.1 Marine pollution biomonitoring

Chemical analyses of heavy metals and POPs have been globally performed in seawater and sediments for pollution monitoring purposes (Zheng & Richardson, 1999; Karlsson & Viklander, 2008; Shanbehzadeh *et al*., 2014; Bellas *et al*., 2020; Avellan *et al*., 2022). However, it should be noted that the environmental concentrations of pollutants barely provide any information regarding their bioavailability and the associated biological and ecological

consequences, which are essential for the diagnosis of ecological risks and the development of waste management plans (Becher & Bjerseth, 1987; Fouzia *et al*., 2019).

To understand the bioavailability of pollutants, one could analyse the bioaccumulated levels of these pollutants in a model animal. Upon potential biotransformation and detoxification, the detectable bioaccumulated levels do not necessarily linearly correlate with the environmental concentrations (Phillips & Yim, 1981; Nicholson & Lam, 2005). Nevertheless, the detectable quantity of bioaccumulation indicates the bioavailable fraction of the pollutant that cannot be easily eliminated from the biological system, and is thus of the greatest concern regarding the animal health and ecological risks. Moreover, the bioaccumulated level provides a time-integrated estimate of the pollution events that occur within the lifespan of the model animal, usually a few years. The coverage of this time-integrated estimate of pollution can even be manipulated by selecting different ages of the model species at the study sites. From the monitoring point of view, this bioaccumulation approach offers clear advantages over the conventional chemical analyses in seawater, from which the results only provide a snapshot of the pollution levels at a particular time point, and in sediment, which represents a sink of pollutants that has been built up for many years and might not accurately indicate recent pollution levels (Becher & Bjerseth, 1987; Wu *et al*., 2005).

The green-lipped mussel *Perna viridis* is a common model species used for marine pollution biomonitoring in the Indo-Pacific region (Nicholson & Lam, 2005). Apart from the use of tissue concentrations to reveal bioavailability of pollutants, a variety of cellular biomarkers have been developed for *P. viridis* to indicate the biological responses to these pollutants (Cheung *et al*., 2001, Cheung *et al*., 2002, Nicholson, 2003c; Cheung *et al*., 2004; Fang *et al*., 2008a; Siu *et al*., 2008; Jena *et al*., 2009; Wang *et al*., 2011, Leung *et al*., 2014; Liu *et al*., 2014; Wang *et al*., 2014; Juhel *et al*., 2017). The cellular damage and defence to pollutants inform the mechanisms of toxicity, which could be relevant to the performance of growth and reproduction and further to the ecological consequences (Wu *et al*., 2005; Lionetto *et al*., 2019; Lomartire *et al*., 2021). With this knowledge, specific biological endpoints could be identified as biomarkers for the target pollutants for pollution biomonitoring purposes (McCarty & Munkittrick, 1996). More information about the application of biomarkers in *P. viridis* is provided in Chapter 2. However, there is no common agreement on how to select the optimal subset of biomarkers for pollution monitoring. The investigation on which subsets of

biomarkers in *P. viridis* best explaining the variability of mixed pollutants was detailed in Chapter 4.

1.2 Case study in Victoria Harbour, Hong Kong

Hong Kong's Victoria Harbour is one of the busiest harbours worldwide. Substantial amounts of chemical pollutants have been released into the harbour through sewage discharge, surface runoff, oil spillage, sludge dumping and reclamation since the beginning of the urban development in the 1960s (Morton, 1989, 1976). For instance, heavy metals, PAHs, PCBs and OCPs were well documented in the seawater and sediments collected from Victoria Harbour (Chan *et al*., 1974; Fung & Yim, 1981; Phillips, 1989; Wong *et al*., 1995; Blackmore, 1998; Connell *et al*., 1998; Hong *et al*., 1999; Zheng & Richardson, 1999; Tanner *et al*., 2000). As a result, marine organisms living in the harbour generally showed higher bioaccumulated levels of these pollutants than other waters in Hong Kong (Phillips, 1985; Chan, 1988, Phillips & Rainbow, 1988; Chan, 1989; Liu & Kueh, 2005; Richardson *et al*., 2001; Fang *et al*., 2008a, 2009; Yeung *et al*., 2017). The wide occurrence of heavy metals and POPs in marine life has raised concerns about the associated ecological and public health risks in the harbour area.

The Harbour Area Treatment Scheme (HATS) has been launched in stages by the Hong Kong Government since 1989 to alleviate the pollution problems in Victoria Harbour (Drainage Service Department, 2019). Under this scheme, the wastewater effluents from the Preliminary Treatment Works (PTWs) on both sides of the harbour are converged to the Stonecutter Island Sewage Treatment Works for a chemically enhanced primary treatment, before being released into the west of Victoria Harbour. Stage 1 of HATS, on the PTWs in Kowloon Peninsula and the eastern part of Hong Kong Island, has been commissioned in 2001. Stage 2A of HATS, on the PTWs in the central and western parts of Hong Kong Island, has been implemented in 2015. As a result, improved water quality was recorded in the harbour (Environmental Protection Department, 2020, 2021), alongside with the generally decreased tissue levels of heavy metals in *P. viridis* (Table 1.1). POPs including PAHs, PCBs and OCPs were also monitored in Victoria Harbour using *P. viridis* by various researchers, but the different analytical approaches make it difficult to directly compare among studies (Table 1.2). With this limitation in mind, the total PAHs in *P. viridis* appeared to have increased in the harbour during the 1990s and 2000s (Liu & Kueh, 2005; Fang *et al*., 2009), suggesting the existence of other sources of PAHs in the adjacent waters, e.g., due to heavy marine traffic and oil spillage. In this connection, the

tissue levels of PAHs and other pollutants in *P. viridis*, along with a suite of biomarkers, were reassessed here and reported in Chapter 3 and Chapter 4 to characterise the latest pollution status in Victoria Harbour after the full implementation of Stage 1 and Stage 2A of HATS.

1.3 Thesis outline

This thesis comprises five chapters. Chapter 1 is a general introduction to the need for pollution biomonitoring in Victoria Harbour. Chapter 2 is an overview on the different types of biomarkers developed in *P. viridis* for marine pollution monitoring purposes, particularly in Hong Kong waters. In Chapter 3, five heavy metals, 16 PAHs, 28 PCBs and 21 OCPs were analysed in *P. viridis* collected from Victoria Harbour seasonally in 2019 to evaluate the performance of HATS. The same mussels were assessed in Chapter 4 to determine nine biomarkers, aiming to develop a multiple biomarker approach that can effectively indicate the bioaccumulation levels of pollutants determined in Chapter 3. Lastly, Chapter 5 is a general discussion on the findings from previous chapters and their implications for marine pollution biomonitoring.

Table 1.1. Concentrations of heavy metals, per g dry weight (dw) of the whole soft tissue in the green-lipped mussel *Perna viridis* collected from Victoria Harbour, Hong Kong. BDL refers to below detection limit.

Sampling period	Sampling strategy (Shell length)	Median (range) of the means among sites (μg g^{-1} dw)					Reference
		Cadmium	Chromium	Copper	Lead	Zinc	
Jul–Aug 1983	Native (57 mm)	0.21 (0.07–1.43)	Not reported	22.8 (11.5–279)	15.5 (7.80–60.5)	129 (115–164)	Phillips (1985)
Apr 1986	Native (50–70 mm)	0.36 (0.22–1.48)	7.60 (4.10–37.6)	29.1 (13.5–219)	12.7 (10.2–47.8)	118 (96.0– 153)	Rainbow & Phillips (1988)
Apr 1986–Jan 1987	Native (Not reported)	0.49 (0.13–1.51)	Not reported	37.6 (17.4–162)	17.2 (9.35–46.7)	116 (72.4–138)	Chan (1988)
Jul 2004–Jul 2005	Native (80 mm)	0.26 (BDL–1.48)	0.97 (0.30–2.21)	14.8 (BDL–67.7)	1.73 (0.41–11.1)	64.73 (21.0– 109)	Fang *et al*. (2008a)
Jan–Sep 2019	Transplanted (72 mm)	0.34 (0.28–0.43)	0.83 (0.59–1.40)	7.29 (4.55–13.5)	2.33 (1.76–3.28)	70.78 (60.5–79.8)	This study (see Chapter 3)

Table 1.2. Concentrations of polycyclic aromatic hydrocarbons (PAHs), polychlorinated biphenyls (PCBs) and organochlorine pesticides (OCPs), such as dichlorodiphenyltrichloroethane (DDT), dichlorodiphenyldichloroethylene (DDE) and dichlorodiphenyldichloroethylene (DDD), per g dry weight (dw) of the whole soft tissue in *Perna viridis* collected from Victoria Harbour, Hong Kong. Concentrations below detection limit (BDL) were assumed to be half of the DL in the calculation of ranges.

Sampling period	Sampling strategy (Shell length)	Median (range) of the means among sites (μg g^{-1} dw)			Reference
		PAHs	PCBs	OCPs	
Jul–Aug 1983	Native (73 mm)	Not reported	Aroclor 1232 + 1242: 0.03 (0.03–1.90)	DDT + DDE + DDD: 0.50 (0.26–2.04)	Phillips (1985)
Sep 1998–Jun 2003	Native (40–120 mm)	3 PAHs: 0.40 (0.21–2.17)	12 PCBs: 0.09 (0.06–0.17)	DDT + DDE + DDD: 0.19 (0.17–0.26)	Liu & Kueh (2005)
Jul 2004–Jul 2005	Native (70–90 mm)	15 PAHs: 4.88 (0.60–22.9)	28 PCBs: 0.09 (0.05–0.13)	Not reported	Fang *et al*. (2009)
Jan–Sep 2019	Transplanted (72 mm)	16 PAHs: 0.26 (0.14–0.31)	28 PCBs: all BDL	21 OCPs: all BDL	This study (see Chapter 3)

Chapter 2: The biomarkers in *Perna viridis* for pollution biomonitoring

The use of biomarkers has been first developed for medical research and later adopted in the field of environmental toxicology. For marine pollution monitoring purposes, a biomarker can be defined as an anthropogenically-induced variation in cellular, biochemical, physiological, or ecological components or processes, structures, or functions that is measurable in a biological sample or system (modified from McCarty & Munkittrick, 1996). In this regard, biomarkers are usually biological responses at lower levels of the biological hierarchy, since they are more easily induced, more specific to the toxic actions of pollutants, and more useful to identify the mechanisms behind (Lam, 2009; Lionetto *et al*., 2019; Lomartire *et al*., 2021). The use of biomarkers should be accompanied with the conventional analytical approach to quantify the ambient or body burden level of pollutants, providing data to establish cause-and-effect relationships between the biological impairment and the exposure level to pollutants (Wu *et al*., 2005).

When selecting a biomarker for pollution biomonitoring, one should understand the exposure time and concentration of the target pollutant required to induce the biomarker response to its initial detectable level and maximum level, and whether the response would decline as a consequence of adaptation during prolonged exposure, or recovery upon abatement of the pollutant (Wu *et al*., 2005; Richardson *et al*., 2008; Hook *et al*., 2014). It should also be noted that the biomarker response could be influenced by environmental variation such as temperature, salinity, pH, dissolved oxygen and tidal movement, and biological variation such as body size, age, sex and the reproductive status of the model animal (Lobel *et al*., 1991; Hole *et al*., 1992; Viarengo *et al*., 2007; Albentosa *et al*., 2012; Nahrgang *et al*., 2013; Schmidt *et al*., 2013; Bellas *et al*., 2014; Amiard-Triquet & Berthet, 2015). Over three decades of research efforts, a lot of these technical concerns have been addressed for mussels, which are widely used as model animals in pollution biomonitoring programmes such as *Mussel Watch* in the USA since the 1980s (Schöne & Krause, 2016).

2.1 Mussels as model animals in pollution biomonitoring

Mussels are sessile organisms that inhabit estuarine and marine environments across intertidal and subtidal zones. They have developed good adaptation to the dynamic environmental

fluctuations and are generally tolerant to water quality changes. Indeed, mussels provide important ecosystem functions. For instance, they produce calcareous shells, which form reefs and can be considered a kind of carbon sequestration. Moreover, mussels filter-feed on phytoplankton and other food particles by pumping and filtering a large quantity of the surrounding water through their gills, a process which can improve the water quality and facilitate nutrient cycling. This filter-feeding process is also associated with bioaccumulation of pollutants from the water column in the mussels, which provides the rationale for using mussels as model animals to bioconcentrate environmental pollutants for monitoring purposes. The bioaccumulated fraction indicates bioavailability of the pollutants (Saavedra & Bachère, 2006; Campos *et al*., 2012; Vaughn & Hoellein, 2018; Świacka *et al*., 2019; López-Pedrouso *et al*., 2020).

Owing to their global distribution and high accessibility for sampling, various species of mussels have been employed in marine pollution assessments worldwide with reference to the body burden of chemical pollutants (Phillips & Yim, 1981; Phillips, 1985; Fang *et al*., 2009; Barhoumi *et al*., 2016; Moschino *et al*., 2016; Li *et al*., 2021), and the change in cellular biomarkers and physiological responses (Verlecar *et al*., 2008; Jena *et al*., 2009; Tsangaris *et al*., 2010; Arockia Vasanthi *et al*., 2012; El Jourmi *et al*., 2012; Rola *et al*., 2012; Giltrap *et al*., 2013; Capolupo *et al*., 2017). One could homogenise the whole soft tissue of mussels for the chemical and biological measurements (Phillips, 1985; Fang *et al*., 2009; Kamaruzzaan *et al*., 2011; Moschino *et al*., 2016), but some measured parameters could be specific to the tissue types (Lau & Wong, 2003), and thus other studies separated haemolymph and organs such as hepatopancreas, gills and adductor muscle in the measurements (Fang *et al*., 2008c; Richardson *et al*., 2008; Juhel *et al*., 2017; Vasanthi *et al*., 2017; Yeung *et al*., 2016). In particular, Faggio *et al*. (2018) have recommended the use of mussel hepatopancreas for pollution monitoring purposes, given the high bioaccumulation of chemical pollutants in this organ (Marigómez *et al*., 2002; Franzellitti *et al*., 2014; Beyer *et al*., 2017; Perić *et al*., 2017; Faggio *et al*., 2018), and the key roles of hepatopancreas in homeostatic regulation, detoxification, and defence against oxidative stress induced by the bioaccumulated pollutants (Marigómez *et al*., 2002; Faggio *et al*., 2016; Pagano *et al*., 2017).

P. viridis is native to the tropical and subtropical waters in the Indo-Pacific, ranging from the Persian Gulf to Papua New Guinea, including Hong Kong, but this species has also been

reported in the Northwest Pacific Ocean (Japan), the Gulf of Mexico (Florida), the Caribbean Sea (Jamaica, Venezuela and Trinidad) and the South Atlantic Ocean (Brazil) (Siddall, 1980; Vakily, 1989; Baker *et al*., 2007; Wood *et al*., 2007; Micklem *et al*., 2016; Dias *et al*., 2018; de Messano *et al*., 2019). *P. viridis* is primarily found on rocky shores in the intertidal to subtidal zones, with the temperature range of 11–32 °C and salinity range of 18–33‰, and can form reefs at a density of up to 35,000 mussels per m^2 (Vakily, 1989; National Introduced Marine Pest Information System, 2002; Gosling, 2003). As a model species for pollution biomonitoring in the Indo-Pacific, *P. viridis* has been considered as a counterpart of the temperate blue mussel *Mytilus edulis* (Nicholson & Lam, 2005). Hoswever, relevant studies on *P. viridis* (375 papers) only accounted for 22% of that on *M. edulis* (1675 papers), according to the literature search results with the keywords "*Perna viridis*" or "*Mytilus edulis*" and "pollution" using the Web of Science search engine on 18 August 2022. Clearly, greater research effort is required on *P. viridis* to catch up with its temperate counterpart regarding the performance of biomarkers in pollution monitoring. To this end, the following section is an overview of the biomarker responses in *P. viridis* to environmental pollutants in five categories, namely genotoxicity, oxidative stress, immune responses, cell signalling and growth potential (Table 2.1). The summary here is not meant to be all inclusive, but rather to provide technical notes for the common biomarkers that can be applicable to *P. viridis* according to key findings from the literature.

2.2 Biomarkers at lower levels of the biological hierarchy

2.2.1 Biomarkers of genotoxicity

Any alteration in the structures of deoxyribonucleic acid (DNA) and nuclei could lead to mutagenesis and carcinogenesis, which might be transgenerational that impacts sustainability of the population. These molecular damages could be induced by genotoxic pollutants, and a number of relevant biomarkers have been proposed in *P. viridis* for marine pollution biomonitoring. Examples of these biomarkers of genotoxicity include DNA strand breaks, DNA adducts, 8-hydroxy-20-deoxyguanosine (8-OHdG) and micronuclei, which are summarised below.

DNA strand breaks refer to the breakage of DNA strands induced by prooxidants, radiation or other genotoxic agents. During the breakage, DNA fragments migrate away from the parent DNA and form a 'comet tail'. The extent of DNA strand breaks can be measured from the

length, intensity or moment of this 'comet tail' using the single-cell alkaline agarose gel electrophoresis, also known as the alkaline comet assay (Müller *et al*., 2000; Singh *et al*., 1988). Under laboratory conditions, the change in DNA strand breaks in hepatopancreatic cells or haemocytes of *P. viridis* was responsive to POPs such as benzo[a]pyrene (B[a]P) and a number of perfluorinated chemicals (Ching *et al*., 2001; Siu *et al*., 2004; Liu *et al*., 2014). However, these DNA damages could probably be healed and were found to return to the control levels upon prolonged exposure to B[a]P (Ching *et al*., 2001; Siu *et al*., 2004). This adaptation response of DNA strand breaks was also reported in a field study, when *P. viridis* was transplanted from a clean site to other sites polluted with PAHs, PCBs and OCPs, only weak correlations were detected between DNA strand breaks in gill cells and the body levels of these pollutants (Siu *et al*., 2008). Nevertheless, the impact of heavy metals on the mussel DNA might be more long-lasting, since significantly stronger DNA strand bsreaks were detected in both gill cells and hepatopancreatic cells of *P. viridis* at sites polluted with heavy metals (Vasanthi *et al*., 2017).

Another form of molecular damage is DNA adducts, which refer to the modification of DNA by forming covalent bonds with xenobiotics that could disable the replication process and give rise to mutagenesis (Shugart, 1998). DNA adducts in marine mussels can be quantified with mass spectrometry, immunological assays or autoradiography (Ching *et al*., 2001; Brown, 2012). As for *P. viridis*, DNA adducts in hepatopancreas appeared to be a suitable biomarker for PAHs, given its dose-related increase along the exposure concentrations of B[a]P under laboratory conditions (Ching *et al*., 2001). However, it remains unclear about the performance of this biomarker in *P. viridis* for other groups of pollutants.

Oxidative free radicals can modify the structures of DNA through hydroxylation of guanin and form 8-OHdG, a predominant product of free radical-induced oxidative lesions which can be used as a biomarker to reveal the degree of oxidative damage on DNA (Valavanidis *et al*., 2009). The concentration of 8-OHdG can be measured with the electrochemical detection method using high-performance liquid chromatography (Nicotera & Bardin, 1998). In a field study using *P. viridis*, the change in 8-OHdG in gills was significantly correlated with the body level of carcinogenic PAHs during the first 12 days, but such alignment with PAHs, as well as PCBs and OCPs, became less clear over a longer-term for 30 days (Siu *et al*., 2008). The

adaptation of 8-OHdG in *P. viridis* to environmental pollutants, and its effectiveness as a biomarker for pollution monitoring, would require further investigation.

The frequency of micronuclei in cells can be an alternative to study genotoxicity. Micronuclei are extra secondary nuclei constituted by damaged chromosomal fragments and are abnormally formed during mitosis (Luzhna *et al*., 2013). Micronuclei can be identified in stained cells under a microscope at 1,000× magnification (Tates *et al*., 1980; Bolognesi & Fenech, 2012). In a 12-day controlled experiment, Siu *et al*. (2004) reported significant increases in the frequency of micronuclei in haemocytes of *P. viridis* upon exposure to sublethal concentrations of B[a]P. Siu *et al*. (2008) further evaluated the use of this biomarker in a field study, where the frequency of micronuclei in the gill cells of *P. viridis* was positively correlated with the body levels of carcinogenic PAHs, total OCPs and total PCBs. More recently, the frequency of micronuclei in haemocytes of *P. viridis* was also found to be generally responsive to perfluorinated chemicals under laboratory conditions, in particular at exposure concentrations > 100 μg L^{-1} (Liu *et al*., 2014).

2.2.2 Biomarkers of oxidative stress

Apart from the oxidative DNA damage that can be indicated by 8-OHdG discussed above, oxidative stress is common in cells and tissues and reflects an imbalance between the production of reactive oxygen species (ROS) and the antioxidant defence. Many POPs and heavy metals are harmful prooxidants that generate ROS. Exposure to these prooxidants could increase the cellular levels of ROS such as hydroxyl radicals, superoxide radicals and hydrogen peroxide (H_2O_2), which inflict oxidative damage.

Lipid peroxidation (LPx) refers to the chain reactions of degradation of lipids into lipid peroxides, in which malondialdehyde (MDA) is another end product and its concentration can reveal the extent of LPx (Alessio, 2000). To counteract oxidative stress, superoxide dismutase (SOD) and catalase (CAT) serve as the primary antioxidant enzymes responsible for the transformation of ROS into less oxidative molecules. SOD catalyses the dismutation of superoxide radicals into H_2O_2 and oxygen, while CAT further catalyses the decomposition of H_2O_2 into water and oxygen (Cheung *et al*., 2002; Weydert & Cullen, 2010). Another important scavenger of ROS is glutathione (GSH), which is a tripeptide antioxidant that turns into glutathione disulphide (GSSG) by reducing ROS into water molecules in reversible redox

reactions. The conjugation of GSH to ROS is facilitated by glutathione S-transferase (GST), while glutathione peroxidase (GPx) and glutathione reductase (GR) catalyse the forward reaction (GSH to GSSG) and backward reaction (GSSG to GSH), respectively (Li, 2009; Aquilano *et al*., 2014).

These antioxidant responses have been used as biomarkers in marine mussels to indicate exposure to ROS induced by environmental pollutants. For instance, SOD, CAT, GSH, GST, GPx, GR and LPx in the gills and hepatopancreas of *P. viridis* upon exposure to PAHs, OCPs and PCBs in field studies were determined (Cheung *et al*., 2001; Cheung *et al*., 2002). Among the tested biomarkers, GSH, GST and GPx appeared to be more sensitive to the pollutants. The roles of physiological states and environmental factors in these antioxidant responses should also be considered, since the changes in SOD, CAT, GST and LPx in marine mussels were found to be influenced by the animal size, tissue type and sampling location (Lau & Wong, 2003). Under controlled laboratory conditions, the occurrence of LPx in the gills and hepatopancreas of *P. viridis* was associated with B[a]P, while SOD, CAT, GSH, GST, GPx and GR in either organ could be induced by PCBs or its combined effect with B[a]P (Cheung *et al*., 2004). Likewise, Richardson *et al*. (2008) recommended GSH and CAT in the hepatopancreas of *P. viridis* to be good biomarkers, according to the sensitivity and correlation of these antioxidant responses to the body burden of PAHs and OCPs. However, it is less clear about the effectiveness of using the antioxidant responses of *P. viridis* in monitoring heavy metals.

2.2.3 Biomarkers of detoxification

There are other proteins in marine mussels more specific to the detoxification of heavy metals, such as metallothionein (MT), which is a family of cysteine-rich proteins which bind to heavy metals and protect the cells from oxidative damage due to excess levels of heavy metals (Leung & Furness, 1999). Two isoforms of MT, namely MT10-I and MT10-II, have been identified in the hepatopancreas of *P. viridis*. The activities of both isoforms could be induced at sublethal concentrations of cadmium, but declined upon prolonged exposure (Leung *et al*., 2014). Another important group of proteins for detoxification is cytochrome P4501A (CYP1A), which is a family of phase 1 enzymes that regulate the metabolism of xenobiotics (Grøsvik *et al*., 2006). CYP1A is mediated by the aryl hydrocarbon receptor (AHR) pathway, which binds to xenobiotics and upregulates CYP1A. Amutha *et al*. (2009) investigated two members of

CYP1A, namely 7-ethoxyresorufin O-deethylase (EROD) and methoxyresorufin-O-dealkylase (MROD), in the hepatopancreas, gills and foot of *P. viridis* collected from PAH-polluted sites, and the changes in EROD and MROD activities well responded to the body levels of PAHs in mussels. These findings were supported by the positive correlation between CYP1A and PAHs in the hepatopancreas of *P. viridis* in another field study reported by Cholumpai *et al*. (2015). EROD in the hepatopancreas of *P. viridis* was also found to be significantly induced by the drug carbamazepine (CBZ) and herbicide atrazine (ATZ) under controlled laboratory conditions (Juhel *et al*., 2017).

2.2.4 Biomarkers of immune responses

Phagocytosis refers to the engulfment process of xenobiotics by phagocytes to form phagosomes, which fuse with lysosomes, and the engulfed items can be destroyed by hydrolytic enzymes and ROS produced in respiratory bursts (Sminia, 1981; Coles *et al*., 1994; Dyrynda *et al*., 1998; Gosling, 2003; Wang *et al*., 2011). Haemocytes are the major cell types of phagocytes in marine mussels, and it has been found that sublethal exposure to environmental pollutants such as Cu could destabilise the haemocytes of *P. viridis*, regarding the lysosomal membrane integrity (Nicholson, 1999a, 1999b, 2001, 2003a). Lysosomes play a key role in the sequestration of xenobiotics, and if the sequestered amount is too high, it could destabilise the proton-pumps, disrupt the ionic equilibrium and compromise material exchange across the lysosomal membrane (Lowe *et al*., 1981; Lowe *et al*., 1995; Moore, 1985). In this connection, (Fang *et al*., 2008c) observed destabilised lysosomal membrane in the haemocytes of *P. viridis* exposed to B[a]P, with quick induction and recovery times, but no adaptation upon prolonged exposure up to 42 days. The high sensitivity to both heavy metals and POPs makes lysosomal membrane destabilisation a suitable biomarker in *P. viridis* for marine pollution biomonitoring.

The lysosomal change in *P. viridis*, however, could be confounded by environmental factors such as dissolved oxygen and ammonia-nitrogen, according to the results from a field study (Fang *et al*., 2008b). Moreover, a number of haemocyte-related parameters in marine mussels, including phagocytosis, total haemocyte count, haemocyte mortality, ROS production, lysosomal content and the non-specific esterase activity, were found to be inducible by the individual or combined effects of hypoxia and nanoparticles of titanium dioxide under laboratory conditions (Wang *et al*., 2014). These findings suggest the non-specific nature of

the immune responses of mussels, which should be considered when biomarkers of this category are used for pollution monitoring purposes.

2.2.5 Biomarkers of cell signalling

Acetylcholinesterase (AChE) is an enzyme that hydrolyses acetylcholine, a neurotransmitter for nerve signal transmission in synapses. AChE could be inactivated by xenobiotics such as PCBs, OPCs, dioxins, organophosphorus compounds and brominated flame retardants through direct inhibition or disruption of its biosynthesis, leading to accumulation of acetylcholine in the postsynaptic terminals, over-stimulation of acetylcholine receptors and subsequently permanent neurological damage and physiological failure (Rickwood & Galloway, 2004; Fu *et al*., 2018). As for *P. viridis*, lower activities of AChE in gills were associated with higher levels of PCBs and Cu in the environment (Lau & Wong, 2003). Juhel *et al*. (2017) also reported inhibition of AChE in the haemolymph of *P. viridis* when exposed to CBZ and ATZ at environmentally realistic levels under laboratory conditions. However, interestingly, AChE appeared to oppositely respond to heavy metals, and was promoted upon exposure to Cd and Pb (Bainy *et al*., 2006). These findings might be explained by the potentially strong association between heavy metals and the acetylcholine receptors, which could reduce the binding sites for AChE on acetylcholine and thus increase the detectible amount of AChE.

Another group of biomarkers of cell signaling is formed by the membrane-bound Na^+, K^+, Mg^{2+} and Ca^{2+} ATPases, which are enzymes that consume adenosine triphosphate (ATP) to pump cations across cell membranes for signal transmission and to maintain the ionic and osmotic gradients (Reddy & Philip, 1992). Upon exposure to Ag and Cr, Vijayavel *et al*. (2007) reported significant inhibition of these membrane-bound ATPases in the gills, hepatopancreas, ovary and adductor muscle of *P. viridis*, potentially leading to ionic imbalance across membranes, osmoregulatory malfunctioning and disruption in neurotransmission. The responses of the ATPases in *P. viridis* to other groups of environmental pollutants are yet to be explored.

2.2.6 Biomarkers of growth potential

Exposure to chemical pollution could interrupt vital metabolic processes and incur extra energy required for detoxification and cellular defence. As a result, the energy available for growth

might be reduced (Calow & Sibly, 1990; Nicholson & Lam, 2005). The nucleic acid ratio of RNA to DNA (R:D) is a biomarker to assess this growth potential at the molecular level. Since DNA normally maintains a fairly stable concentration while RNA increases in concentration during protein synthesis, R:D can be indicative of the relative rate of protein synthesis and growth. The changes in R:D in different tissue parts of *P. viridis* have been confirmed to be positively related to food availability (Yeung & Leung, 2013). Narváez *et al*. (2005) and Yeung *et al*. (2016) furthermore evaluated the responses of R:D in the adductor muscle and hepatopancreas of *P. viridis* upon exposure to Cd and Cu, but clear trends were not observed.

Total energy reserve (Et) is another biomarker that has been used to indicate the growth potential of *P. viridis*, based on the total energy content of lipids, proteins and glycogen in the soft tissue (Yeung *et al*., 2016). In their study, among the four tested combinations between tissue type (adductor muscle or hepatopancreas) and heavy metal (Cd or Cu), only Et in hepatopancreas was found to significantly decrease when exposed to Cd. Further investigation is required to determine the influence of POPs on the responses of R:D and Et.

Apart from the correlation with environmental pollution, an ideal biomarker of growth potential, and of any other category discussed above, should be prognostic of the higher-level physiological responses regarding the actual growth rates, organ functions and behaviour. In this connection, another aspect of using biomarkers in pollution monitoring studies is to provide an early warning signal of any possible deterioration in health and likelihood of survival, which have ecological implication on the population success. However, such correlation between levels of the biological hierarchy is often weak, given the complex metabolic pathways from the cellular level to the whole-organism level. To address this concern, various easy-to-measure physiological endpoints have been developed and incorporated in pollution monitoring programmes along with the use of cellular biomarkers.

2.3 Physiological endpoints at higher levels of the biological hierarchy

Various physiological parameters of *P. viridis* at higher levels of the biological hierarchy have been measured to assess the growth efficiency and energy budgets, the wellness of organs in terms of size and function, and the change in behaviour upon environmental variations. Compared to cellular biomarkers, these physiological endpoints are usually slower-developing and less sensitive to ambient pollution levels, but are more ecologically relevant that could

reveal the overall fitness and survival capability. This section provides technical notes on the common physiological measurements that can be used for *P. viridis* in marine monitoring programmes (Table 2.2).

2.3.1 Condition index

Mussel condition index (CI) is a ratio of soft tissue weight to shell length or shell weight, where a higher value indicates greater somatic growth relative to the shell size that is assumed to be healthier. In comparison with the sole use of tissue weight, CI can be a more reliable indicator of growth and the nutritional state of mussels by taking account of the difference in size or age among individuals. The change in CI is associated with the energy availability for growth and thus SfG, and this indicator of growth was negatively correlated with lysosomal membrane destabilisation and the body burden of B[a]P in *P. viridis* (Fang *et al*., 2008c). Moreover, Yeung *et al*. (2017) reported lower values of CI in *P. viridis* at sites subjected to higher levels of heavy metals. However, there are some limitations using CI in pollution monitoring since it is a parameter of relative somatic growth and is primarily influenced by food availability. For instance, *P. viridis* collected from a polluted and eutrophic site showed higher values of CI compared to a less polluted site (Wendling *et al*., 2013). In this case, the eutrophic condition might be associated with a higher amount of phytoplankton and other food sources that could drive the observed change in CI.

2.3.2 Organ indices

In addition to the mussel CI, more specific indices have been developed to measure the relative growth of different organs, such as hepatosomatic index (HSI) and gonadosomatic index (GSI). HSI is a ratio of hepatopancreas to the whole soft tissue, while GSI is a ratio of gonad to the whole soft tissue, in wet or dry weight. The two indices are commonly used to reveal the energy availability and reproductive maturity of mussels, respectively (Tenuzzo *et al*., 2012; Singh & Srivastava, 2015; Wang *et al*., 2021). In connection to environmental pollution, both HSI and GSI of the brown mussel *Perna perna* were found to decrease upon exposure to tributyltin (TBT), an organic antifoulant (Iyapparaj *et al*., 2013). As for *P. viridis*, the responses of HSI and GSI to TBT and other pollutants are yet to be ascertained. However, such relationships are expected to be weak, if any, since the organ size change is an integrated outcome of changes in volume and number of all cell types in the organ, and these cellular responses could be

influenced by different factors rather than the pollutant-induced effects. For example, the variation of GSI of *P. viridis* was associated with the changes in environmental conditions such as food availability, and biological conditions such as the lipid content in gonad and condition index (Asaduzzaman *et al*., 2019; Noor *et al*., 2021).

2.3.3 Organ morphology

Apart from the organ indices that only provide weight ratios, more specific effects of pollutants on different organs such as tissue deformation and cellular abnormalities can be examined through microscopic observation of stained sections of the organs. These histological alterations provide insight into the impairment of organ functions and likelihood of survival. Using the histological approach, heavy metals were found to damage the gill filaments, hepatopancreas, gonad and adductor muscle of *P. viridis* (Vasanthi *et al*., 2012; Goswami *et al*., 2014; Hariharan *et al*., 2014; Krishnakumar *et al*., 1990; Nagarjuna *et al*., 2019; Viarengo *et al*., 1994; Xu *et al*., 2021). Other studies also identified adverse impacts of organic pollutants, suspended solids and plastic particles on the gills or hepatopancreas of *P. viridis* (Cheung & Shin, 2005; Shin *et al*., 2002; Vasanthi *et al*., 2021; Xu *et al*., 2021). The above morphological changes are summarised in Table 2.3. Among the tested organs, the gills of *P. viridis* appeared to be more sensitive to environmental pollutants, given that the mussel gills provide the first line of defence against foreign substances during the filter-feeding process.

2.3.4 Clearance rate

Mussels filter-feed on planktons and other organic matter from the water column, by ciliary beating in gills to pump seawater, from which the food particles can be filtered out and passed to the labial palps and mouth for feeding (Morton, 1987). The rate of this filter-feeding process is known as the clearance rate, which is indicative of the efficiency of food uptake (Vijayavel *et al*., 2007). The clearance rate of *P. viridis* was found to be inhibited upon exposure to Cd, Cr, Cu, Hg and Ag, as well as suspended solids and the soluble fraction of diesel oil. These effects could be caused by the pollutant-induced morphological changes in gill filaments that altered the ciliary beating behaviour, or due to reduced energy available for the filter-feeding process, since a larger part of the energy budget could be spent on detoxification of the pollutants (Wang *et al*., 1993; Shin *et al*., 2002; Nicholson, 2003b; Cheung & Shin, 2005; Vijayavel *et al*., 2007). Moreover, prolonged closure of the shells to reduce contact with the

exposed pollutants could be another factor leading to the decreased clearance rate of *P. viridis* (Prabhudeva & Menon, 1986; Nicholson & Lam, 2005). The clearance rate of *P. viridis* can be a good indicator of growth since it is a direct estimate of food uptake and thus energy availability.

2.3.5 Respiration rate

Aerobic respiration is the process of cellular respiration that converts food into energy in the presence of oxygen. Respiration rate is referred to as the rate of oxygen consumption in this process and can be used to indicate the amount of energy used for daily maintenance by marine mussels (Vijayavel *et al*., 2007; Zhen *et al*., 2010). The respiration rates of *P. viridis* were found to decrease upon exposure to sublethal levels of Ag, Cr and Cu, but not Zn (Mathew & Menon, 1983; Prabhudeva & Menon, 1986; Vijayavel *et al*., 2007). Since the mussel oxygen uptake relies on the filter-feeding mechanism, the impacts of environmental pollutants on clearance rate such as the compromised structural integrity of gills and prolonged shell closure discussed above, as well as reduced siphonal activity, are applicable to the performance of respiration (Cheung & Shin, 2005).

2.3.6 Scope for growth

Scope for growth (SfG) is an energy balance model to estimate the amount of net energy available for growth. SfG of mussels can be derived as the energy acquired in absorption, corrected by the absorption efficiency, minus the energy consumed via respiration and the energy lost as ammonia excretion. In this calculation, the absorption term and respiration term can be estimated from the clearance rate and respiration rate discussed above, respectively, and converted into the energy equivalent (Vijayavel *et al*., 2007; Zhen *et al*., 2010). In the field study by Wang *et al*. (2005), significantly reduced SfG was detected in *P. viridis* collected from sites polluted with OCPs, and the tissue burden of dichlorodiphenyltrichloroethane (DDT, a major OCP) in these mussels was negatively correlated with the change in SfG. The decrease in SfG indicated reduced energy availability for growth, which might be due to the extra energy allocated for internal defence and detoxification against pollutants. SfG has been shown to be a useful indicator of the energy budget in marine mussels (Widdows & Johnson, 1988; Widdows *et al*., 1990). However, the response of SfG in *P. viridis* could be seasonal and

reduced during winter (< 13 °C), when the mussels became less active with lower rates of clearance and respiration (Wong & Cheung, 2001).

2.3.7 Heart rate

The heart of mussels functions to pump haemolymph and nutrients across different body parts, and facilitate the removal of metabolic waste (Nicholson & Lam, 2005). Hence, the cardiac activity, as quantified by heart rate, can serve as another biological endpoint for the overall health state of mussels with regard to their efficiency of circulation of haemolymph and waste products. Concerning its sensitivity to environmental pollution, the heart rate of *P. viridis* was significantly elevated when the exposure concentration of Cu was increased to > 100 μg L^{-1} under laboratory conditions. In the field, higher heart rates of *P. viridis* were registered at sites with higher levels of suspended sediment particles and TBT. However, it should be noted that the cardiac activity of mussels could be subjected to other influencing factors such as sex of the mussels, the ambient level of dissolved oxygen and the duration of exposure.

2.3.8 Production of byssus

Byssus is a bundle of byssal threads, which are biological filaments secreted by mussels and other bivalves for attaching themselves to solid substrata (Aldred *et al*., 2006). Although its responses to POPs remain unclear, a number of studies have reported significant uptake and bioaccumulation of heavy metals in the byssus of *P. viridis* (Cheung & Wong, 1992; Nicholson & Szefer, 2003; Yap *et al*., 2003a, 2003b). Moreover, the synthesis of byssus could be slowed down upon exposure to sub-lethal concentrations of Ag, Cd, Cu, Hg, Pb and Zn, since the extra energy required for detoxification might reduce the energy available for growth including production of byssus (Ekanath & Menon, 1983; Mathew & Menon, 1983; Yaqin *et al*., 2014). These findings suggest that the *P. viridis* byssus can provide a tool for pollution biomonitoring of heavy metals, based on the relative changes in dry weight, number and density of byssal threads, and their bioaccumulated content of heavy metals. These measurements of byssal threads are simple and low-cost, and more importantly, are relevant to the performance of attachment by mussels and their likelihood of survival.

2.4 Development of a multiple biomarker approach

Chemical pollutants often exist as a cocktail in the environment, and the use of any single biomarker might not be sufficient to reveal the integrated biological impacts of mixed chemicals. The strategy of multiple biomarkers is recommended, but it could be challenging to decide on the optimal combination of biomarkers that can best explain the combined effects of pollutants, yet be cost-effective for routine monitoring purposes. Preferably, the selected group of biomarkers would also be prognostic to higher-level physiological responses that are indicative of the overall fitness and survival capability.

In this thesis, we attempted to develop a multiple biomarker approach, using *P. viridis* as a model species, for monitoring the pollution levels in Victoria Harbour, Hong Kong, for the dry season and the wet season. The bioaccumulated levels of heavy metals, PAHs, PCBs and OCPs in *P. viridis*, which indicated bioavailability of these chemical pollutants in the harbour area, were analysed in Chapter 3. The analytical work was followed by biological assays in Chapter 4, where a suite of biomarkers including SOD, CAT, GSH, AChE, LysD, MN, LPx, R:D and Et were determined in *P. viridis*. Among these biomarkers, the most suitable candidate and the optimal subset that explained the highest variability of the target pollutants were identified with multivariate statistical techniques for each season. Two physiological indices, namely CI and HSI, were used to indicate the general growth conditions of *P. viridis* during the study period. Discussion on the results of bioaccumulation of pollutants and biomarker responses in the mussels and their implications are provided in Chapter 5.

Table 2.1. Biomarkers applicable to *Perna viridis* for marine pollution biomonitoring in the Indo-Pacific region. Common abbreviations used in the literature are provided in brackets.

Category	Biomarker	Description	References
Genotoxicity	DNA strand breaks	Breakage of DNA strands induced by xenobiotics, oxidative agents or irradiation that may be transgenerational	(Ching *et al*., 2001; Siu *et al*., 2004; Siu *et al*., 2008; Vasanthi *et al*., 2012; Liu *et al*., 2014;)
	DNA adducts	Covalent attachment of reactive chemical intermediates to DNA bases that may be carcinogenic or mutagenic	(Ching *et al*., 2001)
	Oxidative DNA damage	Hydroxylation of guanine bases of DNA induced by free radicals to form 8-hydroxy-2'-deoxyguanosine (8-OHdG)	(Siu *et al*., 2008)
	Micronucleus formation	Extra-nuclear body that forms when a damaged chromosome or its fragment is not incorporated into the nucleus during cell division	(Siu *et al*., 2004; Siu *et al*., 2008; Liu *et al*., 2014)
Oxidative Stress	Lipid peroxidation (LPx)	Occurred with free radicals react with lipids that is cytotoxic and usually produces malondialdehyde (MDA) as an end-product	(Cheung *et al*., 2001; Cheung *et al*., 2002; Lau & Wong, 2003; Cheung *et al*., 2004; Davies *et al*., 2005; Jena *et al*., 2009;)
	Superoxide dismutase (SOD)	Enzymes that catalyse the dismutation of superoxide into oxygen and hydrogen peroxide	(Cheung *et al*., 2001; Cheung *et al*., 2002; Lau & Wong, 2003; Cheung *et al*., 2004; Richardson *et al*., 2008; Jena *et al*., 2009;)
	Catalase (CAT)	Enzymes that catalyse the decomposition of hydrogen peroxide to water and oxygen	(Cheung et al., 2001; Cheung et al., 2002; Lau & Wong, 2003; Cheung et al., 2004; Richardson et al., 2008; Jena et al., 2009;)
	Glutathione (GSH)	GSH as a tripeptide that protects against reactive oxygen species (ROS) and is oxidised into glutathione disulphide (GSSG) when reacted with ROS	(Cheung *et al*., 2001; Cheung *et al*., 2002; Richardson *et al*., 2008; Jena *et al*., 2009; Kwok *et al*., 2012;)

	Glutathione reductase (GR)	An enzyme that catalyses the reduction of GSSG back into GSH	(Cheung *et al*., 2001, Cheung *et al*., 2002, Cheung *et al*., 2004; Jena *et al*., 2009)
	Glutathione S-transferase (GST)	Enzymes that catalyse the conjugation of GSH to a range of hydrophobic compounds	(Cheung *et al*., 2001; Cheung *et al*., 2002; Lau & Wong, 2003; Cheung *et al*., 2004; Jena *et al*., 2009; Juhel *et al*., 2017)
	Glutathione peroxidase (GPx)	Enzymes that catalyse the reduction of hydrogen peroxide into water and of lipid peroxides into corresponding alcohols	(Cheung *et al*., 2001, Cheung *et al*., 2002; Davies *et al*., 2005; Jena *et al*., 2009)
Detoxification	Metallothionein (MT)	Cysteine-rich proteins with a high affinity for cations that protect against toxic metals	(Leung *et al*., 2014)
	Cytochrome P4501A (CYP1A)	A family of phase 1 enzymes which are regulated by the aryl hydrocarbon receptor pathway for detoxification of xenobiotics	(Amutha *et al*., 2009; Cholumpai *et al*., 2015; Juhel *et al*., 2017)
Immune responses	Phagocytosis	A process of haemocytes to engulf and eliminate nonself with ROS and lysosomes	(Nicholson, 2003a; Wang *et al*., 2014)
	Production of ROS	ROS released as a respiratory burst to destroy nonself during phagocytosis	(Wang *et al*., 2014)
	Lysosomal membrane destabilisation	Rupture of lysosomes and leakage of hydrolytic enzymes leading to autolysis	(Nicholson, 2001, 2003a; Nicholson, 1999a, 1999b; Nicholson & Lam, 2005; Fang, *et al*., 2008b; Fang, *et al*., 2008c; Fang *et al*., 2010)
	Lysosomal content	Containing hydrolytic enzymes for intracellular degradation and defence against nonself	(Wang *et al*., 2014)
	Total haemocyte count	Immune defence generally accompanied by haemocyte proliferation	(Wang *et al*., 2014)

	Haemocyte mortality	Ratio of dead to live haemocytes that is indicative of the degree of immune-incompetence	(Wang *et al*., 2014)
	Non-specific esterase	For hydrolysis of a number of choline esters including acetylcholine	(Wang *et al*., 2014)
Cell signalling	Acetylcholinesterase (AChE)	An enzyme that hydrolyses the neurotransmitter acetylcholine and is sensitive to organophosphate and carbamate pesticides	(Lau & Wong, 2003; Juhel *et al*., 2017;)
	Membrane-bound Na^+, K^+, Mg^{2+} and Ca^{2+} ATPases	Enzymes that transform ATP into ADP to pumps Na^+, K^+, Mg^{2+} and Ca^{2+} across plasma membranes for signal transmission and maintenance of the cellular ionic gradient	(Vijayavel *et al*., 2007)
Growth potential	RNA to DNA ratio	Ratio to estimate the relative rate of protein synthesis and growth potential	(Yeung *et al*., 2016, 2017)
	Energy reserves	Total concentration of glycogen, lipids and proteins converted into an energy equivalent	(Yeung *et al*., 2016, 2017)

Table 2.2. Physiological endpoints applicable to *Perna viridis* for marine pollution biomonitoring in the Indo-Pacific region. Common abbreviations used in the literature are provided in brackets.

Physiological endpoint	Description	References
Condition index	Ratio of tissue weight to shell weight or length that indicates relative somatic growth efficiency	(Nicholson, 1999a)
Gonadosomatic index (GSI)	Proportion of weight of gonad in the whole tissue that indicates sexual maturity and potential endocrine disruption	(Asaduzzaman *et al*., 2019; Noor *et al*., 2021)
Hepatosomatic index (HSI) or digestive gland index (DGI)	Proportion of weight of hepatopancreas in the whole tissue that reveals the amount of energy reserve	(Iyapparaj *et al*., 2013)
Organ morphology	Histological observation of tissue impairment in organs	(see Table 2.3)

Clearance rate	Feeding efficiency on microalgae to quantify energy acquisition, which can be part of SfG	(Nicholson, 2003b; Vijayavel *et al*., 2007; Tateda *et al*., 2015)
Respiration rate	Oxygen consumption rate as a measure of metabolic activity, which can be part of SfG	(Vijayavel *et al*., 2007; Wendling *et al*., 2013, Tateda *et al*., 2015)
Scope for growth (SfG)	SfG as an energy balance model among energy acquired via feeding, consumed via respiration and lost via excretion	(Wong & Cheung, 2001, 2003; Wang, *et al*., 2011)
Heart rate	Haemolymph pumping rate as a measure of cardiac activity, which indicates efficiency of transport of haemolymph, production of urine and movement of faeces	(Nicholson, 1999a, 1999b, 2002, 2003b; Nicholson & Lam, 2005)
Byssus thread production	Quantity of secreted proteinaceous fibre bundles for adhesive attachment to solid substrata	(Ekanath & Menon, 1983; Mathew & Menon, 1983; Yaqin *et al*., 2014)

Table 2.3. Histological alterations in different organs of *Perna viridis* under the stress of environmental pollution.

Organ	Description	References
Gills	Structural damages and cellular abnormalities of gill filaments such as rupture of cilia, distortion of lamellae, hyperplasia, hypertrophy, necrosis and haemolytic proliferation	(Viarengo *et al*., 1994; Shin *et al*., 2002; Cheung & Shin, 2005; Vasanthi *et al*., 2012; Goswami *et al*., 2014; Hariharan *et al*., 2014; Nagarjuna *et al*., 2019; Vasanthi *et al*., 2021; Xu *et al*., 2021)
Hepatopancreas	Structural damages and cellular abnormalities of digestive diverticula such as rupture of cilia, microtubules, internal star-like structures, compressed digestive cells, loss of basophilic cells, necrosis and dilation of lumen	(Krishnakumar *et al*., 1990; Vasanthi *et al*., 2012; Vasanthi *et al*., 2021)
Gonad	Gonadal degradation in form of reduction of gonadal follicles, gonadal atrophy, atresia and increase of lipofuscin	(Xu *et al*., 2021)
Adductor muscle	Myodegeneration and connective tissue damages leading to muscle fragmentation and atrophy	(Vasanthi *et al*., 2012)

Chapter 3: Biomonitoring of persistent organic pollutants and heavy metals using a mussel transplantation approach

3.1 Introduction

The exponential urbanisation of Hong Kong, in particular along the iconic Victoria Harbour, has resulted in significant coastal pollution since the 1960s. Earlier research efforts identified a wide range of persistent organic pollutants (POPs) and heavy metals in the sediment and biota collected from Victoria Harbour, such as polycyclic aromatic hydrocarbons (PAHs), polychlorinated biphenyls (PCBs) and organochlorine pesticides (OCPs) (Phillips, 1985, 1989; Zheng & Richardson, 1999), as well as cadmium (Cd), chromium (Cr), copper (Cu), lead (Pb) and zinc (Zn) (Chan, 1988, 1989; Chan, 1995; Wong *et al*., 1995; Phillips, 1985, 1989; Phillips & Rainbow, 1988; Tanner *et al*., 2000; Tang *et al*., 2008). The pollution sources could be sewage discharges, urban runoff, land reclamation, oil spillage and liberation from sediments, among others (Morton, 1976, 1989; Wong *et al*., 1999; Wong *et al*., 2004; Lai *et al*., 2016). POPs and heavy metals can be bioaccumulated in marine organisms and biomagnified along the food chains. Apart from the environmental impacts, the trophic transfer provides a route for these pollutants to enter the human diet through the consumption of seafood and has raised human health risk concerns since a lot of POPs and heavy metals are considered carcinogenic and mutagenic (Alharbi *et al*., 2018; Briffa *et al*., 2020).

Aiming to address the pollution issues in Victoria Harbour, the Government has implemented the Harbour Area Treatment Scheme (HATS) to convey sewage from both sides of the harbour to the Stonecutters Island Sewage Treatment Works for a chemically enhanced primary treatment (Drainage Service Department, 2019; Figure 3.1). Since then, a number of studies have confirmed improvement of water quality in the Harbour (Liu & Kueh, 2005; Fang, 2008a). However, pollution sources still exist in the adjacent waters. For instance, PAHs and heavy metals are expected due to heavy maritime traffic, industrial discharges and reclamation activities (Alharbi *et al*., 2018; Briffa *et al*., 2020). Other examples include PCBs and OCPs, which have been banned or phased out since the 1980s, but they are long-lasting in the environment and can still be detected in Victoria Harbour and elsewhere (Zhang *et al*., 2002; Fu *et al*., 2003; Liu & Kueh, 2005; Fang *et al*., 2009). The spread of PCBs and OCPs, as well as other POPs, could be further enhanced by long-distance transport in air, rivers and ocean currents (Chen *et al*., 2006; Kueh & Lam, 2008).

The analytical methods for POPs and heavy metals have been well established and can be combined with the biomonitoring approach to indicate the bioavailability of the target pollutants in marine environments. Marine bivalves such as mussels are model organisms commonly used for pollution biomonitoring due to their global distribution and sedentary lifestyle, and more importantly, to their filter-feeding nature, bioaccumulation capability for a wide range of pollutants and high tolerance to environmental stress (Hamza-Chaffai, 2014; Beyer *et al*., 2017; Świacka *et al*., 2019; Kucuksezgin *et al*., 2020;). In the Indo-Pacific region including Hong Kong, the green-lipped mussel *Perna viridis* represents the most important mussel species for this biomonitoring purpose and has been regarded as effective for both POPs and heavy metals (Chan, 1988, Phillips, 1985; Chan, 1989; Liu & Kueh, 2005; Fang *et al*, 2008a; Fang *et al*., 2009; Yeung *et al*., 2017). However, it should be noted that native mussels may not exist at all intended sampling sites, for example, in heavily polluted waters with high mortality or on feeding grounds of fish where mussels are under high predation stress. These site-specific factors could restrict the scope of pollution biomonitoring using native mussels. An alternative strategy is the use of mussel transplantation, in which mussels are collected from a reference site and redeployed among the target sites for pollution biomonitoring. The main advantage of the transplantation approach is to guarantee all mussels have the same origin and thus pre-exposure history to pollution (Chan, 1989; Kucuksezgin *et al*., 2013, 2020; Moschino *et al*., 2016; Yeung *et al*., 2017; Bashnin *et al*., 2019). After deployment for weeks or months, the tissue levels of pollutants in mussels and their cellular stress responses can be indicative of the recent pollution status of the target sites. The transplantation approach can also minimise the potential confounding effects due to any long-term adaptation developed by native mussels to the target pollutants (Felten *et al*., 2013).

The aim of this Chapter was to determine the pollution status in Victoria Harbour in terms of the bioavailable levels of PAHs, PCBs, OCPs and heavy metals in *P. viridis* using the mussel transplantation approach. Mussels were collected from a reference site outside the harbour and redeployed in the dry season and wet season in 2019. This biomonitoring work would allow us to evaluate the effectiveness of HATS and the seasonal influence on the bioavailability of pollutants. More importantly, the obtained data of the body burden of pollutants would provide the scientific basis to develop an integrated biomarker approach of *P. viridis* for routine biomonitoring purposes in Chapter 4.

3.2 Methods and materials

3.2.1 Experimental design

A pollution biomonitoring study was carried out in Victoria Harbour, Hong Kong, using *P. viridis* with two rounds of transplantation in a dry season (December 2018–March 2019) and a wet season (July–September 2019). All mussels were collected from Tung Lung Chau (TLC), a reference site in this study which is close to Victoria Harbour but was found to be less polluted with POPs and heavy metals (Phillips & Yim, 1981; Fang *et al*, 2008a; Tang *et al*., 2008; Fang *et al*., 2009). About 800 mussels per season were acclimated in nylon cages at TLC for two weeks, after which 120 healthy individuals with similar shell lengths (72 mm on average) were selected and redeployed at each of the four study sites within Victoria Harbour, namely Yau Ma Tei (YMT), Causeway Bay (CWB), Kwun Tong (KT) and Yau Tong (YT) (Figure 3.1). Another 120 mussels were maintained at TLC as the control group. The 120 mussels per site were kept in a nylon cage (1 m height × 0.3 m diameter) with four layers, 30 mussels on each layer, and hung at 2–3 m water depth. All mussels were retrieved after five weeks of deployment and transported live in a cool box to the laboratory. The five-week redeployment period was considered appropriate, given that the tissue concentrations of heavy metals in mussels transplanted at polluted sites for four weeks were generally similar to those for a longer period of 8–16 weeks (Wu *et al*., 2007; Gonzalez-Rey *et al*., 2011), while mussels redeployed at another polluted site also reached the highest tissue levels of POPs in about 4–7 weeks (Peven *et al*., 1996).

3.2.2 Sample preparation

Retrieved mussels were gently separated from each other by cutting the byssal threads. Out of the 120 mussels per site, 100 intact individuals were selected for the chemical analyses (this Chapter) and biological assays (Chapter 4) following the sampling scheme presented in Figure 3.2. Shell length of *P. viridis* was measured. The mussel valves were pried apart by 5 mm and haemolymph (0.8 mL) was freshly extracted from the adductor muscle. The mussels were then thoroughly opened and the hepatopancreas was collected. The isolated hepatopancreas, and the remaining soft tissue, were blot-dried and weighed. The above steps yielded 100 samples for each sample type (haemolymph, hepatopancreas and remaining tissue) per site. These 100 samples were pooled by 10, leading to 10 homogenised composite samples per sample type per site. The composite samples of haemolymph and hepatopancreas were used in Chapter 4, where various cellular biomarkers and physiological indices were determined. The composite samples

of remaining tissue were used in this Chapter for the analyses of POPs and heavy metals. Each of the composite tissue samples was divided into three portions, one for POPs (PAHs, PCBs and OCPs), one for heavy metals (Cd, Cr, Cu, Pb and Zn), and one as a backup. All portions were freeze-dried, ground to powder, dry-weighed and kept at –20 °C prior to the chemical analyses.

3.2.3 Analyses of PCHs, PCBs and OCPs

The modified sample preparation technique of QuEChERS, which stands for "Quick, Easy, Cheap, Effective, Rugged and Safe", was employed in this study to extract PAHs, OCPs and PCBs from the *P. viridis* tissue samples (Rashid *et al*., 2010; Kutty *et al*., 2012). Homogenised tissue powder (2 g) was resuspended in 13 mL of Milli-Q water (Merck, Darmstadt, Germany) at 4 °C and added with 15 mL of 1% acetic acid in acetonitrile as the extraction solvent, which was spiked with three internal standards, namely 1.5 µg of m-terphenyl (45801, Sigma-Aldrich, St Louis, MO) for analysis of PAHs, 1.5 µg of PCB 185 (DRE-C20018500, LGC Standards, Middlesex, UK) for analysis of PCBs, and 1.5 µg of quintozene (45653, Sigma-Aldrich) for analysis of OCPs. The sample mixture was vortexed for 1 min, added with 1.5 g of sodium acetate and 6 g of magnesium sulphate, shaken by hand for 2 min and centrifuged at 4000 rpm for 5 min, after which 10 mL of the acetonitrile layer was transferred to a new tube containing 1 g of anhydrous sodium sulphate. The solution of acetonitrile was shaken by hand for 1 min and evaporated to 0.5 mL by nitrogen blowing. The concentrated content was resuspended by adding 20 mL of dichloromethane and evaporated again to 0.5 mL using nitrogen. The resuspension and evaporation steps were repeated for two more rounds by adding 10 mL of dichloromethane and 10 mL of hexane, respectively.

The concentrated content, at this stage in 0.5 mL of hexane, underwent three steps of solid-phase extraction (SPE). In step 1, the concentrated content was applied to a silica-based SPE cartridge (SLSPE1K12SI, Hawach Scientific, Xi'an, China), which had been pre-conditioned with 10 mL of dichloromethane and 20 mL of hexane. In step 2, the SPE cartridge was eluted with 13 mL of dichloromethane and hexane (4:6). In step 3, the extract after SPE was evaporated to 0.5 mL by nitrogen blowing. Steps 1–3 were repeated to ensure complete extraction. The final extract was completely dried by nitrogen evaporation and resuspended in 1 mL of isooctane. Concentrations of PAHs, PCBs and OCPs in the final extract were analysed with a 30 m fused-silica capillary column (Agilent CP8944, Santa Clara, CA) using a gas

chromatography (Agilent 7890, Santa Clara, CA) electron ionisation-quadrupole mass spectrometer (Agilent 5977, Santa Clara, CA). We followed the method of Kutty *et al*. (2012) with modification. In brief, 1 μL of the final extract was injected into the capillary column in a pulsed splitless mode at 325 °C. The oven temperature was set at 60 °C for the first 2 min and raised to 175 °C at 20 °C per min, then to 250 °C at 5 °C per min, and finally to 325 °C at 10 °C per min. The detector temperature was set at 325 °C. The total acquisition time was 35.25 min. Three analytical standard mixes, namely polynuclear aromatic hydrocarbons mix (CRM47543, Sigma-Aldrich), chlorinated biphenyl congeners in isooctane (NIST2262, Sigma-Aldrich), and EPA8081 pesticide standard mix (CRM46845, Sigma-Aldrich), were used in the quantification of PAHs, PCBs and OCPs, respectively.

Target PAHs included 16 forms, namely naphthalene (2 rings), acenaphthylene, acenaphthene, anthracene, fluorene and phenanthrene (3 rings), benzo[a]anthracene, chrysene, fluoranthene and pyrene (4 rings), benzo[b]fluoranthene, benzo[k]fluoranthene, benzo[a]pyrene and dibenz[a,h]anthracene (5 rings), and benzo[ghi]perylene and indeno[1,2,3-cd]pyrene (6 rings). The PAHs with 2–3 and 4–6 fused aromatic rings were defined as low molecular weight PAHs (LMW PAHs) and high molecular weight PAHs (HMW PAHs), respectively. Target PCBs included 28 congeners, including numbers 1, 8, 18, 28, 29, 44, 50, 52, 66, 77, 87, 101, 104, 105, 118, 126, 128, 138, 153, 154, 170, 180, 187, 188, 194, 195, 201 and 206. Target OCPs included 21 types, namely aldrin, cis-chlordane, trans-chlordane, decachlorobiphenyl, 4,4'-dichlorodiphenyldichloroethane, 4,4'-dichlorodiphenyldichloroethylene, 4,4'-dichlorodiphenyltrichloroethane, dieldrin, endosulfan, endosulfan sulfate, endrin, endrin-aldehyde, endrin ketone, heptachlor, cis-heptachlor epoxide, alpha-hexachlorocyclohexane, beta-hexachlorocyclohexane, gamma-hexachlorocyclohexane, sigma-hexachlorocyclohexane, methoxychlor and 2,3,5,6-tetrachloro-m-xylene. Summation of the individual PAHs, PCBs and OCPs yielded concentrations of 16ΣPAH, 28ΣPCB and 21ΣOCP, respectively.

Spiked recovery tests were performed for the compounds of 16 PAHs, 28 PCBs and 21 OCPs using the three analytical standard mixes. Homogenised tissue powder of *P. viridis* was divided into two portions, of which one (2 g) was spiked with 200 ng of each analyte, while the other portion (2 g) served as the background control. The two portions were subject to the same analytical procedures described above. Differences in the measured quantity of each target analyte between the two portions, divided by the spiked quantity, yielded the recovery rate of

our method. The mean recovery rates of PAHs, OCPs and PCBs in the tissue matrix of *P. viridis* were determined to be 80–120% (n = 3). Data of PAHs, PCBs and OCPs were standardised to unit dry weight (DW) of the tissue samples. The method detection limits of PAHs, PCBs and OCPs were determined to be 1 ng g^{-1}, which was the lowest tested concentration that showed a signal-to-noise ratio of at least 3.0 (Brunetti & Desimoni, 2015).

3.2.4 Analyses of Cd, Cr, Cu, Pb and Zn

The ultrasonic acid digestion method was employed for the analyses of Cd, Cr, Cu, Pb and Zn following (Kazi *et al*., 2009). All glassware was precleaned in 10% nitric acid overnight and thoroughly rinsed with Milli-Q water. Homogenised tissue powder (200 mg) was added with 50 ng of indium (CGIN1, Inorganic Ventures, Christiansburg, VA) as an internal standard and was digested in 2 mL of 65% nitric acid mixed with 1 mL of 30% hydrogen peroxide at 70°C for 60 min. The solution was then ultrasonicated at 35 kHz at 70 °C for 30 min, added with 4 mL of Milli-Q water, ultrasonicated for another 5 min, and diluted to 10 mL using Milli-Q water. The diluted solution was vacuum-filtered through a cellulose acetate membrane with 0.45 μm pores (CH4525-CA, Thermo Fisher Scientific, Waltham, MA) and kept at –20 °C until the analyses of heavy metals. Cd, Cr and Pb in the filtered solution were analysed using an inductively coupled plasma mass spectrometer (ICP-MS; Agilent 7500). The concentrations of Cu and Zn were 1–2 orders of magnitude higher than those of Cd, Cr and Pb and were determined with an Inductively coupled plasma optical emission spectrometer (ICP-OES; Agilent 710).

Spiked recovery tests were performed for Cd, Cr, Cu, Pb and Zn using the analytical standards supplied by Inorganic Ventures with the product codes of CGCD10, CGCR(3)1, CGCU1, CGPB1 and CGZN1, respectively. Homogenised tissue powder of *P. viridis* was divided into two portions, of which one (200 mg) was spiked with 0.01 μg of Cd, 0.01 μg of Cr and 0.01 μg of Pb, while the other portion (200 mg) served as the background control. The same process was repeated for another pair of portions but spiked with 1 μg of Cu and 1 μg of Zn. The two pairs of spiked and unspiked samples were subject to the same analytical procedures described above using ICP-MS (for Cd, Cr and Pb) or ICP-OES (for Cu and Zn). Differences in the measured quantity between each pair, divided by the spiked quantity, yielded the recovery rate of each heavy metal. The recovery rates of Cd, Cr, Cu, Pb and Zn in the mussel tissue matrix were determined to be 70–110% (n = 3). The data of Cd, Cr, Cu, Pb and Zn were expressed

per unit g of DW of the tissue samples. The limits of detection for heavy metals were calculated as the mean plus three times of the standard deviation of the blank following the AOAC method 2015.01 (Briscoe *et al*., 2015), and were estimated to be 0.05 ng g^{-1} for Cd, 0.05 ng g^{-1} for Cr, 0.05 ng g^{-1} for Cu, 2.5 µg g^{-1} for Pb, and 2.5 µg g^{-1} for Zn.

3.2.5 Univariate statistical analysis

The seven datasets of LMW PAHs, HMW PAHs, Cd, Cr, Cu, Pb and Zn in *P. viridis* at five sites in two seasons were used in the statistical analysis. The concentrations of all target PCBs and OCPs were below the detection limits and not statistically analysed (see Table 3.1). Most of the datasets, even after data transformations, did not fulfil the assumptions of normality or homogeneity of variance required for the analysis of variance (ANOVA). Therefore, the site effect on each pollutant in each season was analysed with Kruskal-Wallis *H* test, which is the non-parametric analogue of ANOVA.

Since there were 14 rounds of *H* test required for the seven pollutants in two seasons, the significant level ($\alpha = 0.05$) in each round was corrected by the sequential Bonferroni method to reduce the chance of committing the family-wise Type I error (Fang *et al*., 2017). The lowest *p* value obtained among the 14 rounds was tested at $\alpha/c = 0.0036$, with the second lowest tested at $\alpha/(c - 1) = 0.0038$, and the third lowest tested at $\alpha/(c - 2) = 0.0042$, and so on, where c was set to be 14. The sequential correction continued until a non-significant result was detected. When the site effect was significant in the *H* test, Dunn's multiple comparisons were used to compare all sites pairwise at $\alpha = 0.05$. The univariate statistical procedures were performed with the statistical software SigmaPlot 14.0 (Systat Software, Palo Alto, CA).

3.2.6 Multivariate statistical analyses

The multivariate statistical procedures for the mussel tissue data of pollutants were performed using the software PRIMER 7 (PRIMER-e, Auckland, New Zealand). Seven variables, namely LMW PAHs, HMW PAHs, Cd, Cr, Cu, Pb and Zn, in *P. viridis* at the five sites were analysed separately for the dry season and wet season in the multivariate statistical procedures. Strong correlations did not exist among these variables ($\rho < 0.62$ in Spearman's correlation test). Square root transformation was applied to the seven variables, and the transformed data were normalised to a common dimensionless scale by subtracting the mean and being divided by the

standard deviation (SD) of each variable. Principal component analysis (PCA) was conducted on the normalised data using Euclidean distance to project the multi-dimensional cloud of data on a two-dimensional plane using the first principal component (PC1) and second principal component (PC2), the two most important PCs to explain the total variation of the seven variables.

A resemblance matrix of Euclidean distance was constructed to define the pairwise similarities among the 50 tissue samples per season, which were subject to hierarchical agglomerative clustering using group-average linkage (CLUSTER). The CLUSTER routine was coupled with similarity profile analysis (SIMPROF), using 9999 permutations, which provided an objective *a posteriori* approach to identify significantly dissimilar groups among the 50 samples at $p < 0.05$ (Clarke *et al.*, 2008). The SIMPROF groups were overlayed on a plot of non-metric multidimensional scaling (nMDS) to visualise the similarity rankings among these samples in two dimensions. The stress value provided by nMDS, which varies between 0 and 1, represents the level of distortion from reducing the dimensionality into lower dimensions. A value closer to zero indicates a better fit, where stress < 0.2 is generally considered acceptable.

The *a posteriori* groups identified by SIMPROF were validated *a priori* using analysis of similarity (ANOSIM) (Clarke & Gorley, 2016). ANOSIM is the non-parametric multivariate analogue of ANOVA. The test statistic R of ANOSIM has a range of 0–1 and is a scaled measure of dissimilarity between groups. A higher value of R indicates higher dissimilarity, where $R = 1$ indicates completely different assemblages. In this study, two-way crossed ANOSIM (site × season) was adopted to determine the dissimilarity among the five sites (YMT, CWB, KT, YT and TLC) across all seasons, and between the dry and wet seasons across all sites, using the seven variables of pollutants in *P. viridis* (LMW PAHs, HMW PAHs, Cd, Cr, Cu, Pb and Zn). Since the spatial compositions of these pollutants were found to be significantly dissimilar between the dry and wet seasons in the crossed ANOSIM (see Figure 3.7b), data of the five sites were separately analysed for each of the two seasons using one-way ANOSIM, and if significant, post hoc pairwise ANOSIM was used to determine the dissimilarity in each pair of sites. The ANOSIM procedures were followed by similarity percentages analysis (SIMPER), which was used to identify the percent contribution of each variable in the compositional differences between sites.

3.3 Results

3.3.1 Univariate statistical results

The tissue burden concentrations of POPs and heavy metals in *P. viridis* redeployed at the five study sites in Victoria Harbour in the dry season and wet season are summarised in Table 3.1. The composition of LMW PAHs (with 2–3 fused aromatic rings) consisted mainly of naphthalene, acenaphthylene, anthracene and phenanthrene in the tissue of *P. viridis* during the two study periods. The tissue burden of HMW PAHs (with 4–6 fused aromatic rings) was dominated by fluoranthene and pyrene, while benzo[a]anthracene and benzo[a]pyrene were only found at KT and CWB, respectively, in the dry season. The ratio of LMW PAHs to HMW PAHs, which is indicative of the pyrolytic (if < 1) or petrogenic sources of PAHs (if > 1), ranged at 1.76–9.41 within the harbour area (YMT, CWB, KT and YT), but higher values of 14.4–19.9 were found at the reference site TLC. Another ratio used to reveal the origin of PAH pollution was phenanthrene to anthracene, which are two isomers of LMW PAHs with equal molecular mass but different thermodynamic stability (pyrolytic if > 10, or petrogenic if < 10; (Sałata *et al*., 2019), and this ratio showed a range of 0.70–1.33 among all sites. The concentrations of 16ΣPAH at TLC (135–139 ng g^{-1}) were lower than those at other sites within Victoria Harbour (189–307 ng g^{-1}) in the two seasons. However, none of the 28 congeners of PCBs and 21 types of OCPs reached the method detection limit at 1 ng g^{-1} and therefore 28ΣPCB and 21ΣOCP were not determined. As for heavy metals, all mussel samples showed detectable levels of Cd (0.28–0.43 µg g^{-1}), Cr (0.59–1.40 µg g^{-1}), Cu (4.55–13.5 µg g^{-1}), Pb (1.76–3.28 µg g^{-1}) and Zn (60.5–79.7 µg g^{-1}; Table 3.1).

The spatial pollution patterns of LMW PAHs, HMW PAHs, Cd, Cr, Cu, Pb and Zn in the dry and wet seasons are illustrated in Figures 3.3 and 3.4. The site effects were significant for all these pollutants regardless of which season, as indicated by Kruskal-Wallis *H* test with sequential Bonferroni correction ($p < 0.001$ or = 0.006), except that for Zn in the wet season ($p = 0.058$; Table 3.2). The results of Dunn's pairwise comparison test furthermore revealed the significantly lowest pollution levels at the reference site TLC among all sites, except those of Pb and Zn in the wet season (Table 3.2).

3.3.2 Multivariate statistical results

The data of LMW PAHs, HMW PAHs, Cd, Cr, Cu, Pb and Zn in *P. viridis* were visualised with PCA, in which PC1 and PC2 accounted for 42.1% and 20.2% of the total variance in the dry season, and for 36.9% and 20.6% in the wet season, respectively (Table 3.3). According to the directions and magnitudes of the eigenvectors, *P. viridis* at the reference site TLC appeared to contain lower concentrations of pollutants compared to the other sites in the dry season (Figure 3.5a). However, this spatial pattern was less pronounced in the wet season under the influence of high Pb in some mussels at TLC (Figure 3.5b).

The *a posteriori* hierarchical cluster analysis using CLUSTER and SIMPROF identified five significantly dissimilar groups and one outlier among the 50 tissue samples in the dry season ($p < 0.05$; Figure 3.6a). The groups identified by SIMPROF were illustrated on the nMDS plot for the dry season (2D stress = 0.16; Figure 3.6c). All ten samples of TLC (reference site) formed a unique group. All ten samples of YMT (western-harbour site) formed another distinct group which contained two clusters. All ten samples of YT (eastern-harbour site), and two samples of CWB, were clustered together, while the other eight samples of CWB and all ten samples of KT (two central-harbour sites) formed the largest cluster in the dry season. However, the grouping was less distinct in the wet season, and three significantly dissimilar groups were formed in addition to one outlier according to the results of SIMPROF ($p < 0.05$; Figure 3.6b) and nMDS (2D stress = 0.19; Figure 3.6d). Eight out of ten samples of TLC remained unique but were clustered with two samples of CWB and YT. The remaining nine samples of YT joined with five samples of the other sites to form another group. The largest cluster of CWB and KT still existed but was merged with most samples of YMT in the wet season.

The *a priori* approach of ANOSIM was used to test the dissimilarity among the five sites in the dry season and wet season based on the seven variables of pollutants in *P. viridis*. The overall site effect (global $R = 0.65$; Figure 3.7a) and season effect (global $R = 0.43$; Figure 3.7b) were both significant in two-way crossed ANOSIM. The site effect in each season was then assessed in one-way ANOSIM. In the dry season, the site effect was significant (global $R = 0.72$; Figure 3.7c), and pairwise ANOSIM tests revealed that the pollution levels at most sites were highly dissimilar to each other ($R = 0.70–0.93$), except those between CWB and KT and between CWB and YT ($R = 0.48–0.50$; Table 3.4a). In the wet season, significance was also detected among sites (global $R = 0.58$; Figure 3.7d), and TLC was still distinct when compared

with CWB, KT and YT (R = 0.76–0.80; Table 3.4b). However, the dissimilarity between TLC and YMT, and between all other sites became less clear in the wet season (R = 0.06–0.66) than in the dry season. The three most important variables that resulted in the compositional difference in each pair of sites in the two seasons were identified using SIMPER. For instance, the two types of PAHs contributed to 23.9%–58.9% of the dissimilarity of TLC with the other sites, except that with CWB and KT in the dry season, where the mixture of heavy metals showed a greater influence. The major contributors to other pairwise site differences are summarised in Table 3.5.

Discussion on the above results of bioaccumulation of pollutants, together with the biomarker responses in *P. viridis* assessed in Chapter 4, is provided as a whole in Chapter 5.

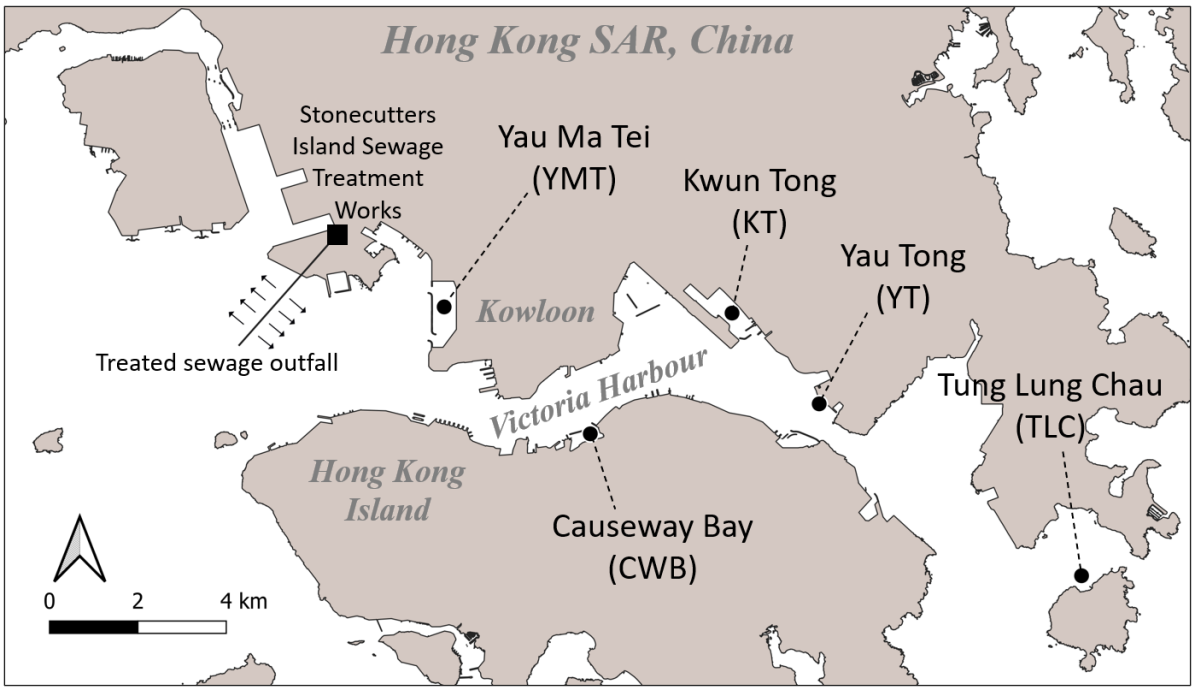

Figure 3.1. Five study sites of the pollution biomonitoring work using the green-lipped mussel *Perna viridis* in Victoria Harbour, Hong Kong, namely Yau Ma Tei (YMT), Causeway Bay (CWB), Kwun Tong (KT) and Yau Tong (YT) within the harbour, and Tung Lung Chau (TLC) in the east outside the harbour as a reference site. Mussels were collected from the reference site and redeployed at all five sites for five weeks in the transplantation approach. The arrows indicate the treated sewage discharge points of the Stonecutters Island Sewage Treatment Works in the west of Victoria Harbour.

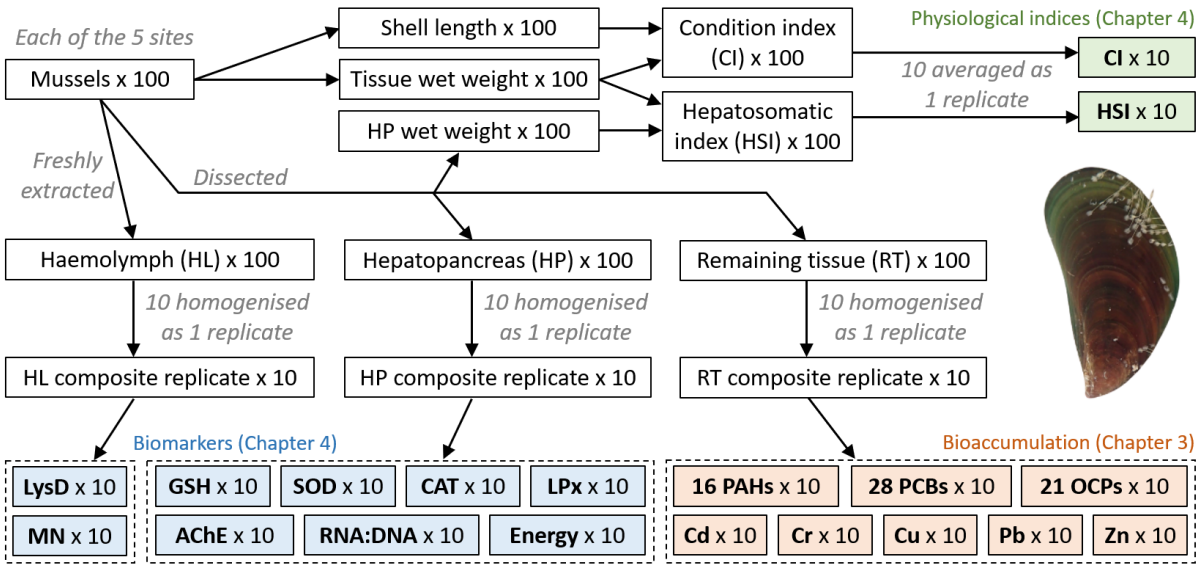

Figure 3.2. Sampling scheme of *Perna viridis* for the biomonitoring study in Victoria Harbour, Hong Kong. At each site, 100 mussels generated 10 composite replicates for each chemical analysis or biological assay. The data of the body burden of pollutants (brown cells) are presented in this Chapter, namely polycyclic aromatic hydrocarbons (PAHs), polychlorinated biphenyls (PCBs), organochlorine pesticides (OCPs), cadmium (Cd), chromium (Cr), copper (Cu), lead (Pb) and zinc (Zn). The data of biomarkers (blue cells) and physiological indices (green cells) and their abbreviations are reported in Chapter 4.

Table 3.1. Data summary of **(a)** persistent organic pollutants (POPs) and **(b)** heavy metals determined in *Perna viridis* redeployed at the five sites (YMT, CWB, KT, YT and TLC) in the dry and wet seasons (mean ± SD, n = 10). If the concentration of any polycyclic aromatic hydrocarbon (PAH) is below the detection limit (BDL; < 1 ng g^{-1}), it is assumed to be 0.5 ng g^{-1} in the calculation for low molecular weight (LMW) PAHs, high molecular weight (HMW) PAHs and 16ΣPAH. The numbers of fused aromatic rings in PAHs are indicated in the brackets. All polychlorinated biphenyls (PCBs) and organochlorine pesticides (OCPs) are below the detection limit. Please refer to Figure 3.1 for the site abbreviations.

Pollutant in *P. viridis*	YMT, dry	CWB, dry	KT, dry	YT, dry	TLC, dry	YMT, wet	CWB, wet	KT, wet	YT, wet	TLC, wet
(a) POPs (ng g^{-1} dry weight)										
Naphthalene (rings: 2)	102 ± 40.2	105 ± 42.2	65.9 ± 32.6	119 ± 45.1	60.0 ± 23.0	115 ± 32.2	76.9 ± 36.1	94.6 ± 37.5	97.2 ± 18.1	39.7 ± 16.1
Acenaphthylene (3)	6.49 ± 7.74	10.6 ± 6.98	3.05 ± 5.38	2.05 ± 4.91	BDL	BDL	5.06 ± 7.37	1.99 ± 4.70	2.05 ± 4.89	BDL
Acenaphthene (3)	BDL	BDL	BDL	BDL	BDL	BDL	BDL	BDL	BDL	BDL
Anthracene (3)	65.5 ± 5.04	48.4 ± 13.7	36.0 ± 14.2	41.4 ± 6.84	33.4 ± 5.55	49.5 ± 19.1	34.9 ± 17.9	46.6 ± 5.82	59.5 ± 8.30	43.3 ± 19.4
Fluorene (3)	BDL	BDL	BDL	BDL	BDL	BDL	BDL	BDL	BDL	BDL
Phenanthrene (3)	46.8 ± 4.22	39.1 ± 6.64	33.0 ± 5.56	31.2 ± 4.94	23.4 ± 4.29	45.0 ± 4.96	35.4 ± 5.43	34.2 ± 4.47	45.6 ± 7.02	38.6 ± 3.40
Benzo[a]anthracene (4)	BDL	BDL	2.26 ± 5.56	BDL	BDL	BDL	BDL	BDL	BDL	BDL
Chrysene (4)	BDL	BDL	BDL	BDL	BDL	BDL	BDL	BDL	BDL	BDL
Fluoranthene (4)	41.5 ± 2.11	36.5 ± 5.16	26.4 ± 18.0	42.8 ± 15.3	3.04 ± 8.02	BDL	5.77 ± 11.1	35.3 ± 2.23	25.6 ± 17.5	BDL
Pyrene (4)	10.1 ± 20.2	3.14 ± 8.35	18.2 ± 22.9	65.3 ± 5.92	10.1 ± 12.6	51.0 ± 18.0	34.3 ± 18.4	42.8 ± 15.0	47.0 ± 17.5	11.3 ± 23.2
Benzo[b]fluoranthene (5)	BDL	BDL	BDL	BDL	BDL	BDL	BDL	BDL	BDL	BDL
Benzo[k]fluoranthene (5)	BDL	BDL	BDL	BDL	BDL	BDL	BDL	BDL	BDL	BDL
Benzo[a]pyrene (5)	BDL	10.6 ± 16.4	BDL	BDL	BDL	BDL	BDL	BDL	BDL	BDL
Dibenz[a,h]anthracene (5)	BDL	BDL	BDL	BDL	BDL	BDL	BDL	BDL	BDL	BDL
Benzo[ghi]perylene (6)	BDL	BDL	BDL	BDL	BDL	BDL	BDL	BDL	BDL	BDL
Indeno[1,2,3-cd]pyrene (6)	BDL	BDL	BDL	BDL	BDL	BDL	BDL	BDL	BDL	BDL
LMW PAHs (2–3)	222 ± 46.0	204 ± 58.1	139 ± 42.4	195 ± 52.2	118 ± 30.7	211 ± 43.9	153 ± 55.8	178 ± 37.3	205 ± 21.9	123 ± 30.2

HMW PAHs (4–6)	55.6 ± 20.4	53.8 ± 15.9	50.4 ± 35.5	112 ± 18.4	17.1 ± 13.0	55.5 ± 18.0	44.1 ± 17.5	82.1 ± 14.4	76.6 ± 31.5	15.8 ± 23.2
LMW/HMW PAHs	4.30 ± 1.38	4.20 ± 1.88	9.41 ± 13.1	1.76 ± 0.42	14.4 ± 11.5	8.19 ± 15.2	7.63 ± 14.8	2.31 ± 1.01	5.91 ± 10.5	19.9 ± 10.6
Phenanthrene/anthracene	0.71 ± 0.04	0.93 ± 0.61	1.13 ± 0.67	0.75 ± 0.04	0.70 ± 0.03	1.20 ± 0.89	1.33 ± 0.75	0.73 ± 0.03	0.77 ± 0.02	0.93 ± 0.55
16ΣPAH	277 ± 55.5	258 ± 52.0	189 ± 57.2	307 ± 61.0	135 ± 31.6	267 ± 39.0	197 ± 56.5	260 ± 37.3	282 ± 46.2	139 ± 38.6
28 congeners of PCBs	BDL	BDL	BDL	BDL	BDL	BDL	BDL	BDL	BDL	BDL
21 types of OCPs	BDL	BDL	BDL	BDL	BDL	BDL	BDL	BDL	BDL	BDL
(b) Heavy metals (μg g^{-1} dry weight)										
Cadmium (Cd)	0.30 ± 0.02	0.36 ± 0.04	0.33 ± 0.04	0.30 ± 0.03	0.28 ± 0.04	0.39 ± 0.07	0.30 ± 0.03	0.35 ± 0.08	0.43 ± 0.05	0.37 ± 0.05
Chromium (Cr)	0.71 ± 0.09	1.23 ± 0.52	0.93 ± 0.23	1.32 ± 0.15	0.87 ± 0.22	0.59 ± 0.22	0.79 ± 0.20	0.66 ± 0.23	1.40 ± 0.67	0.60 ± 0.12
Copper (Cu)	6.41 ± 0.38	7.55 ± 0.54	10.8 ± 0.94	6.01 ± 0.69	4.55 ± 0.49	7.03 ± 1.93	13.5 ± 2.89	9.70 ± 2.91	9.62 ± 3.20	5.38 ± 0.68
Lead (Pb)	1.86 ± 0.15	3.28 ± 0.49	2.37 ± 0.22	2.49 ± 0.21	2.25 ± 0.35	1.76 ± 0.53	2.29 ± 0.21	1.85 ± 0.35	2.94 ± 0.17	2.57 ± 0.44
Zinc (Zn)	61.6 ± 3.30	76.3 ± 11.3	79.7 ± 6.28	66.3 ± 5.37	60.5 ± 5.25	77.7 ± 19.7	67.9 ± 5.37	73.7 ± 12.4	76.6 ± 7.32	65.6 ± 9.47

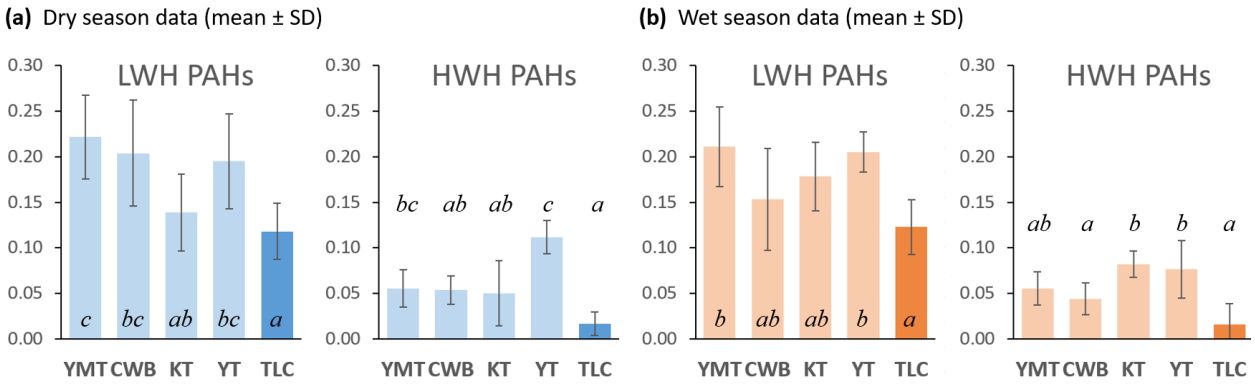

Figure 3.3. Tissue burden concentrations (µg g^{-1} dry weight) of low molecular weight (LMW) polycyclic aromatic hydrocarbons (PAHs) and high molecular weight (HMW) PAHs in *Perna viridis* assessed at the five sites (YMT, CWB, KT, YT and TLC) in the **(a)** dry season and **(b)** wet season (n = 10). Please refer to Figure 3.1 for the site abbreviations. The darker bars indicate the reference site. Significant pairwise site differences are indicated by different italic small letters (Kruskal-Wallis *H* test followed by Dunn's multiple comparisons, $p < 0.05$).

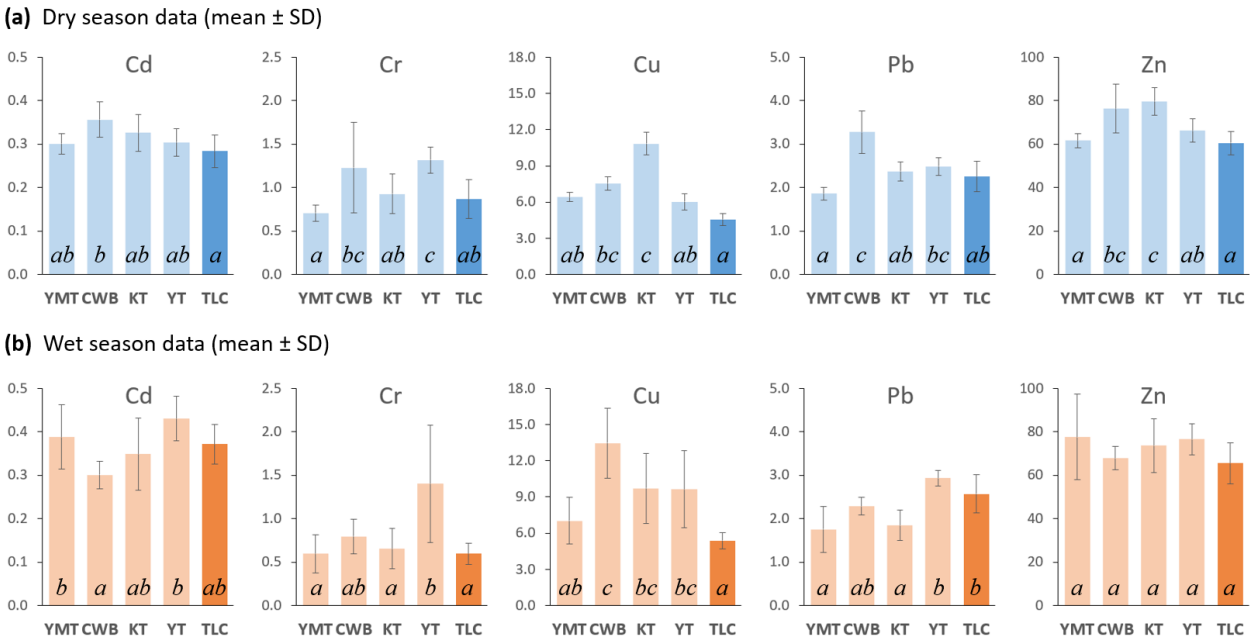

Figure 3.4. Tissue burden concentrations (µg g^{-1} dry weight) of cadmium (Cd), chromium (Cr), copper (Cu), lead (Pb) and zinc (Zn) in *Perna viridis* assessed at the five sites (YMT, CWB, KT, YT and TLC) in the **(a)** dry season and **(b)** wet season (n = 10). Please refer to Figure 3.1 for the site abbreviations. The darker bars indicate the reference site. Significant pairwise site differences are indicated by different italic small letters (Kruskal-Wallis *H* test followed by Dunn's multiple comparisons, $p < 0.05$).

Table 3.2. Results of Kruskal-Wallis *H* test with sequential Bonferroni correction and post hoc Dunn's multiple comparisons for the spatial difference of pollutants in *Perna viridis* among the five sites (YMT, CWB, KT, YT and TLC) in the **(a)** dry season and **(b)** wet season. Different italic small letters indicate significantly different pollutant concentrations among sites ($p < 0.05$). The results of pairwise comparisons are overlaid in Figures 3.3–3.4. Please refer to Figures 3.1–3.4 for the abbreviations of sites and pollutants.

Kruskal-Wallis *H* test				Dunn's multiple comparisons				
Pollutant	Degree of freedom	*H* value	*p* value	YMT	CWB	KT	YT	TLC
(a) Dry season								
LMW PAHs	4	24.337	< 0.001	*c*	*bc*	*ab*	*bc*	*a*
HMW PAHs	4	32.569	< 0.001	*bc*	*ab*	*ab*	*c*	*a*
Cd	4	14.558	0.006	*ab*	*b*	*ab*	*ab*	*a*
Cr	4	31.263	< 0.001	*a*	*bc*	*ab*	*c*	*ab*
Cu	4	43.698	< 0.001	*ab*	*bc*	*c*	*ab*	*a*
Pb	4	34.376	< 0.001	*a*	*c*	*ab*	*bc*	*ab*
Zn	4	31.327	< 0.001	*a*	*bc*	*c*	*ab*	*a*
(b) Wet season								
LMW PAHs	4	20.791	< 0.001	*b*	*ab*	*ab*	*b*	*a*
HMW PAHs	4	27.371	< 0.001	*ab*	*a*	*b*	*b*	*a*
Cd	4	21.126	< 0.001	*b*	*a*	*ab*	*b*	*ab*
Cr	4	23.903	< 0.001	*a*	*ab*	*a*	*b*	*a*
Cu	4	30.696	< 0.001	*ab*	*c*	*bc*	*bc*	*a*
Pb	4	30.075	< 0.001	*a*	*ab*	*a*	*b*	*b*
Zn	4	9.147	0.058	*a*	*a*	*a*	*a*	*a*

Table 3.3. Principal component analysis (PCA) for the tissue burden data of pollutants in *Perna viridis* in the **(a)** dry season and **(b)** wet season summarised in Figures 3.3–3.4 (7 variables × 10 tissue samples × 5 sites per season). Reported parameters include eigenvalues of five principal components (PC1 to PC5) and their contribution to the total variation, and eigenvectors of the seven variables of pollutants (LMW PAHs, HMW PAHs, Cd, Cr, Cu, Pb and Zn). Please refer to Figures 3.3–3.4 for the abbreviations of pollutants.

	PC1	PC2	PC3	PC4	PC5
(a) Dry season					
Eigenvalue	2.95	1.41	1.06	0.72	0.43
% Variation	42.1	20.2	15.2	10.3	6.20
% Cumulative variation	42.1	62.3	77.4	87.8	94.0
Eigenvector					
LMW PAHs	–0.058	0.627	–0.336	0.595	–0.354
HMW PAHs	–0.138	0.679	–0.105	–0.459	0.545
Cd	–0.467	–0.137	0.011	0.449	0.403
Cr	–0.353	0.261	0.564	–0.249	–0.512
Cu	–0.363	–0.156	–0.596	–0.392	–0.377
Pb	–0.489	–0.012	0.367	0.129	0.057
Zn	–0.515	–0.186	–0.259	–0.025	0.089
(b) Wet season					
Eigenvalue	2.58	1.44	1.17	0.74	0.54
% Variation	36.9	20.6	16.7	10.6	7.80
% Cumulative variation	36.9	57.5	74.1	84.7	92.5
Eigenvector					
LMW PAHs	–0.206	0.502	–0.448	0.496	–0.402
HMW PAHs	–0.383	0.482	0.093	–0.009	0.631
Cd	0.425	–0.240	–0.441	–0.276	0.364
Cr	–0.500	–0.187	0.119	0.475	0.006
Cu	–0.278	0.174	0.757	–0.027	–0.158
Pb	–0.341	–0.607	0.036	0.195	–0.153
Zn	–0.432	0.154	–0.090	–0.643	–0.510

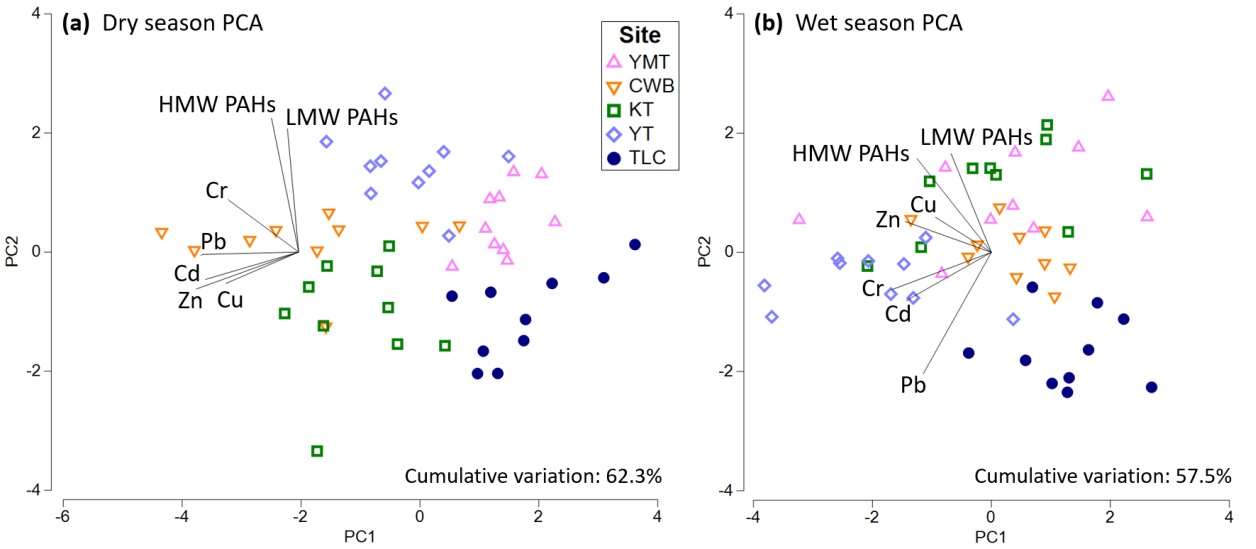

Figure 3.5. Graphical presentation of the first two principal components (PC1 and PC2) to compress the variation of the seven variables of pollutants in *Perna viridis* into two dimensions, among the five sites in the **(a)** dry season and **(b)** wet season. Eigenvectors of the seven variables in PC1 and PC2 are visualised on the plots. The full results of principal component analysis (PCA) are provided in Table 3.3. Please refer to Figures 3.1–3.4 for the abbreviations of sites and pollutants.

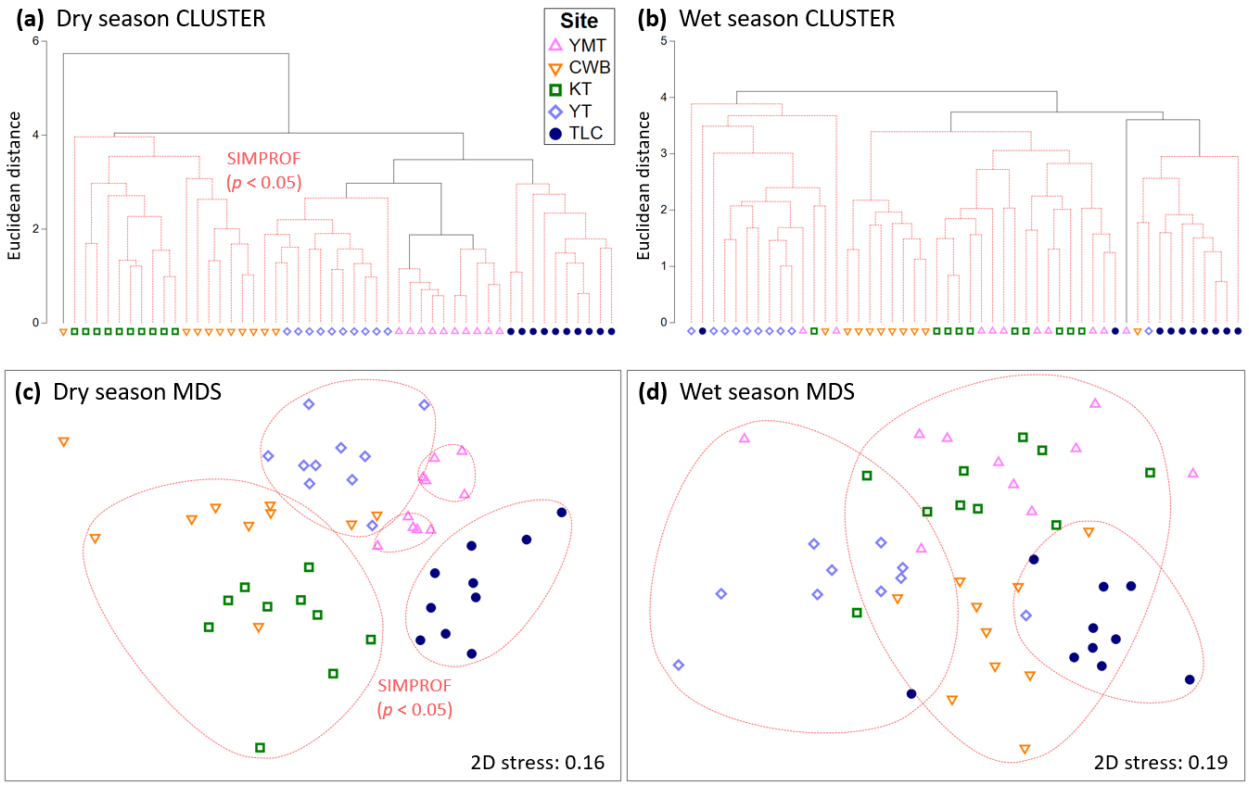

Figure 3.6. Hierarchical cluster analysis (CLUSTER) for **(a)** 50 tissue samples of *Perna viridis* collected from the five sites (10 replicates per site) in the dry season and **(b)** 50 other tissue samples in the wet season. Please refer to Figure 3.1 for the site abbreviations. The two resemblance matrices were constructed using Euclidean distance of the seven variables of pollutants reported in Figures 3.3–3.4. Significantly dissimilar groups among samples were identified by the black cluster lines using similarity profile analysis with 9999 permutations (SIMPROF; $p < 0.05$). Statistically similar samples are grouped in the same bunches of red dashed lines. The SIMPROF groups are overlaid on the plots of non-metric multi-dimensional scaling (nMDS) for the same resemblance matrices obtained in the **(c)** dry season and **(d)** wet season.

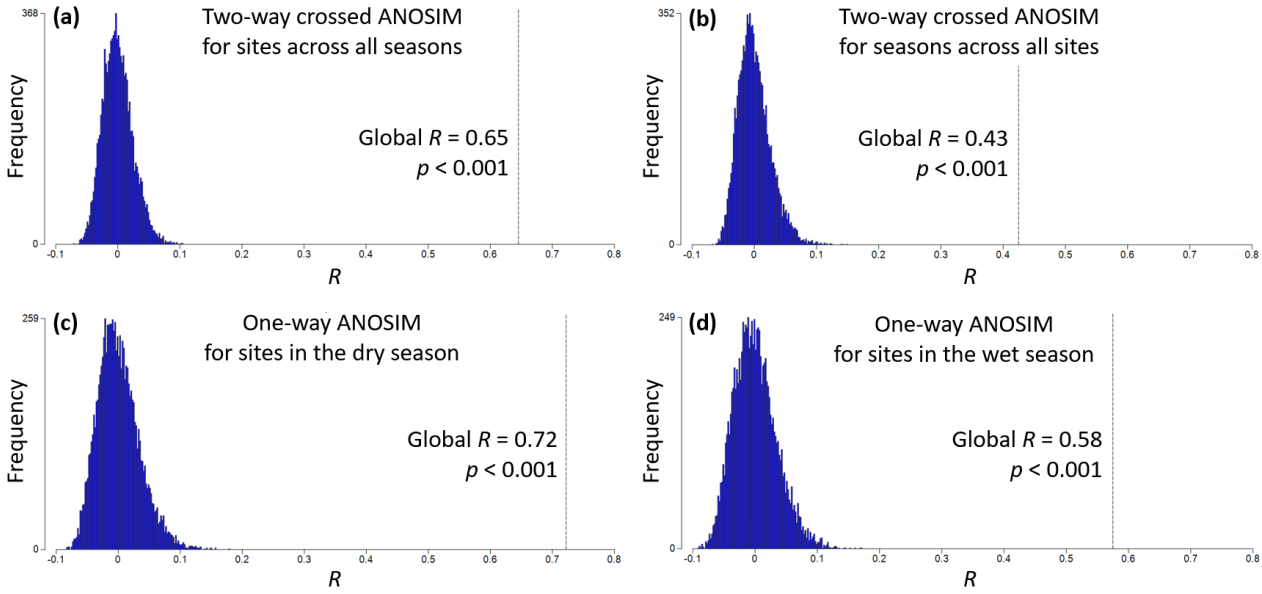

Figure 3.7. Global test results of two-way crossed analysis of similarity (ANOSIM) for **(a)** the five sites across all seasons and **(b)** the two seasons across all sites, and of one-way ANOSIM for the five sites separately in the **(c)** dry season and **(d)** wet season, based on Euclidean distance with 9999 permutations. The one-way ANOSIM in each season was followed by post hoc pairwise ANOSIM to determine the dissimilarity in all pairs of sites (see Table 3.4). Please refer to Figures 3.3–3.4 for the seven variables of pollutants in *Perna viridis* used in ANOSIM.

Table 3.4. Results of pairwise ANOSIM among the five sites in the **(a)** dry season and **(b)** wet season. A higher value of *R* indicates higher dissimilarity between two sites, in terms of the tissue levels of pollutants in *Perna viridis* (see Figures 3.3–3.4). The strength of *R* is indicated in a greyscale gradient. Please refer to Figure 3.1 for the site abbreviations.

		YMT (western)	CWB (central)	KT (central)	YT (eastern)
(a)	Dry season				
	CWB (central)	$R = 0.70, p < 0.001$			
	KT (central)	$R = 0.81, p < 0.001$	$R = 0.50, p < 0.001$		
	YT (eastern)	$R = 0.90, p < 0.001$	$R = 0.48, p < 0.001$	$R = 0.84, p < 0.001$	
	TLC (reference)	$R = 0.75, p < 0.001$	$R = 0.75, p < 0.001$	$R = 0.93, p < 0.001$	$R = 0.89, p < 0.001$
(b)	Wet season				
	CWB (central)	$R = 0.61, p < 0.001$			
	KT (central)	$R = 0.06, p = 0.13$	$R = 0.42, p < 0.001$		
	YT (eastern)	$R = 0.52, p < 0.001$	$R = 0.66, p < 0.001$	$R = 0.54, p < 0.001$	
	TLC (reference)	$R = 0.60, p < 0.001$	$R = 0.80, p < 0.001$	$R = 0.79, p < 0.001$	$R = 0.76, p < 0.001$

Table 3.5. Results of similarity percentages analysis (SIMPER) for the **(a)** dry season and **(b)** wet season, reporting the percent contribution of the topmost three variables leading to the dissimilarity in each pair of sites and their average squared distance (SqD). Please refer to Figure 3.1 for the site abbreviations.

		YMT (western)	CWB (central)	KT (central)	YT (eastern)
(a)	Dry season				
	CWB (central)	Pb, 38.6% Cr, 20.8% Zn, 16.7% (SqD = 19.03)			
	KT	Cu, 24.0%	Pb, 21.1%		

	(central)	Zn, 23.4%	Cr, 16.9%		
		LMW PAHs, 18.2%	LMW PAHs, 16.7%		
		(SqD = 15.24)	(SqD = 14.99)		
		Cr, 39.0%	Cd, 21.1%	Cu, 28.1%	
	YT	Pb, 17.6%	Pb, 19.7%	HMW PAHs, 21.1%	
	(eastern)	HMW PAHs, 16.2%	Zn, 17.4%	Zn, 14.0%	
		(SqD = 9.95)	(SqD = 12.76)	(SqD = 16.15)	
		LMW PAHs, 35.2%	Cd, 19.3%	Cu, 41.3%	HMW PAHs, 40.9%
	TLC	HMW PAHs, 20.4%	Pb, 18.5%	Zn, 20.7%	LMW PAHs, 17.1%
	(reference)	Cd, 12.4%	Zn, 16.3%	Cd, 13.2%	Cr, 15.7%
		(SqD = 10.57)	(SqD = 22.95)	(SqD = 20.30)	(SqD = 15.52)
(b)	Wet season				
		Cu, 23.1%			
	CWB	LMW PAHs, 18.8%			
	(central)	Zn, 17.5%			
		(SqD = 16.03)			
		Zn, 27.8%	LMW PAHs, 18.5%		
	KT	Cd, 21.4%	Cu, 18.5%		
	(central)	Cu, 13.3%	Cd, 17.8%		
		(SqD = 11.42)	(SqD = 10.27)		
		Pb, 29.0%	Cd, 25.4%	Cr, 29.3%	
	YT	Cr, 28.9%	Cr, 21.1%	Pb, 25.3%	
	(eastern)	Zn, 13.3%	LMW PAHs, 15.6%	Cd, 18.3%	
		(SqD = 18.15)	(SqD = 15.42)	(SqD = 15.66)	
		LMW PAHs, 23.9%	Cu, 40.2%	HMW PAHs, 31.6%	HMW PAHs, 25.5%
	TLC	Zn, 21.3%	HMW PAHs, 16.9%	Pb, 15.2%	Cr, 25.2%
	(reference)	Pb, 21.1%	LMW PAHs, 14.5%	Cu, 14.2%	LMW PAHs, 17.1%
		(SqD = 16.74)	(SqD = 13.70)	(SqD = 16.28)	(SqD = 19.33)

Chapter 4: Development of a multiple biomarker approach using mussels for pollution biomonitoring

4.1 Introduction

The presence of pollutants in environments, even at high concentrations, do not necessarily indicate bioavailability. In cases where pollutants are bioavailable, they do not necessarily induce any adverse biological effects. Assessing environmental vulnerability through chemical measurements alone is therefore of limited health or ecological relevance, unless such data can be directly linked to biological responses (Becher & Bjerseth, 1987; Zheng & Richardson, 1999; Karlsson & Viklander, 2008; Shanbehzadeh *et al*., 2014; Avellan *et al*., 2022). In this connection, the use of biomarkers has been incorporated into marine pollution assessments worldwide to evaluate the biological impacts upon exposure to various pollutants (Nicholson & Lam, 2005; Lionetto *et al*., 2019; Lomartire *et al*., 2021). Biomarkers can be broadly divided into three categories in terms of the purpose of prognosis, namely (1) biomarkers of exposure, e.g. cellular defence mechanisms against xenobiotics, (2) biomarkers of effect, e.g. cellular damage caused by xenobiotics, and (3) biomarkers of growth potential, e.g. biological indices that are prognostic to the growth efficiency.

The strategy of multiple biomarkers is recommended to cope with the situations of mixed pollutants, which are common in urban coastal waters with diverse pollution sources. However, the multi-biomarker approach could be costly, in particular for routine monitoring purposes. Moreover, the responses of biomarkers are often nonspecific that can be induced by more than one type of pollutants and influenced by environmental factors. It is therefore important, but could be challenging, to identify one or a small group of biomarker(s) that can accurately indicate the biological impacts of mixed pollutants on selected organisms, among which mussels represent a popular group of model species in marine biomonitoring programmes worldwide owing to their filter-feeding and sessile nature (Saavedra & Bachère, 2006; Campos *et al*., 2012; Świacka *et al*., 2019; López-Pedrouso *et al*., 2020). More details and rationale for the use of biomarkers and mussels in marine pollution assessments have been provided in Chapter 2. The present Chapter aimed to develop a multiple biomarker approach for pollution biomonitoring based on the green-

lipped mussel *Perna viridis*, a common marine species in the Indo-Pacific region. The work on biomarkers was carried out in Victoria Harbour, Hong Kong, where the tissue concentrations of pollutants in *P. viridis* were analysed in Chapter 3. The mussels were confirmed to contain polycyclic aromatic hydrocarbons of low molecular weight (LMW PAHs) and high molecular weight (HMW PAHs), as well as cadmium (Cd), chromium (Cr), copper (Cu), lead (Pb) and zinc (Zn). Nine biomarkers from the three categories of exposure, effect and growth potential were selected and determined in the same mussels to investigate the biological effects of these pollutants on *P. viridis*.

Four cellular biomarkers of exposure were proposed, namely superoxide dismutase (SOD), catalase (CAT), glutathione (GSH) and acetylcholinesterase (AChE). SOD and CAT are antioxidant enzymes that protect cells from oxidative damage caused by reactive oxygen species. SOD catalyses the transformation of superoxide into less reactive species such as hydrogen peroxide (H_2O_2), which is readily decomposed to water by CAT (Weydert & Cullen, 2010). GSH is a tripeptide antioxidant that modulates cellular homeostasis and neutralises reactive oxygen species via conversion to its oxidised state known as glutathione disulphide (Aquilano *et al*., 2014). The mechanisms of SOD, CAT and GSH are centred around oxidative stress, and increases in their activities or concentrations have been reported in marine organisms upon exposure to POPs and heavy metals (Cheung *et al*., 2001, Cheung *et al*., 2002; Geret *et al*., 2008; Boudjema *et al*., 2014; Trevisan *et al*., 2014). Another proposed biomarker, AChE, is an enzyme that hydrolyses the neurotransmitter acetylcholine and is particularly sensitive to neurotoxic POPs such as pesticides, which inhibit the activity of AChE (Juhel *et al*., 2017). However, interestingly, suppression and promotion of AChE have both been reported in marine organisms exposed to heavy metals under different exposure conditions (Bainy *et al*., 2006 and references therein).

The use of these biomarkers of exposure were accompanied by three biomarkers of effect at the cellular level, namely lysosomal destabilisation (LysD), micronucleus frequency (MN) and lipid peroxidation (LPx). LysD can be induced by sequestration of xenobiotics such as POPs and heavy metals, and has been widely used to indicate cell integrity based on histology of lysosomes (Nicholson, 2003a, Fang, *et al*., 2008b; Fang, *et al*., 2008c). MN is a biomarker of genotoxicity which quantifies the occurrence of extra secondary nuclei resulting from chromosomal damage

(Siu *et al*., 2008; Liu *et al*., 2014), while LPx refers to the process of oxidative degradation of lipids into lipid peroxides in the cell membrane that can be inflicted by reactive oxygen species (Cheung *et al*., 2001, Cheung *et al*., 2002, Cheung *et al*., 2004; Juhel *et al*., 2017). Furthermore, two biomarkers of growth potential were used to link the pollution-induced cellular stress to growth of the individual, namely the nucleic acid ratio of RNA to DNA (R:D) at the molecular level and total energy reserve (Et) at the tissue level. A higher value of R:D indicates a greater potential of growth, since the amount of DNA is relative stable, but the quantity of RNA is associated with protein synthesis and can vary in different environmental conditions (Yeung *et al*., 2016). As for Et, the potential energy available for growth can be derived from the total energy content of lipids, proteins and glycogen, and is indicative of the health status (Yeung *et al*., 2016).

Overall, the biomarker responses of SOD, CAT, GSH, AChE, LysD, MN, LPx, R:D and Et to the detectable pollutants of LMW PAHs, HMW PAHs, Cd, Cr, Cu, Pb and Zn in *P. viridis* were evaluated using univariate and multivariate statistical methods. Our goal was to identify the most suitable biomarkers, and the optimal subsets, to explain the variability of the whole suite of biomarkers and of the mixed pollutants.

4.2 Methods and materials

4.2.1 Experimental design

Pollution biomonitoring in Victoria Harbour, Hong Kong, was carried out in the dry season and wet season of 2019, using a transplantation approach on *P. viridis*. The rationale and sampling plan have been described in Chapter 3 and Figure 3.2. In brief, all mussels were collected from the reference site, Tung Lung Chau (TLC), and redeployed at four other sites within Victoria Harbour, namely Yau Ma Tei (YMT), Causeway Bay (CWB), Kwun Tong (KT) and Yau Tong (YT), in addition to TLC as the control group. The redeployment lasted five weeks, after which all mussels were retrieved and transported to the laboratory. One hundred mussels from each site were processed. The shell length of each mussel was measured. The valves were pried apart by 5 mm and haemolymph (0.8 mL) was freshly extracted from the adductor muscle. Each mussel was then thoroughly opened to collect hepatopancreas. The whole tissue and hepatopancreas were freshly

weighed. The haemolymph and hepatopancreas samples were used for biomarkers in this Chapter, while the remaining tissue was used for the chemical analyses reported in Chapter 3.

The sampling plan resulted in 100 samples of haemolymph and 100 samples of hepatopancreas per site for the biological assays. These samples were homogenised and pooled by 10 to produce 10 composite samples of haemolymph and 10 composite samples of hepatopancreas per site. Each of the haemolymph composite was divided for LysD and MN. Each of the hepatopancreas composite was divided for SOD, CAT, GSH, AChE, LPx, R:D and Et. The remaining of each composite sample was kept at –80 °C as a reserve. The protocols for the biomarkers of SOD, CAT, GSH, AChE, LysD, MN, LPx, R:D and Et are provided below.

4.2.2 Superoxide dismutase (SOD)

The enzymatic activity of SOD (EC 1.15.1.1) in hepatopancreas of *P. viridis* was measured using the Solarbio SOD assay kit (BC0175, Beijing, China). The working principle is based on the reaction between nitro-blue tetrazolium and superoxide to form a product that absorbs 560 nm. This reaction is inhibited by SOD, which removes superoxide, and the SOD activity is proportional to the decrease in absorption at 560 nm. About 100 mg of tissue was homogenised in 1 mL of the provided extraction solution on ice. The homogenate was centrifuged at 12,000 × g at 4 °C for 10 min. The supernatant was used in the assay and processed with the provided reagents according to the manufacturer's instructions. The specific activity of SOD in the sample was measured at 560 nm with a SpectraMax M3 microplate reader (Molecular Devices, San Jose, CA) and expressed as U mg^{-1} in protein, which was measured in the tissue using the Quick Start Bradford protein assay kit (Bio-Rad, Hercules, CA).

4.2.3 Catalase (CAT)

The enzymatic activity of CAT (EC 1.11.1.6) in hepatopancreas of *P. viridis* was measured with the ferrithiocyanate method of Cohen *et al.* (1996), based on the removal rate of H_2O_2 by CAT. About 100 mg of tissue was homogenised in 1 mL of a 28 mM phosphate buffer at pH 7, and centrifuged at 12,000 × g at 4 °C for 10 min. An aliquot (25 µL) of the supernatant was diluted with 75 µL of deionised water and 800 µL of the phosphate buffer at pH 7. The dilued solution

was added with 100 µL of 60 mM H_2O_2 to initiate the reaction. After 0.5 and 2 min of reaction time, aliquots (100 µL) were quenched with 4 mL of 0.6 N sulphuric acid, and mixed with 1 mL of 10 mM ferrous sulphate and 400 µL of 2.5 M potassium thiocyanate for colour development. Absorbance of the solution was measured at 492 nm using the SpectraMax M3. The specific activity of CAT was calculated from the absorbance measured at the two time points following Cohen *et al*. (1996), and expressed as U mg^{-1} in protein.

4.2.4 Glutathione (GSH)

The concentration of GSH in hepatopancreas of *P. viridis* was measured with the Solarbio GSH assay kit (BC1175). The working principle is based on the reaction between GSH and 5,5'-dithiobis-2-nitrobenzoic acid (DTNB), which forms a product with absorbance at 412 nm. Homogenisation of tissue (about 100 mg) in the provided extraction solution (1 mL) was done on ice. The homogenate was centrifuged at 12,000 × g at 4 °C for 10 min, after which the supernatant was collected and processed with the provided reagents following the manufacturer's instructions. The concentration of GSH was measured at 412 nm using the SpectraMax M3 and was expressed as in µg mg^{-1} in protein.

4.2.5 Acetylcholinesterase (AChE)

The enzymatic activity of AChE (EC 3.1.1.7) in hepatopancreas of *P. viridis* was measured with the Solarbio AChE assay kit (BC2025). The working principle is based on the catalysed hydrolysis of acetylcholine by AChE to form thiocholine, which reacts with DTNB, and the reaction product absorbs 412 nm. About 100 mg of tissue was homogenised in 1 mL of the provided extraction solution on ice and centrifuged at 12,000 × g at 4 °C for 10 min. The supernatant was used in the assay and added with the provided reagents according to the manufacturer's instructions. The specific activity of AChE was measured at 412 nm using the SpectraMax M3 and was expressed as U mg^{-1} in protein.

4.2.6 Lysosomal destabilisation (LysD)

The haemolymph extracted from *P. viridis* was diluted by 50% in a calcium- and magnesium-free saline (CMFS). This suspension of haemocytes was immediately processed for LysD using the

neutral red assay (Ringwood *et al*., 2003; Fang, *et al*., 2008). The primary stock of neutral red (NR) was made by dissolving 4 mg of the NR stain (Sigma-Aldrich N4638, Merck, Darmstadt, Germany) in 1 mL of dimethyl sulfoxide. A further dilution of 20 µL of the primary stock to 2 mL in CMFS produced the NR working solution. The cell suspension was added with the NR working solution at a 1:1 ratio and agitated in a light-proof humidified chamber with ice for 60 min, after which 50 µL of cells with stained lysosomes were spread on a glass slide and mounted with a coverslip. At least 100 cells were observed under a light microscope at 400× magnification. The ratio of destabilised cells (lysosomes burst and leaking NR) to stable cells (NR intact within lysosomes) was counted as LysD.

4.2.7 Micronucleus frequency (MN)

The MN assay was performed on the haemolymph extracted from *P. viridis* using a method modified from Bolognesi & Fenech (2012). The suspension of haemocytes in CMFS (50 µL) was centrifuged at 1,000 rpm at 4 °C for 5 min. The supernatant was discarded, while the pellet was resuspended and fixed in 100 µL of methanol for 20 min. The fixed cells (50 µL) was spread on a glass slide, air-dried in a fume hood overnight, and stained with 100 µL of 3% Giemsa stain (Sigma-Aldrich 109204) for 10 min. The stained cells were washed with a Sorensen buffer. At least 1,000 cells were observed under a light microscope at 1,000× magnification with oil immersion to determine the ratio of cells with MN. The criteria to define MN were provided in Bolognesi & Fenech (2012).

4.2.8 Lipid peroxidation (LPx)

The extent of LPx in hepatopancreas of *P. viridis* was indicated by the concentration of malondialdehyde (MDA), which is an end product of LPx, using the Solarbio MDA assay kit (BC0025). Homogenisation of about 100 mg of tissue was performed in 1 mL of the provided extraction solution on ice, which was then centrifuged at 12,000 × g at 4 °C for 10 min. The supernatant was collected and treated with the provided reagents following the manufacturer's instructions. The concentration of MDA was measured at 532 nm using the SpectraMax M3 and was expressed as pmol mg^{-1} in wet weight of tissue.

4.2.9 Ratio of RNA to DNA (R:D)

RNA and DNA in hepatopancreas of *P. viridis* were determined using the TRIzol protocol of Triant & Whitehead (2009). About 100 mg of tissue was homogenised in 1 mL of the Invitrogen TRIzol reagent (Thermo Fisher Scientific, Waltham, MA), centrifuged at 12,000 × g at 4 °C for 10 min, and incubated at 4 °C for another 5 min. The supernatant was collected and mixed with 0.2 mL of chloroform for 3 min and centrifuged at 12,000 × g at 4 °C for 15 min, after which the upper aqueous phase was used for RNA extraction, while the interphase and lower organic phase were used for DNA extraction.

The aqueous phase was collected and mixed with 0.5 mL of isopropanol for 10 min to precipitate RNA. The solution was centrifuged at 12,000 × g at 4 °C for 10 min. The supernatant was discarded, while the pellet was resuspended in 1 mL of 75 % ethanol for cell lysis and centrifuged at 7,500 × g at 4 °C for 5 min. The supernatant was discarded. The remaining pellet was air-dried for 10 min, resuspended in 50 µL of RNase-free water containing 0.1 mM ethylenediaminetetraacetic acid (AM9912, Thermo Fisher Scientific, Waltham, MA) and 0.5% sodium dodecyl sulphate. The mixture was incubated at 60 °C for 10 min, after which 2 µL was measured for absorbance at 260 nm with a Nanodrop One spectrometer (Thermo Fisher Scientific, Waltham, MA) to determine the concentration of RNA (ng μL^{-1}). The purity of RNA was confirmed to be high, as indicated by the absorbance ratio of 260 nm to 280 nm that was determined to be around 2.0.

DNA was extracted from the interphase and organic phase, which were mixed with 250 µL of a back extraction buffer containing 4 M guanidine thiocyanate, 50 mM sodium citrate and 1 M tris. The solution was incubated at 4 °C for 10 min, and centrifuged at 13,200 rpms at 4 °C for another 15 min. The upper layer was discarded, while the lower layer was mixed with 100% isopropanol in a 1:1 ratio, incubated at −80 °C overnight, and then centrifuged at 13,200 rpms at 4 °C for 15 min. The supernatant was discarded. The pellet was washed in 70% ethanol by pipetting up and down, and then the ethanol was removed. The washed pellet was dried in air for 5 min, and dissolved in a 50 µL solution of 10 mM tris and 0.1 mM ethylenediaminetetraacetic acid at pH 8. The concentration of DNA in the solution (2 µL) was measured at 260 nm using the Nanodrop One (ng μL^{-1}). The absorbance ratio of 260 nm to 280 nm was around 1.8 and thus the purity of DNA was regarded high. The concentration ratio of RNA to DNA yielded R:D.

4.2.10 Total energy reserve (Et)

The total energy content of lipids, proteins and glycogen in hepatopancreas was used to indicate Et of *P. viridis*. The concentration of lipids was determined in the Sulphophosphovanillin assay following Gessner & Neumann (2005). About 100 mg of tissue was soaked in 7 mL of methanol and chloroform (2:1) overnight to extract lipids. The extract (5 mL) was transferred to another glass tube, mixed with 1 mL of 0.9% sodium chloride, and centrifuged at 1,720 × g for 15 min. The upper aqueous layer was discarded. The glass tube's inner wall was gently rinsed with a 2 mL solution of methanol, chloroform and water (2:47:48). The rinsing solution, left on top of the extract, was discarded. The remaining lower layer was blown to dryness using a nitrogen stream, added with 1 mL of chloroform, blown to dryness again, and then resuspended in 1 mL of chloroform. An aliquot (100 µL) was transferred to a new tube, blown to dryness, and resuspended in 200 µL of sulphuric acid, which was heated at 100 °C for 10 min, and let cool at 20 °C for 5 min. The solution was mixed with 2.5 mL of a phosphoric acid-vanillin reagent (85% phosphoric acid and 0.6% vanillin) and incubated for 60 min, after which the lipid content was measured as cholesterol equivalents at 528 nm using the SpectraMax M3 and were converted into µg mg^{-1} in wet weight of tissue.

The concentration of proteins was determined using the Bio-Rad Quick Start Bradford kit. About 100 mg of tissue was homogenised in 1 mL of a lysis buffer containing 42% urea, 15% thiourea and 0.5% tris. The solution was incubated on ice for 10 min to solubilise protein, centrifuged at 13,000 × g at 4 °C for 5 min, and remained on ice for another 15 min. The supernatant was used in the Bradford assay and processed with the provided reagents following the manufacturer's instructions. The protein content in the solution was measured at 595 nm using the SpectraMax M3 and were converted into µg mg^{-1} in wet weight of tissue. The value of Et was derived from the concentrations of lipids, proteins and glycogen, where the glycogen content was assumed to be 40 µg mg^{-1} in wet tissue of *P. viridis* (Yeung *et al*., 2016). These concentrations were converted into energy contents, using the energy equivalents of lipids (39.5 J mg^{-1}), proteins (24 J mg^{-1}) and glycogen (17.5 J mg^{-1}) provided by Verslycke *et al.* (2004), and summed to yield Et that was expressed as J mg^{-1} in wet weight of tissue.

4.2.11 Univariate statistical analysis

The biomarker levels of SOD, CAT, GSH, AChE, LysD, MN, LPx, R:D and Et in *P. viridis* were compared among sites in the dry and wet seasons. Most of the datasets, even after data transformations, did not fulfil the assumptions of normality or homogeneity of variance required for the analysis of variance. The non-parametric Kruskal-Wallis *H* test was therefore used to determine the site effect on each biomarker. There were 18 rounds of *H* test required for nine biomarkers in two seasons. The potential family-wise Type I error associated with this multiple testing procedure was reduced by using the sequential Bonferroni correction, where the lowest *p* value obtained among the 18 rounds was tested at $\alpha/c = 0.0028$, with the second lowest tested at $\alpha/(c - 1) = 0.0029$, and the third lowest tested at $\alpha/(c - 2) = 0.0031$, and so on, where the significant level (α) and correction factor (c) were set to be 0.05 and 18, respectively (Fang *et al*., 2017). The sequential correction continued until a non-significant result was detected. Kruskal-Wallis *H* test, if significant among sites, was followed by Dunn's pairwise comparisons as a post hoc procedure at $\alpha = 0.05$. The above statistical tests were carried out with the software SigmaPlot 14.0 (Systat Software, Palo Alto, CA).

4.2.12 Multivariate statistical analyses

Nine variables of biomarkers, namely SOD, CAT, GSH, AChE, LysD, MN, LPx, R:D and Et, in *P. viridis* at the five sites were separately analysed for the dry season and wet season (10 samples × 5 sites = 50 samples per season) using the multivariate statistical software PRIMER 7 (PRIMER-e, Auckland, New Zealand). Strong inter-correlations did not exist among the variables ($\rho < 0.43$ in Spearman's correlation test). Each variable was transformed by a square root and normalised to a common dimensionless scale by subtracting the mean and being divided by the standard deviation (SD). The normalised data were converted into Euclidean distance and subject to Principal component analysis (PCA), in which the first and second principal components (PC1 and PC2, respectively) were used to project the nine-dimensional cloud of data on a two-dimensional plane.

The pairwise similarities among the 50 samples per season were arranged as a resemblance matrix of Euclidean distance, which was used in hierarchical cluster analysis (CLUSTER, group-average linkage) combined with similarity profile analysis (SIMPROF) to identify significantly dissimilar groups *a posteriori* among the 50 samples at $p < 0.05$ under 9999 permutations (Clarke *et al*., 2008). Moreover, non-metric multidimensional scaling (nMDS) was employed to visualise the similarity rankings among these samples in two dimensions. The nMDS stress level, with a range of 0–1, indicates the extent of distortion from reducing the dimensionality into lower dimensions. A lower stress level shows a better fit, where stress < 0.2 is generally considered acceptable. The nMDS plots were overlaid with the corresponding SIMPROF groups.

The similarity matrices of biomarkers (SOD, CAT, GSH, AChE, LysD, MN, LPx, R:D and Et) determined in *P. viridis* in the dry and wet seasons were linked to the tissue burden levels of seven detectable pollutants, namely LMW PAHs, HMW PAHs, Cd, Cr, Cu, Pb and Zn, in the same mussels reported in Chapter 3. The routine for comparing resemblance matrices (RELATE) was used to assess the concordance of inter-sample similarity between the patterns of biomarkers and pollutants in each season, based on Spearman's rank correlation under 9999 permutations (Clarke & Gorley, 2016). The RELATE analysis was followed by the routine for linking of biota to environment (BIOENV) to identify the most sensitive biomarker or subset of biomarkers that explained the highest variability of the whole suite of biomarkers, and to derive the optimal combination of biomarkers that provided the best match to the similarity pattern of pollutants and vice versa (Clarke *et al*., 2008). Spearman's rank correlation coefficient (ρ) was used as the 'matching' statistic, with a range of 0–1, where a highest ρ value indicated a better match. The best three subsets of maximum four variables were solved from all possible combinations.

4.3 Results

4.3.1 Univariate statistical results

In addition to the chemical data of PAHs, PCBs, OCPs and heavy metals reported in Chapter 3, the biological responses of the same mussels were determined in the present Chapter. The biological data of *P. viridis* redeployed at the five study sites in Victoria Harbour in the dry season and wet season are provided in Figure 4.1. Investigated parameters included four biomarkers of

exposure, namely SOD (99.8–254 U mg^{-1}), CAT (429–684 U mg^{-1}), GSH (2.99–23.7 µg mg^{-1}) and AChE (31.3–67.4, U mg^{-1}; Figure 4.1a), three biomarkers of effect, namely LysD (0.21–0.71), MN (0.003–0.010) and LPx (51.0–112 pmol mg^{-1}; Figure 4.1b), and two biomarkers of growth potential, namely R:D (1.91–3.61) and Et (2.73–7.54 J mg^{-1}; Figure 4.1c). The mean ranges of condition index and hepatosomatic index of *P. viridis* at all sites were determined to be 0.06–0.13 and 0.11–0.17, respectively.

The results of Kruskal-Wallis *H* test revealed significant spatial effects on most of the tested biomarkers in both seasons ($p \leq 0.006$), except those for CAT and R:D in the dry season after sequential Bonferroni correction ($p = 0.292$ and 0.038, respectively; Table 4.1). Pairwise comparison among the five sites were performed with Dunn's test. For instance, *P. viridis* at the reference site TLC showed the significantly lowest levels of LysD, MN and Et but highest levels of SOD and AChE in the dry season, and the significantly lowest levels of GSH and LysD but highest levels of CAT, AChE and R:D in the wet season. The changes in mussel biological responses at other sites are summarised in Table 4.1.

4.3.2 Multivariate statistical results

PCA was used to convert the nine-dimensional data cloud of biomarkers in *P. viridis* (SOD, CAT, GSH, AChE, LysD, MN, LPx, R:D and Et) into PCs, of which the first two cumulatively accounted for 50.1% and 48.7% in the dry season and wet season, respectively (Table 4.2). In the plots of PC1 versus PC2, samples from the same sites were generally scattered closer to each other. Directions of the eigenvectors formed radial patterns, with the CWB samples generally at the centres surrounded by samples from the other sites, but the spatial patterns were caused by different combinations of biomarkers between the dry season (Figure 4.2a) and wet season (Figure 4.2a).

The CLUSTER and SIMPROF routines separated the 50 samples of multiple biomarkers into two significantly dissimilar groups, with two outliers, in the dry season ($p < 0.05$; Figure 4.3a), and the results of clustering were overlaid on the nMDS plot (2D stress = 0.19; Figure 4.3c). Seven out of ten samples of TLC (reference site) and one sample of YT formed a distinct group, while most of the other samples were clustered together in the dry season. The grouping of most TLC samples

remained in the wet season, which showed stronger spatial effects and three other significantly dissimilar groups were formed by all samples of YT, half of the KT samples, and the other KT samples plus most samples of CWB and YMT, respectively. These spatial clusters, and two outliers, in the wet season were identified by SIMPROF ($p < 0.05$; Figure 4.3b) and nMDS (2D stress = 0.19; Figure 4.3d).

The BIOENV routine was employed to determine the single best predictor and optimal subset of biomarkers that could represent the whole suite of biological responses in each season, in terms of inter-sample similarity under 9999 permutations. The selection outcomes of three topmost single predictors and subsets are listed in Table 4.3a–b, where LysD ($\rho = 0.479$) and the subset of LysD, Et, R:D and LPx ($\rho = 0.789$), and LPx ($\rho = 0.401$) and the subset of LPx, MN, CAT and SOD ($\rho = 0.789$), explained the highest variability of all tested biomarkers in the dry season and wet season, respectively. The biomarker responses (SOD, CAT, GSH, AChE, LysD, MN, LPx, R:D and Et) were interpreted with the tissue burden levels of pollutants in the same mussels (LMW PAHs, HMW PAHs, Cd, Cr, Cu, Pb and Zn; see Chapter 3). Using the RELATE routine under 9999 permutations, the inter-sample similarity of biomarkers showed significant concordance with that of chemical data in the dry season ($\rho = 0.209$, $p < 0.001$) and wet season ($\rho = 0.184$, $p < 0.001$). Furthermore, indicated in BIOENV, the variability of chemical data was best explained by LysD ($\rho = 0.200$) and the subset of LysD, GSH, AChE and R:D ($\rho = 0.331$) in the dry season (Table 4.3c), and by R:D ($\rho = 0.136$) and the subset of R:D, Et, CAT and LysD ($\rho = 0.251$) in the wet season (Table 4.3d). Vice versa, the chemical data of Cu ($\rho = 0.259$) and the subset of Cu, HMW PAHs and Cd ($\rho = 0.318$) in the dry season (Table 4.3e), and Pb ($\rho = 0.288$) and the subset of Pb, HMW PAHs and Cr ($\rho = 0.308$) in the wet season (Table 4.3f), were selected by BIOENV to provide the most optimal match to the similarity patterns of biomarkers in *P. viridis*.

Discussion on the above findings of biomarkers, along with the bioaccumulation of pollutants in *P. viridis* determined in Chapter 3, is provided as a whole in Chapter 5.

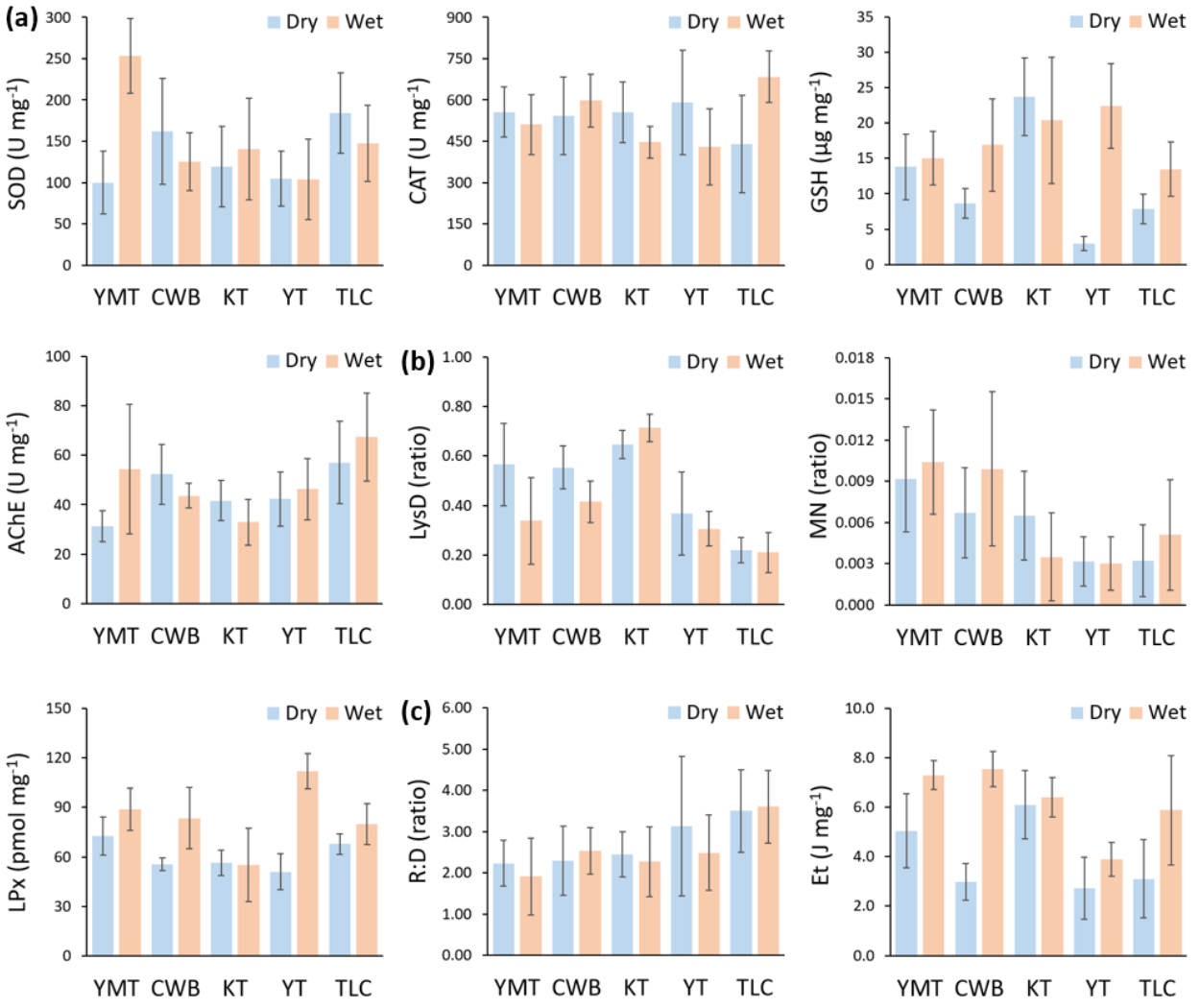

Figure 4.1. **(a)** Biomarkers of exposure, namely superoxide dismutase (SOD), catalase (CAT), glutathione (GSH) and acetylcholinesterase (AChE), **(b)** biomarkers of effect, namely lysosomal destabilisation (LysD), micronucleus frequency (MN) and lipid peroxidation (LPx), and **(c)** biomarkers of growth potential, namely ratio of RNA to DNA (R:D) and total energe reserve (Et), determined in *Perna viridis* at five sites in Hong Kong waters, namely Yau Ma Tei (YMT), Causeway Bay (CWB), Kwun Tong (KT), Yau Tong (YT) and Tung Lung Chau (TLC), in the dry season and wet season (mean ± SD; n = 10). The univariate statistical results of spatial differences among sites are reported in Table 4.1.

Table 4.1. Results of Kruskal-Wallis *H* test and post hoc Dunn's pairwise comparisons of nine biomarkers in *Perna viridis* among five sites (YMT, CWB, KT, YT and TLC) in the **(a)** dry season and **(b)** wet season. The hash sign indicates no significant difference in the *H* test after sequential Bonferroni correction. Different italic small letters indicate significantly different spatial levels among sites ($p < 0.05$). Please refer to Figure 4.1 for the abbreviations of biomarkers and sites.

Kruskal-Wallis *H* test				Dunn's multiple comparisons				
Biomarker	Degree of freedom	*H* value	*p* value	YMT	CWB	KT	YT	TLC
(a) Dry season								
SOD	4	16.058	0.003	*a*	*ab*	*ab*	*a*	*b*
CAT	4	4.952	#0.292					
GSH	4	41.155	< 0.001	*bc*	*ab*	*c*	*a*	*ab*
AChE	4	25.397	< 0.001	*a*	*b*	*ab*	*ab*	*b*
LysD	4	30.183	< 0.001	*bc*	*bc*	*c*	*ab*	*a*
MN	4	20.188	< 0.001	*b*	*ab*	*ab*	*a*	*a*
LPx	4	25.501	< 0.001	*c*	*a*	*ab*	*a*	*bc*
R:D	4	10.159	#0.038					
Et	4	25.892	< 0.001	*ab*	*a*	*b*	*a*	*a*
(b) Wet season								
SOD	4	23.782	< 0.001	*b*	*a*	*a*	*a*	*ab*
CAT	4	23.849	< 0.001	*ab*	*ab*	*a*	*a*	*b*
GSH	4	14.348	0.006	*ab*	*ab*	*ab*	*b*	*a*
AChE	4	19.663	< 0.001	*ab*	*ab*	*a*	*ab*	*b*
LysD	4	32.998	< 0.001	*ab*	*bc*	*c*	*ab*	*a*
MN	4	23.202	< 0.001	*b*	*b*	*a*	*a*	*ab*
LPx	4	27.002	< 0.001	*bc*	*ab*	*a*	*c*	*ab*
R:D	4	15.365	0.004	*a*	*ab*	*a*	*ab*	*b*
Et	4	26.123	< 0.001	*b*	*b*	*ab*	*a*	*ab*

Table 4.2. Principal component analysis (PCA) for the nine biomarkers in *Perna viridis* in the **(a)** dry season and **(b)** wet season summarised in Figures 4.1 (10 samples × 5 sites per season). Reported parameters include eigenvalues of five principal components (PC1 to PC5) and their contribution to the total variation, and eigenvectors of the variables of biomarkers (SOD, CAT,

GSH, AChE, LysD, MN, LPx, R:D and Et). Please refer to Figures 4.1 for the abbreviations of biomarkers.

	PC1	PC2	PC3	PC4	PC5
(a) Dry season					
Eigenvalue	2.99	1.52	1.00	0.91	0.73
% Variation	33.2	16.9	11.1	10.1	8.10
% Cumulative variation	33.2	50.1	61.2	71.3	79.4
Eigenvector					
SOD	0.229	–0.344	0.414	–0.604	0.227
CAT	–0.243	0.494	0.245	–0.202	–0.224
GSH	–0.356	–0.364	0.368	0.359	0.174
AChE	0.374	–0.043	0.579	0.126	0.139
LysD	–0.449	0.082	0.052	–0.055	0.495
MN	–0.403	–0.060	–0.211	–0.448	0.329
LPx	–0.05	–0.582	–0.216	–0.284	–0.461
R:D	0.329	–0.192	–0.433	0.236	0.497
Et	–0.384	–0.345	0.132	0.331	–0.187
(b) Wet season					
Eigenvalue	2.21	2.17	1.30	0.98	0.72
% Variation	24.6	24.2	14.4	10.8	8.00
% Cumulative variation	24.6	48.7	63.2	74.0	82.1
Eigenvector					
SOD	0.118	0.418	–0.025	0.639	0.021
CAT	–0.229	0.371	0.385	–0.415	0.263
GSH	0.169	–0.397	–0.087	0.112	0.885
AChE	–0.434	0.144	0.044	0.552	0.145
LysD	0.519	–0.203	0.227	0.118	–0.173
MN	0.154	0.488	–0.315	–0.288	0.245
LPx	–0.393	–0.004	–0.580	–0.059	–0.012
R:D	–0.393	–0.086	0.574	0.007	0.094
Et	0.338	0.473	0.156	0.036	0.163

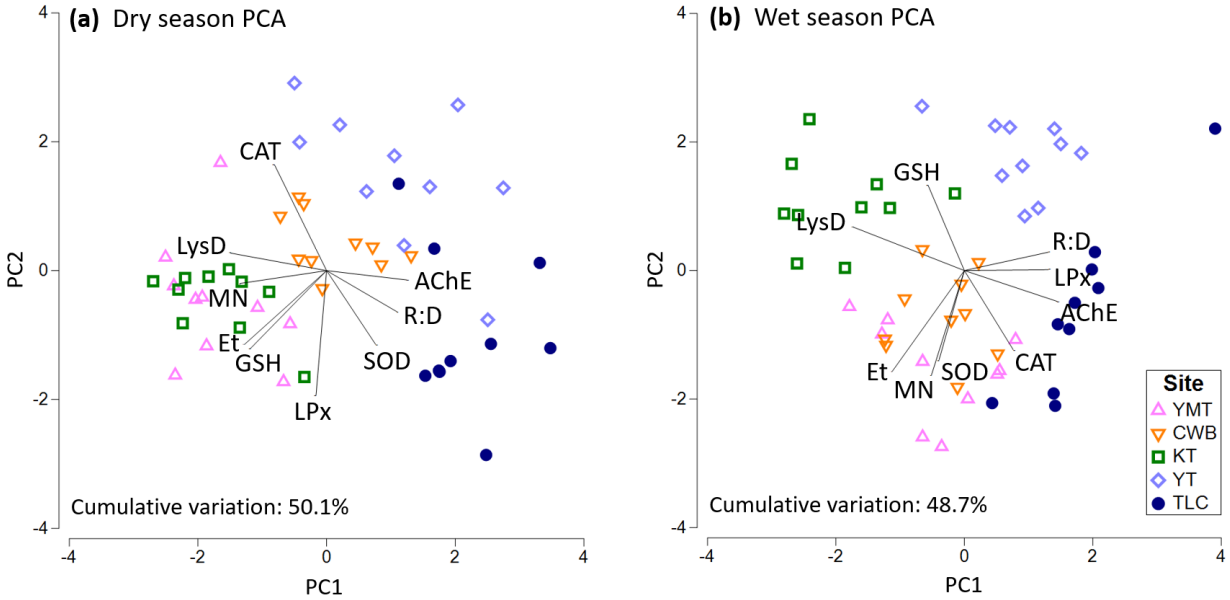

Figure 4.2. Two-dimensional plots of the principal component analysis (PCA) for biomarkers in *Perna viridis* among five sites in the **(a)** dry season and **(b)** wet season, 50 samples per season. Eigenvectors of the nine variables of biomarkers in PC1 and PC2 are visualised on the plots. The full results of PCA are provided in Table 4.2. Please refer to Figures 4.1 for the abbreviations of biomarkers and sites.

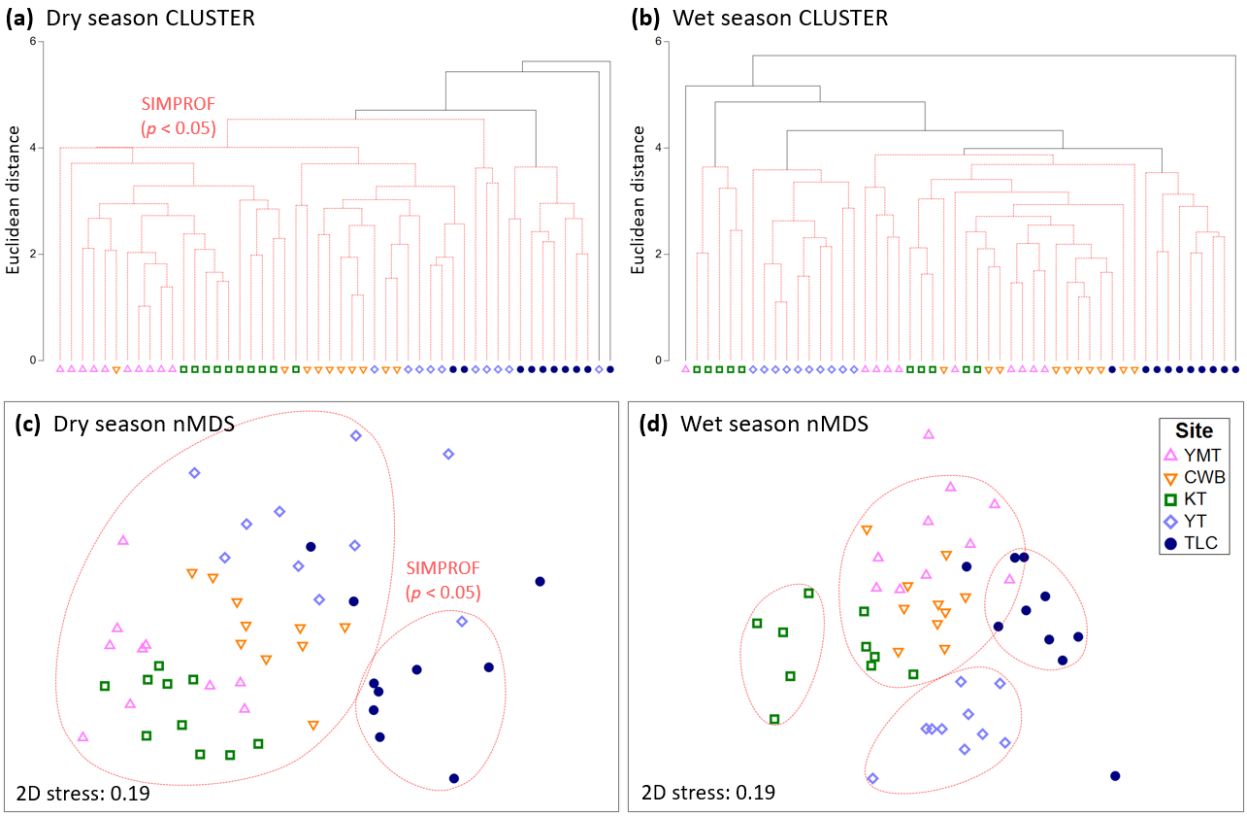

Figure 4.3. Hierarchical cluster analysis (CLUSTER) for biomarkers in *Perna viridis* among five sites in the **(a)** dry season and **(b)** wet season, 50 samples per season, based on Euclidean distance of the nine variables reported in Figure 4.1. Significantly dissimilar groups among samples were identified by the black cluster lines using similarity profile analysis with 9999 permutations (SIMPROF; $p < 0.05$). Statistically similar samples are grouped in the same bunches of red dashed lines. The groups identified by SIMPROF are overlaid on two-dimensional plots of non-metric multi-dimensional scaling (nMDS) for the same resemblance matrices obtained in the **(c)** dry season and **(d)** wet season.

Table 4.3. Results of the routine for linking of biota to environment (BIOENV) to identify **(a, b)** the single best predictor and optimal subset predictors of biomarkers that had the highest correlation with the similarity matrix, and to derive **(c, d)** the single best predictor and optimal subset predictors of biomarkers for the similarity matrix of seven pollutants determined in the same mussels, and **(e, f)** the single best predictor and optimal subset predictors of pollutants for the similarity matrix of biomarkers. The data of seven detectable pollutants, namely low molecular

weight and high molecular weight polycyclic aromatic hydrocarbons (LMW PAHs and HMW PAHs, respectively), and cadmium (Cd), chromium (Cr), copper (Cu), lead (Pb) and zinc (Zn), are reported in Chapter 3. Please refer to Figures 4.1 for the abbreviations of biomarkers. The numbers of variables (Var) was set to be 1 and ≤ 4 for the single best predictor and optimal subset predictors, respectively. Spearman's rank correlation coefficient (ρ) was used as the test statistic, with the value closer to 1 indicated a higher correlation under 9999 permutations. The best three predictors are shown for each group.

Dry season			Wet season		
Var	ρ value	Selections	Var	ρ value	Selections
(a) Optimal subset of biomarkers ($p < 0.001$)			**(b)** Optimal subset of biomarkers ($p < 0.001$)		
1	0.479	**LysD**	1	0.401	**LPx**
1	0.387	MN	1	0.383	MN
1	0.348	Et	1	0.367	LysD
4	0.789	**LysD, Et, R:D, LPx**	4	0.789	**LPx, MN, CAT, SOD**
4	0.774	LysD, MN, Et, LPx	4	0.781	LPx, MN, CAT, AChE
4	0.771	MN, R:D, SOD, GSH	4	0.766	LPx, MN, LysD, CAT
(c) Optimal subset of biomarkers to explain the variability of pollutants ($p < 0.001$)			**(d)** Optimal subset of biomarkers to explain the variability of pollutants ($p = 0.003$)		
1	0.200	**LysD**	1	0.136	**R:D**
1	0.184	GSH	1	0.132	Et
1	0.150	AChE	1	0.117	AChE
4	0.331	**LysD, GSH, AChE, R:D**	4	0.251	**R:D, Et, CAT, LysD**
3	0.313	LysD, GSH, AChE	3	0.250	R:D, Et, CAT
3	0.295	GSH, AChE, R:D	4	0.246	R:D, Et, AChE, CAT
(e) Optimal subset of pollutants to explain the variability of biomarkers ($p < 0.001$)			**(f)** Optimal subset of pollutants to explain the variability of biomarkers ($p < 0.001$)		
1	0.259	**Cu**	1	0.288	**Pb**
1	0.175	HMW PAHs	1	0.152	HMW PAHs
1	0.112	Cd	1	0.093	Cr
3	0.318	**Cu, HMW PAHs, Cd**	3	0.308	**Pb, HMW PAHs, Cr**
4	0.304	Cu, HMW PAHs, Cd, Cr	2	0.300	Pb, HMW PAHs
3	0.298	Cu, Cd, Cr	2	0.273	Pb, Cr

Chapter 5: General discussion

The green-lipped mussel *Perna viridis* used to be abundant in Victoria Harbour, Hong Kong, by the 2000s (Phillips, 1985; Phillips & Rainbow, 1988; Chan, 1988, 1989; Richardson *et al*., 2001; Liu & Kueh, 2005; Fang *et al*., 2009), but was found rare in the harbour area during a number of surveys carried out in 2018–2019 (KL Leung, pers. obs.). The actual cause of this decline in *P. viridis* remains unclear, but the possible return of fish populations due to the improved water quality under the Harbour Area Treatment Scheme (HATS) might have increased the predation pressure on mussel spats in the harbour (KMY Leung, pers. comm.). Given the limited number of native mussels, passive biomonitoring (sampling of mussels at their native sites) was not feasible in the present study, and thus we adopted the approach of active biomonitoring (retrieval of mussels transplanted from a reference site to the study sites; Felten *et al*., 2013). All transplanted *P. viridis* had a similar size and the same origin (the reference site; Figure 3.1), which minimised the biological variation among individuals such as age, reproductive stage and pre-exposure history to pollution. Moreover, the use of transplanted mussels informed the recent pollution levels at the study sites, and avoided any long-term adaptation to pollution that might have been developed by native mussels. With this active approach, the biomonitoring work was extended to sites where *P. viridis* was absent, and we have successfully completed the mussel transplantation studies at five sites in the dry season and wet season of 2019 (Figure 3.2).

Our results in Chapter 3 confirmed bioaccumulation of heavy metals, namely cadmium (Cd), chromium (Cr), copper (Cu), lead (Pb) and zinc (Zn), and polycyclic aromatic hydrocarbons with low molecular weights (LMW PAHs) and high molecular weights (HMW PAHs), in the soft tissue of P. viridis. All tested polychlorinated biphenyls (PCBs) and organochlorine pesticides (OCPs) were under the method detection limits. The integrated biological effects of these pollutants were evaluated with nine biomarkers in *P. viridis* in Chapter 4, including four biomarkers of exposure, namely superoxide dismutase (SOD), catalase (CAT), glutathione (GSH) and acetylcholinesterase (AChE), three biomarkers of effect, namely lysosomal destabilisation (LysD), micronucleus frequency (MN) and lipid peroxidation (LPx), as well as two biomarkers of growth potential, namely the nucleic acid ratio of RNA to DNA (R:D) and total energy reserve (Et). The chemical and biological datasets were analysed with multivariate statistical techniques, from which the most

suitable biomarker, and the optimal subset of biomarkers, were identified to explain the spatial pollution pattern per season.

5.1 Sources of PAHs and heavy metals

Anthropogenically released PAHs can be categorised into petrogenic or pyrogenic sources. Petrogenic PAHs are primarily LMW (2–3 fused aromatic rings) and formed in association with fossil fuels under moderate temperatures (100−300 °C) and high pressure over millions of years. In contrast, pyrogenic PAHs are primarily HMW (4–6 fused aromatic rings) and produced in incomplete combustion of fossil fuels and organic compounds at rapid and high temperatures (>350 °C) (Abdel-Shafy & Mansour, 2016). The occurrence of petrogenic PAHs in marine environments is often attributed to maritime activities, e.g., through spillage of petroleum products from vessels, while the sources of pyrogenic PAHs vary, e.g., including vehicle exhausts, waste incineration, and commercial cooking (Baek *et al*., 1991; Yang *et al*., 1998; Zhu *et al*., 2009). Any PAHs emitted into the atmosphere can bind to air particles and be deposited on the ground and in the sea. For those PAHs on the ground, a lot of them could be eventually washed into the sea by surface runoff (Galarneau, 2008; Zhao *et al*., 2008; Wang *et al*., 2013). PAHs in the sea are dispersed by water currents and bioaccumulated in marine organisms. Sediment represents another major sink of PAHs in marine environments.

Both LMW PAHs (petrogenic) and HMW PAHs (pyrogenic) were found in the soft tissue of *P. viridis* in the present study. According to their ratio, as well as the ratio of phenanthrene to anthracene, petrogenic sources appeared to be more important than pyrogenic sources for these PAHs bioaccumulated in *P. viridis* at all study sites (Figure 3.3, Table 3.1). A major petrogenic source of PAHs could be oil spillage associated with the heavy maritime traffic in the harbour and adjacent waters (Lai *et al*., 2016). Moreover, the coastal reclamation and channel dredging activities in Hong Kong waters over the years could resuspend and liberate the legacy pollutants from the sediment in the water column (Chan *et al*., 2017). These legacy pollutants include PAHs, as well as heavy metals.

Heavy metal pollution has been an environmental problem worldwide since the industrial revolution. Highly urbanised areas, including the two sides of Victoria Harbour, are filled with innumerable sources of heavy metals that could be associated with roadworks, building construction, landfills, industries and the use of motor vehicles, to name a few (Briffa *et al*., 2020). The target heavy metals serve as important materials in the modern society (e.g., Cd for alloys, paints and batteries, Cr for welding and electroplating, Cu for alloys, electronics and pipes, Pb for batteries and solders, and Zn for galvanising and die-casting) and were detected in *P. viridis* in the present study (Figure 3.4). Apart from the sediment resuspension effect, heavy metals could enter marine environments through municipal runoff, stormwater discharge, wastewater discharge and atmospheric deposition (Zhang *et al*., 1992; Nabizadeh *et al*., 2005; Al-Musharafi *et al*., 2013; Sakson *et al*., 2018).

5.2 Pollution abatement in Victoria Harbour

Compared to the biomonitoring data reported in the 1980s through 2000s, the pollution levels in Victoria Harbour have been generally alleviated, according to the tissue concentrations in *P. viridis* (Tables 1.1 and 1.2). In particular, the total quantities of PAHs and Cu in mussels in 2019 were substantially reduced by about 95% and 49%, respectively, from the levels reported in 2004–2005 (Fang *et al*., 2008a; Fang *et al*., 2009). Besides, the presence of PCBs and OCPs was confirmed in *P. viridis* back in 1998–2005 (Fang *et al*., 2009; Liu & Kueh, 2005), but the concentrations of these compounds decreased to be undetectable in the present study, apparently owing to the ban or phaseout of PCBs and OCPs in the region (Table 1.2). As for Cd, Cr, Pb and Zn, the tissue levels in *P. viridis*, however, remained similar between the earlier study in 2004–2005 (Fang *et al*., 2008a) and our work in 2019 (Table 1.1). Overall, our results from *P. viridis* indicated pollution abatement of PAHs, PCBs, OCPs and Cu in the harbour area, findings which were in line with the conclusion of water quality improvement made by other recent marine monitoring studies (Environmental Protection Department, 2020, 2021).

HATS, a large-scale wastewater collection and treatment scheme in Hong Kong, was expected to be the primary driving force to the observed pollution abatement in Victoria Harbour. Stage 1 and Stage 2A of HATS have been implemented since 2001 and 2015, respectively, and have upgraded

the wastewater treatment facilities on both sides of the harbour and converged the wastewater for a chemically enhanced primary treatment (CEPT) at the Stonecutter Island Sewage Treatment Works in the west of Victoria Harbour. CEPT involves the addition of ferric chloride and an anionic polymer as chemical coagulants in the wastewater to facilitate removal of suspended solids and sedimentation of sludge (Drainage Service Department, 2019). It has also been shown that the CEPT process can effectively reduce organic compounds and heavy metals from treated wastewater (Shewa & Dagnew, 2020), providing an explanation for the reduced pollution levels in the harbour water and thus *P. viridis* therein.

Spatial bioaccumulation pattern of pollutants

Compared to the four study sites in Victoria Harbour (YMT, CWB, KT and YT), *P. viridis* at the reference site TLC showed the lowest tissue concentrations of LMW PAHs, HMW PAHs and Cu, regardless of the season (Figures 3.3 and 3.4). The lowest levels of Cd and Zn in the dry season, and Cr in the wet season, were also found in the TLC mussels. However, the body burden of Pb in *P. viridis* was relatively high in the wet season.

The overall bioaccumulation pattern in *P. viridis* at TLC was the most dissimilar from the other study sites, based on the results of non-metric multi-dimensional scaling (nMDS) and similarity profile analysis (SIMPROF), using seven variables of LMW PAHs, HMW PAHs, Cd, Cr, Cu, Pb and Zn (Figure 3.6). The dissimilarity of TLC from other sites was more pronounced in the dry season than wet season, and could be driven by LMW PAHs and HMW PAHs, as suggested by the results of principal component analysis (PCA; Figure 3.5). Findings from these a posteriori tests were in line with those obtained a priori from analysis of similarity (ANOSIM; Table 3.4) and similarity percentages analysis (SIMPER; Table 3.5), which confirmed the relatively least polluted environment at TLC among all study sites.

Within the harbour, the body burden patterns of pollutants in *P. viridis* at YT were generally dissimilar from those at YMT, CWB and KT in both seasons, although the patterns among sites became less clear in the wet season (MDS and SIMPROF; Figure 3.6). One possible explanation is that, different from YT, the study sites YMT, CWB and KT are all located within typhoon shelters with weaker water circulation (Figure 3.1), and thus the water quality could be more alike

to each other and more influenced by surface runoff and stormwater discharge, particularly in the wet season. By contrast, the site YT is open to strong currents in the harbour that are regulated by the seasonal monsoons, namely the Kuroshio and Taiwan currents flowing from east to west in the dry season, and the Hainan current flowing from west to east in the wet season (Morton & Wu, 1975). It has been speculated that, following the Hainan current, the Pearl River estuarine water entering Victoria Harbour would bring extra nutrients and pollutants in the wet season (Watts, 1971; Ramu *et al*., 2005; Chen *et al*., 2006). However, this seasonal effect of Pearl River was not observed from our results of bioaccumulated pollutants in *P. viridis*, and its biomarker responses discussed below.

5.3 Biomarker responses to the pollutants

The biological impacts of the seven groups of pollutants were investigated using nine biomarkers in *P. viridis*, including SOD, CAT, GSH, AChE, LysD, MN, LPx, R:D and Et. In the dry season, *P. viridis* at the reference site TLC showed the highest rates of SOD and AChE but lowest levels of LysD, MN and Et, compared to the four within-harbour sites (YMT, CWB, KT and YT). In the wet season, the highest values of CAT, AChE and R:D but lowest extents of GSH and LysD were found in *P. viridis* at TLC among all sites (Figure 4.1; Table 4.1).

In line with the findings from bioaccumulation of pollutants, the overall patterns of biomarkers in the TLC mussels appeared to be dissimilar from those at the within-harbour sites, regardless of the season, as indicated in the results of MDS and SIMPROF using the nine variables of biomarkers. The changes in the biomarker responses in *P. viridis* at the within-harbour sites were more alike to each other in the dry season than in wet season (Figure 4.3). The key biomarkers driving the similarity patterns appeared to be CAT, LysD and MN in the dry season, and GSH and LysD in the wet season, as identified by PCA (Figure 4.2).

Using the routine for linking of biota to environment (BIOENV), the optimal subsets of biomarkers in *P. viridis* that best represented the overall biological responses were identified to be LysD, Et, R:D and LPx (dry season), and LPx, MN, CAT and SOD (wet season), and that best explained the bioaccumulation patterns of mixed pollutants were derived to be LysD, GSH, AChE and R:D (dry

season), and R:D, Et, CAT and LysD (wet season; Table 4.3a–d). Each of the subsets is listed in descending order of the relative contribution, with the first variable representing the single best predictor. In these BIOENV results, LysD and R:D were respectively selected in three out of the four optimal subsets of biomarkers, and were regarded as the two most suitable biomarkers in *P. viridis* for pollution monitoring purposes. Vice versa, the optimal subsets of pollutants that most influenced the overall biomarker responses were found to be Cu, HMW PAHs and Cd (dry season), and Pb, HMW PAHs and Cr (wet season; Table 4.3e–f). Selection of these pollutants were mainly driven by the differences between the reference site TLC and the within-harbour sites (Figures 3.3 and 3.4).

Based on these findings, we recommend LysD and R:D in *P. viridis* to be two core biomarkers for marine pollution monitoring in Victoria Harbour and other waters in South China. LysD is a cytohistological biomarker of effect, which quantifies the proportion of swelling or bursting of lysosomes induced by sequestration and overload of xenobiotics (Lowe *et al*., 1981; Moore, 1985; Lowe *et al*., 1995). R:D is a biomarker of growth potential at the molecular level, with the rationale that the quantity of DNA is relatively stable but that of RNA increases along with protein synthesis (Buckley *et al*., 1999; Foley *et al*., 2016). Both assays of LysD and R:D are relatively simple and low-cost compared to many other biochemical measurements, and can be readily implemented in the existing biomonitoring programmes using mussels. The responses of LysD and R:D are non-specific that can be induced by various environmental pollutants (Lowe *et al*., 1981; Danovaro *et al*., 1995; Lowe *et al*., 1995; Ringwood *et al*., 1998; Nicholson 1999b, 2001; Acosta & Lodeiros, 2001; Nicholson, 2003a; Choi *et al*., 2014; Da Ros *et al*., 2002; Hwang *et al*., 2002; Fang, *et al*., 2008c; Li *et al*., 2010; Moschino *et al*., 2016;). This non-specific nature makes the combined use of LysD and R:D a suitable screening tool to pinpoint the pollution hotspots, which can then be assessed with other more specific biomarkers and sophisticated chemical analyses to characterise the pollutants and their biological impacts.

5.4 Conclusions and implications

The present study provided a case study of active pollution biomonitoring in Victoria Harbour, Hong Kong, by means of transplantation of caged *P. viridis* from a reference site to the within-

harbour sites in two seasons. We used a multiple-biomarker approach, which has been regarded as a useful tool for assessing the health of model organisms across different levels of the biological hierarchy (Lam & Gray, 2003; Lam, 2009; Bellas *et al*., 2014; Hook *et al*., 2014; Lionetto *et al*., 2019; Lomartire *et al*., 2021). On top of the use of biomarkers, we furthermore quantified the bioaccumulated levels of major groups of chemical pollutants in the mussels. Obtained datasets of all tested biomarkers and chemical concentrations were analysed with multivariate statistical techniques, which allowed us to identify the optimal subsets of biomarkers that could best explain the overall biological responses and bioaccumulation patterns of pollutants in *P. viridis* between seasons. A better knowledge of these interrelationships among biomarkers and bioaccumulated pollutants is required for assessing the bioavailability of these pollutants and their modes of toxic action (Lionetto *et al*., 2019; Lomartire *et al*., 2021), and for developing biomarkers that can be prognostic to higher-level biological changes and provide early warning signals for routine pollution monitoring (Nicholson & Lam, 2005; Wu *et al*., 2005; Hook *et al*., 2014). As a whole, the present study identified two biomarkers in *P. viridis*, namely LysD and R:D, that could serve these purposes. Our findings are applicable to other Indo-Pacific areas where *P. viridis* is abundant.

Bibliography

Abdel-Shafy, H. I., & Mansour, M. S. M. (2016). A review on polycyclic aromatic hydrocarbons: Source, environmental impact, effect on human health and remediation. *Egyptian Journal of Petroleum*, *25*(1), 107–123.

Acosta, V., & Lodeiros, C. (2001). Evaluation of Copper Effect on Juveniles of the Green Mussel *Perna viridis* by DNA Concentration and a RNA/DNA Ratio of Abductor Muscle. *Revista Científica de Veterinaria*, *11*(6), 485–490.

Al-Musharafi, S. K., Mahmoud, I. Y., & Al-Bahry, S. N. (2013). Heavy Metal Pollution from Treated Sewage Effluent. *APCBEE Procedia*, *5*, 344–348.

Albentosa, M., Viñas, L., Besada, V., Franco, A., & González-Quijano, A. (2012). First measurements of the scope for growth (SFG) in mussels from a large scale survey in the North-Atlantic Spanish coast. *Science of the Total Environment*, *435–436*, 430–445.

Aldred, N., Ista, L. K., Callow, M. E., Callow, J. A., Lopez, G. P., & Clare, A. S. (2006). Mussel (*Mytilus edulis*) byssus deposition in response to variations in surface wettability. *Journal of the Royal Society Interface*, *3*(6), 37–43.

Alessio, H. M. (2000). Lipid peroxidation in healthy and diseased models: influence of different types of exercise. In *Handbook of Oxidants and Antioxidants in Exercise* (pp. 115–127). Elsevier Science B.V.

Alharbi, O. M. L., Basheer, A. A., Khattab, R. A., & Ali, I. (2018). Health and environmental effects of persistent organic pollutants. *Journal of Molecular Liquids*, *263*, 442–453.

Amiard-Triquet, C., & Berthet, B. (2015). Individual Biomarkers. In C. Amiard-Triquet, J.-C. Amiard, & C. Mouneyrac (Eds.), *Aquatic Ecotoxicology: Advancing Tools for Dealing with Emerging Risks* (pp. 153–182). Academic Press.

Amutha, C., Bupesh, G., Ramesh, R., Kavitha, P., & Subramanian, P. (2009). Cytochrome P450-dependent mixed function oxidases (MFO) system dynamics during the poly aromatic hydrocarbon (PAH) metabolism in green mussel *Perna viridis* (Linnaeus, 1758). *Environmental Bioindicators*, *4*(1), 97–116.

Aquilano, K., Baldelli, S., & Ciriolo, M. R. (2014). Glutathione: New roles in redox signalling for an old antioxidant. *Frontiers in Pharmacology*, *5 AUG*, 196.

Vasanthi, A. L., Revathi, P., Arulvasu, C., & Munuswamy, N. (2012). Biomarkers of metal toxicity and histology of *Perna viridis* from Ennore estuary, Chennai, south east coast of India. *Ecotoxicology and Environmental Safety*, *84*, 92–98.

Asaduzzaman, M., Noor, A. R., Rahman, M. M., Akter, S., Hoque, N. F., Shakil, A., & Wahab, M. A. (2019). Reproductive biology and ecology of the green mussel *Perna viridis*: A multidisciplinary approach. *Biology*, *8*(4), 88.

Avellan, A., Duarte, A., & Rocha-Santos, T. (2022). Organic contaminants in marine sediments and seawater: A review for drawing environmental diagnostics and searching for informative predictors. *Science of The Total Environment*, *808*, 152012.

Baek, S. O., Goldstone, M. E., Kirk, P. W. W., Lester, J. N., & Perry, R. (1991). Phase distribution and particle size dependency of polycyclic aromatic hydrocarbons in the urban atmosphere. *Chemosphere*, *22*(5–6), 503–520.

Bainy, A. C. D., Gennari de Medeiros, M. H., Mascio e, P., & de ALmeida, E. A. (2006). In vivo effects of metals on the acetylcholinesterase activity of the *Perna perna* mussel's digestive gland. *Biotemas*, *19*(1), 35–39.

Baker, P., Fajans, J. S., Arnold, W. S., Ingrao, D. A., Marelli, D. C., & Baker, S. M. (2007). Range and dispersal of a tropical marine invader, the Asian green mussel, *Perna viridis*, in subtropical waters of the southeastern United States. *Journal of Shellfish Research*, *26*(2), 345–355.

Barhoumi, B., El Megdiche, Y., Clérandeau, C., Ameur, W. Ben, Mekni, S., Bouabdallah, S., Derouiche, A., Touil, S., Cachot, J., & Driss, M. R. (2016). Occurrence of polycyclic aromatic hydrocarbons (PAHs) in mussel (*Mytilus galloprovincialis*) and eel (*Anguilla anguilla*) from Bizerte lagoon, Tunisia, and associated human health risk assessment. *Continental Shelf Research*, *124*, 104–116.

Barletta, M., Lima, A. R. A., & Costa, M. F. (2019). Distribution, sources and consequences of nutrients, persistent organic pollutants, metals and microplastics in South American estuaries. *Science of the Total Environment*, *651*, 1199–1218.

Bashnin, T., Verhaert, V., De Jonge, M., Vanhaecke, L., Teuchies, J., & Bervoets, L. (2019). Relationship between pesticide accumulation in transplanted zebra mussel (*Dreissena polymorpha*) and community structure of aquatic macroinvertebrates. *Environmental Pollution*, *252*, 591–598.

Becher, G., & Bjerseth, A. (1987). Monitoring of Environmental Chemicals. *Methods For Assessing the Effects of Mixtures of Chemicals*, 225–248.

Bellas, J., Albentosa, M., Vidal-Liñán, L., Besada, V., Franco, M. Á., Fumega, J., González-Quijano, A., Viñas, L., & Beiras, R. (2014). Combined use of chemical, biochemical and physiological variables in mussels for the assessment of marine pollution along the N-NW Spanish coast. *Marine Environmental Research*, *96*, 105–117.

Bellas, J., Hylland, K., & Burgeot, T. (2020). Editorial: New Challenges in Marine Pollution Monitoring. *Frontiers in Marine Science*, *6*, 820.

Beyer, J., Green, N. W., Brooks, S., Allan, I. J., Ruus, A., Gomes, T., Bråte, I. L. N., & Schøyen, M. (2017). Blue mussels (*Mytilus edulis spp.*) as sentinel organisms in coastal pollution monitoring: A review. *Marine Environmental Research*, *130*, 338–365.

Blackmore, G. (1998). An overview of trace metal pollution in the coastal waters of Hong Kong. *Science of the Total Environment*, *214*, 21–48.

Bolognesi, C., & Fenech, M. (2012). Mussel micronucleus cytome assay. *Nature Protocols*, *7*(6), 1125–1137.

Boudjema, K., Kourdali, S., Bounakous, N., Meknachi, A., & Badis, A. (2014). Catalase activity in brown mussels (*Perna perna*) under acute cadmium, lead, and copper exposure and depuration tests. *Journal of Marine Biology*, *2014*.

Briffa, J., Sinagra, E., & Blundell, R. (2020). Heavy metal pollution in the environment and their toxicological effects on humans. *Heliyon*, *6*(9), e04691.

Briscoe, M., Sullivan, D., Alewijn, M., Austad, J., Boison, J., Christiansen, S., Cook, J. M., De Vries, J., Indyk, H., Joseph, G., Konings, E., Krynitsky, A., Phillips, T., Popping, B., Reddy, M., & Wong, J. (2015). Determination of heavy metals in food by inductively coupled plasma-mass spectrometry: First action 2015.01. *Journal of AOAC International*, *98*(4), 1113–1120.

Brown, K. (2012). Methods for the detection of DNA adducts. *Methods in Molecular Biology*, *817*, 207–230.

Brunetti, B., & Desimoni, E. (2015). About Estimating the Limit of Detection by the Signal to Noise Approach. *Pharmaceutica Analytica Acta*, *06*(04).

Buckley, L., Caldarone, E., & Ong, T. L. (1999). RNA-DNA ratio and other nucleic acid-based indicators for growth and condition of marine fishes. *Hydrobiologia*, *401*(0), 265–277.

Calow, P., & Sibly, R. M. (1990). A Physiological Basis of Population Processes: Ecotoxicological Implications. *Functional Ecology*, *4*(3), 283.

Campos, A., Tedesco, S., Vasconcelos, V., & Cristobal, S. (2012). Proteomic research in bivalves. Towards the identification of molecular markers of aquatic pollution. *Journal of Proteomics*, *75*(14), 4346–4359.

Capolupo, M., Franzellitti, S., Kiwan, A., Valbonesi, P., Dinelli, E., Pignotti, E., Birke, M., & Fabbri, E. (2017). A comprehensive evaluation of the environmental quality of a coastal lagoon (Ravenna, Italy): Integrating chemical and physiological analyses in mussels as a biomonitoring strategy. *Science of the Total Environment*, *598*, 146–159.

Chan, H. M. (1988). A survey of trace metals in *Perna viridis* (L.)(Bivalvia: Mytilacea) from the coastal waters of Hong Kong. *Asian Marine Biology*, *5*, 89–102.

Chan, H. M. (1989). Temporal and spatial fluctuations in trace metal concentrations in transplanted mussels in Hong Kong. *Marine Pollution Bulletin*, *20*(2), 82–86.

Chan, J. P., Cheung, M. T., & Li, F. P. (1974). Trace metals in Hong Kong waters. *Marine Pollution Bulletin*, *5*(11), 171–174.

Chan, J. T. K., Leung, H. M., Yue, P. Y. K., Au, C. K., Wong, Y. K., Cheung, K. C., Li, W. C., & Yung, K. K. L. (2017). Combined effects of land reclamation, channel dredging upon the bioavailable concentration of polycyclic aromatic hydrocarbons (PAHs) in Victoria Harbour sediment, Hong Kong. *Marine Pollution Bulletin*, *114*(1), 587–591.

Chan, K. M. (1995). Concentrations of copper, zinc, cadmium and lead in rabbitfish (*Siganus oramin*) collected in Victoria Harbour, Hong Kong. *Marine Pollution Bulletin*, *31*(4–12), 277–280.

Chen, S. J., Luo, X. J., Mai, B. X., Sheng, G. Y., Fu, J. M., & Zeng, E. Y. (2006). Distribution and mass inventories of polycyclic aromatic hydrocarbons and organochlorine pesticides in sediments of the pearl river estuary and the northern South China Sea. *Environmental Science and Technology*, *40*(3), 709–714.

Cheung, C. C. C., Siu, W. H. L., Richardson, B. J., De Luca-Abbott, S. B., & Lam, P. K. S. (2004). Antioxidant responses to benzo[a]pyrene and Aroclor 1254 exposure in the green-lipped mussel, Perna viridis. *Environmental Pollution*, *128*(3), 393–403.

Cheung, C. C. C., Zheng, G. J., Lam, P. K. S., & Richardson, B. J. (2002). Relationships between tissue concentrations of chlorinated hydrocarbons (polychlorinated biphenyls and

chlorinated pesticides) and antioxidative responses of marine mussels, *Perna viridis*. *Marine Pollution Bulletin*, *45*(1–12), 181–191.

Cheung, C. C. C., Zheng, G. J., Li, A. M. Y., Richardson, B. J., & Lam, P. K. S. (2001). Relationships between tissue concentrations of polycyclic aromatic hydrocarbons and antioxidative responses of marine mussels, *Perna viridis*. *Aquatic Toxicology*, *52*(3–4), 189–203.

Cheung, S. G., & Shin, P. K. S. (2005). Size effects of suspended particles on gill damage in green-lipped mussel *Perna viridis*. *Marine Pollution Bulletin*, *51*(8–12), 801–810.

Cheung, Y. H., & Wong, M. H. (1992). Comparison of trace metal contents of sediments and mussels collected within and outside Tolo Harbour, Hong Kong. *Environmental Management*, *16*(6), 743–751.

Ching, E. W. K., Siu, W. H. L., Lam, P. K. S., Xu, L., Zhang, Y., Richardson, B. J., & Wu, R. S. S. (2001). DNA adduct formation and DNA strand breaks in green-lipped mussels (*Perna viridis*) exposed to benzo[a]pyrene: Dose- and time-dependent relationships. *Marine Pollution Bulletin*, *42*(7), 603–610.

Choi, E. H., Choi, J. K., Lee, W. Y., Yoon, J. H., Shim, N. Y., Kim, S. K., & Lim, H. J. (2014). The change of the physiological response of the *Crassostrea gigas* exposed to PAHs. *The Korean Journal of Malacology*, *30*(3), 169–175.

Cholumpai, V., Celander, M. C., & Kanchanopas-Barnette, P. (2015). Accumulation and clearance of PAHs and CYP1A levels in farmed green mussels (*Perna viridis* L.) from a coastal industrial area in Thailand. *EnvironmentAsia*, *8*(2), 109–117.

Clarke, K. R., & Gorley, R. N. . (2016). PRIMER v7: User Manual/Tutorial. In *PRIMER v7: User Manual/Tutorial*. PRIMER-e.

Clarke, K. Robert, Somerfield, P. J., & Gorley, R. N. (2008). Testing of null hypotheses in exploratory community analyses: similarity profiles and biota-environment linkage. *Journal of Experimental Marine Biology and Ecology*, *366*(1–2), 56–69.

Cohen, G., Kim, M., & Ogwu, V. (1996). A modified catalase assay suitable for a plate reader and for the analysis of brain cell cultures. *Journal of Neuroscience Methods*, *67*(1), 53–56.

Coles, J. A., Farley, S. R., & Pipe, R. K. (1994). Effects of fluoranthene on the immunocompetence of the common marine mussel, *Mytilus edulis*. *Aquatic Toxicology*, *30*(4), 367–379.

Connell, D. W., Wu, R. S. S., Richardson, B. J., Leung, K., Lam, P. S. K., & Connell, P. A. (1998). Occurrence of persistent organic contaminants and related substances in Hong Kong marine areas: An overview. *Marine Pollution Bulletin*, *36*(5), 376–384.

Da Ros, L., Meneghetti, F., & Nasci, C. (2002). Field application of lysosomal destabilisation indices in the mussel *Mytilus galloprovincialis*: Biomonitoring and transplantation in the Lagoon of Venice (north-east Italy). *Marine Environmental Research*, *54*(3–5), 817–822.

Danovaro, R., Fabiano, M., & Albertelli, G. (1995). Possible use of RNA: DNA ratio for detecting oil induced disturbance: A field report. *Chemistry and Ecology*, *11*(1), 1–10.

Davies, W. R., Siu, W. H. L., Jack, R. W., Wu, R. S. S., Lam, P. K. S., & Nugegoda, D. (2005). Comparative effects of the blue green algae *Nodularia spumigena* and a lysed extract on detoxification and antioxidant enzymes in the green lipped mussel (*Perna viridis*). *Marine Pollution Bulletin*, *51*(8–12), 1026–1033.

de Messano, L. V. R., Gonçalves, J. E. A., Messano, H. F., Campos, S. H. C., & Coutinho, R. (2019). First report of the Asian green mussel *Perna viridis* (Linnaeus, 1758) in Rio de Janeiro, Brazil: a new record for the southern Atlantic Ocean. *BioInvasions Records*, *8*(3), 653–660.

Dias, P. J., Gilg, M. R., Lukehurst, S. S., Kennington, W. J., Huhn, M., Madduppa, H. H., McKirdy, S. J., De Lestang, P., Teo, S. L. M., Lee, S. S. C., & McDonald, J. I. (2018). Genetic diversity of a hitchhiker and prized food source in the anthropocene: The asian green mussel *Perna viridis* (mollusca, mytilidae). *Biological Invasions*, *20*(7), 1749–1770.

Drainage Service Department. (2019). *Harbour Area Treatment Scheme*. https://www.dsd.gov.hk/others/HATS2A/en/index.html

Dyrynda, E. A., Pipe, R. K., Burt, G. R., & Ratcliffe, N. A. (1998). Modulations in the immune defences of mussels (*Mytilus edulis*) from contaminated sites in the UK. *Aquatic Toxicology*, *42*(3), 169–185.

Ekanath, A. E., & Menon, N. R. (1983). Mercury toxicity in two intertidal tropical marine molluscs. *Fishery Technology*, *20*(2), 84–89.

El Jourmi, L., Amine, A., Boutaleb, N., Lazar, S., & El Antri, S. (2012). Multiple Biomarker Response in the Mussel, Perna Perna To Assess the Marine Quality in the Big Casablanca Area. *Scientific Study & Research. Chemistry & Chemical Engineering, Biotechnology, Food Industry;*, *13*(4), 377–386.

Environmental Protection Department. (2020). *HATS Stage 1*. https://www.epd.gov.hk/epd/english/environmentinhk/water/cleanharbour/milestones.html

Environmental Protection Department. (2021). *Environmental Protection Interactive Centre : Marine Water Quality Monitoring Data Searching Paramater*. Environmental Protection Department, HKSAR. https://cd.epic.epd.gov.hk/EPICRIVER/marine/?lang=en%0Ahttp://epic.epd.gov.hk/EPICRIVER/marine/history/

Faggio, C., Pagano, M., Alampi, R., Vazzana, I., & Felice, M. R. (2016). Cytotoxicity, haemolymphatic parameters, and oxidative stress following exposure to sub-lethal concentrations of quaternium-15 in *Mytilus galloprovincialis*. *Aquatic Toxicology*, *180*, 258–265.

Faggio, C., Tsarpali, V., & Dailianis, S. (2018). Mussel digestive gland as a model tissue for assessing xenobiotics: An overview. *Science of the Total Environment*, *636*, 220–229.

Fang, J. K.H., Au, D. W. T., Wu, R. S. S., Zheng, G. J., Chan, A. K. Y., Lam, P. K. S., & Shin, P. K. S. (2009). Concentrations of polycyclic aromatic hydrocarbons and polychlorinated biphenyls in green-lipped mussel *Perna viridis* from Victoria Harbour, Hong Kong and possible human health risk. *Marine Pollution Bulletin*, *58*(4), 615–620.

Fang, J. K.H., Wu, R. S. S., Chan, A. K. Y., & Shin, P. K. S. (2008a). Metal concentrations in green-lipped mussels (*Perna viridis*) and rabbitfish (*Siganus oramin*) from Victoria Harbour, Hong Kong after pollution abatement. *Marine Pollution Bulletin*, *56*(8), 1486–1491.

Fang, J. K.H., Wu, R. S. S., Chan, A. K. Y., Yip, C. K. M., & Shin, P. K. S. (2008b). Influences of ammonia-nitrogen and dissolved oxygen on lysosomal integrity in green-lipped mussel *Perna viridis*: Laboratory evaluation and field validation in Victoria Harbour, Hong Kong. *Marine Pollution Bulletin*, *56*(12), 2052–2058.

Fang, J. K.H., Wu, R. S. S., Zheng, G. J., Lam, P. K. S., & Shin, P. K. S. (2008c). Induction, adaptation and recovery of lysosomal integrity in green-lipped mussel *Perna viridis*. *Marine Pollution Bulletin*, *57*(6–12), 467–472.

Fang, James K.H., Schönberg, C. H. L., Hoegh-Guldberg, O., & Dove, S. (2017). Symbiotic plasticity of Symbiodinium in a common excavating sponge. *Marine Biology*, *164*(5), 1–11.

Fang, James K.H., Wu, R. S. S., Zheng, G. J., Lam, P. K. S., & Shin, P. K. S. (2010). Seasonality

of bioaccumulation of trace organics and lysosomal integrity in green-lipped mussel *Perna viridis*. *Science of the Total Environment*, *408*(6), 1458–1465.

Felten, V., Tixier, G., & Guérold, F. (2013). Active Biomonitoring. *Encyclopedia of Aquatic Ecotoxicology*, 15–20.

Foley, C. J., Bradley, D. L., & Höök, T. O. (2016). A review and assessment of the potential use of RNA:DNA ratios to assess the condition of entrained fish larvae. *Ecological Indicators*, *60*, 346–357.

Fouzia, H., Redouane Larbi, B., Amina, A., Nacera, C., & Nour El Islam, B. (2019). Introductory Chapter: Marine Monitoring Pollution. In H. Fouzia (Ed.), *Monitoring of Marine Pollution*. IntechOpen.

Franzellitti, S., Buratti, S., Capolupo, M., Du, B., Haddad, S. P., Chambliss, C. K., Brooks, B. W., & Fabbri, E. (2014). An exploratory investigation of various modes of action and potential adverse outcomes of fluoxetine in marine mussels. *Aquatic Toxicology*, *151*, 14–26.

Fu, H., Xia, Y., Chen, Y., Xu, T., Xu, L., Guo, Z., Xu, H., Xie, H. Q., & Zhao, B. (2018). Acetylcholinesterase Is a Potential Biomarker for a Broad Spectrum of Organic Environmental Pollutants. *Environmental Science and Technology*, *52*(15), 8065–8074.

Fu, J., Mai, B., Sheng, G., Zhang, G., Wang, X., Peng, P., Xiao, X., Ran, R., Cheng, F., Peng, X., Wang, Z., & Tang, U. W. (2003). Persistent organic pollutants in environment of the Pearl River Delta, China: An overview. *Chemosphere*, *52*(9), 1411–1422.

Fung, K. W., & Yim, W. W. S. (1981). Heavy metals in marine sediments of Hong Kong. *Hong Kong Engineer*.

Fuoco, R., & Giannarelli, S. (2019). Integrity of aquatic ecosystems: An overview of a message from the South Pole on the level of persistent organic pollutants (POPs). *Microchemical Journal*, *148*, 230–239.

Galarneau, E. (2008). Source specificity and atmospheric processing of airborne PAHs: Implications for source apportionment. *Atmospheric Environment*, *42*(35), 8139–8149.

Geret, F., Serafim, A., Barreira, L., & Bebianno, M. J. (2008). Effect of cadmium on antioxidant enzyme activities and lipid peroxidation in the gills of the clam *Ruditapes decussatus*.

Gessner, M. O., & Neumann, P. T. M. (2005). Total lipids. In *Methods to Study Litter Decomposition: A Practical Guide* (pp. 91–95). Springer Netherlands.

Giltrap, M., Ronan, J., Hardenberg, S., Parkes, G., McHugh, B., McGovern, E., & Wilson, J. G. (2013). Assessment of biomarkers in Mytilus edulis to determine good environmental status for implementation of MSFD in Ireland. *Marine Pollution Bulletin*, *71*(1–2), 240–249.

Gonzalez-Rey, M., Lau, T. C., Gomes, T., Maria, V. L., Bebianno, M. J., & Wu, R. (2011). Comparison of metal accumulation between "Artificial Mussel" and natural mussels (*Mytilus galloprovincialis*) in marine environments. *Marine Pollution Bulletin*, *63*(5–12), 149–153.

Gosling, E. (2003). Bivalve Molluscs. In *Bivalve Molluscs*. Blackwell Publishing Ltd.

Goswami, P., Hariharan, G., Godhantaraman, N., & Munuswamy, N. (2014). An integrated use of multiple biomarkers to investigate the individual and combined effect of copper and cadmium on the marine green mussel (*Perna viridis*). *Journal of Environmental Science and Health - Part A Toxic/Hazardous Substances and Environmental Engineering*, *49*(13), 1564–1577.

Grøsvik, B. E., Jonsson, H., Rodríguez-Ortega, M. J., Roepstorff, P., & Goksøyr, A. (2006). CYP1A-immunopositive proteins in bivalves identified as cytoskeletal and major vault proteins. *Aquatic Toxicology*, *79*(4), 334–340.

Hamza-Chaffai, A. (2014). Usefulness of Bioindicators and Biomarkers in Pollution Biomonitoring. *International Journal of Biotechnology for Wellness Industries*, *3*(1), 19–26.

Hariharan, G., Purvaja, R., & Ramesh, R. (2014). Toxic effects of lead on biochemical and histological alterations in green mussel (*Perna viridis*) induced by environmentally relevant concentrations. *Journal of Toxicology and Environmental Health - Part A: Current Issues*, *77*(5), 246–260.

Hole, L. M., Moore, M. N., & Bellamy, D. (1992). Age-related differences in the recovery of lysosomes from stress-induced pathological reactions in marine mussels. *Marine Environmental Research*, *34*(1–4), 75–80.

Hong, H., Chen, W., Xu, L., Wang, X., & Zhang, L. (1999). Distribution and fate of organochlorine pollutants in the Pearl River Estuary. *Marine Pollution Bulletin*, *39*(1–12), 376–382.

Hook, S. E., Gallagher, E. P., & Batley, G. E. (2014). The role of biomarkers in the assessment of aquatic ecosystem health. *Integrated Environmental Assessment and Management*, *10*(3), 327–341.

Hwang, H. M., Wade, T. L., & Sericano, J. L. (2002). Relationship between lysosomal membrane destabilization and chemical body burden in eastern oysters (*Crassostrea virginica*) from Galveston Bay, Texas, USA. *Environmental Toxicology and Chemistry*, *21*(6), 1268–1271.

Iyapparaj, P., Revathi, P., Ramasubburayan, R., Prakash, S., Anantharaman, P., Immanuel, G., & Palavesam, A. (2013). Antifouling activity of the methanolic extract of Syringodium isoetifolium, and its toxicity relative to tributyltin on the ovarian development of brown mussel *Perna indica*. *Ecotoxicology and Environmental Safety*, *89*, 231–238.

Jena, K. B., Verlecar, X. N., & Chainy, G. B. N. (2009). Application of oxidative stress indices in natural populations of *Perna viridis* as biomarker of environmental pollution. *Marine Pollution Bulletin*, *58*(1), 107–113.

Juhel, G., Bayen, S., Goh, C., Lee, W. K., & Kelly, B. C. (2017). Use of a suite of biomarkers to assess the effects of carbamazepine, bisphenol A, atrazine, and their mixtures on green mussels, *Perna viridis*. *Environmental Toxicology and Chemistry*, *36*(2), 429–441.

Kamaruzzaan, B. Y., Mohd Zahir, M. S., Akbar John, B., Jalal, K. C. A., Shahbudin, S., Al-Barwani, S. M., & Goddard, J. S. (2011). Bioaccumulation of some metals by Green mussel *Perna viridis* (Linnaeus 1758) from Pekan, Pahang, Malaysia. *International Journal of Biological Chemistry*, *5*(1), 54–60.

Karaouzas, I., Kapetanaki, N., Mentzafou, A., Kanellopoulos, T. D., & Skoulikidis, N. (2021). Heavy metal contamination status in Greek surface waters: A review with application and evaluation of pollution indices. *Chemosphere*, *263*, 128192.

Karlsson, K., & Viklander, M. (2008). Polycyclic aromatic hydrocarbons (PAH) in water and sediment from gully pots. *Water, Air, and Soil Pollution*, *188*(1–4), 271–282.

Kazi, T. G., Jamali, M. K., Arain, M. B., Afridi, H. I., Jalbani, N., Sarfraz, R. A., & Ansari, R. (2009). Evaluation of an ultrasonic acid digestion procedure for total heavy metals determination in environmental and biological samples. *Journal of Hazardous Materials*, *161*(2–3), 1391–1398.

Krishnakumar, P. K., Asokan, P. K., & Pillai, V. K. (1990). Physiological and cellular responses to copper and mercury in the green mussel *Perna viridis* (Linnaeus). *Aquatic Toxicology*, *18*(3), 163–173.

Kucuksezgin, F., Gonul, L. T., Pazi, I., Ubay, B., & Guclusoy, H. (2020). Monitoring of

polycyclic aromatic hydrocarbons in transplanted mussels (*Mytilus galloprovincialis*) and sediments in the coastal region of Nemrut Bay (Eastern Aegean Sea). *Marine Pollution Bulletin*, *157*, 111358.

Kucuksezgin, F., Pazi, I., Yucel-Gier, G., Akcali, B., & Galgani, F. (2013). Monitoring of heavy metal and organic compound levels along the Eastern Aegean coast with transplanted mussels. *Chemosphere*, *93*(8), 1511–1518.

Kueh, C. S. W., & Lam, J. Y. C. (2008). Monitoring of toxic substances in the Hong Kong marine environment. *Marine Pollution Bulletin*, *57*(6–12), 744–757.

Kumar, V., Parihar, R. D., Sharma, A., Bakshi, P., Singh Sidhu, G. P., Bali, A. S., Karaouzas, I., Bhardwaj, R., Thukral, A. K., Gyasi-Agyei, Y., & Rodrigo-Comino, J. (2019). Global evaluation of heavy metal content in surface water bodies: A meta-analysis using heavy metal pollution indices and multivariate statistical analyses. *Chemosphere*, *236*, 124364.

Kutty, P., Gravell, A., & Thompson, K. (2012). Determination Of Chemical Contaminants In Marine Shellfish Using The Agilent 7000 Triple Quadrupole GC/MS. *Chemical & Engineering News Archive*, *90*(29), 31.

Kwok, C. T., van de Merwe, J. P., Chiu, J. M. Y., & Wu, R. S. S. (2012). Antioxidant responses and lipid peroxidation in gills and hepatopancreas of the mussel *Perna viridis* upon exposure to the red-tide organism Chattonella marina and hydrogen peroxide. *Harmful Algae*, *13*, 40–46.

Lai, R. W. S., Perkins, M. J., Ho, K. K. Y., Astudillo, J. C., Yung, M. M. N., Russell, B. D., Williams, G. A., & Leung, K. M. Y. (2016). Hong Kong's marine environments: History, challenges and opportunities. *Regional Studies in Marine Science*, *8*, 259–273.

Lam, P. K. S. (2009). Use of biomarkers in environmental monitoring. *Ocean and Coastal Management*, *52*(7), 348–354.

Lam, P. K. S., & Gray, J. S. (2003). The use of biomarkers in environmental monitoring programmes. *Marine Pollution Bulletin*, *46*(2), 182–186.

Lau, P. S., & Wong, H. L. (2003). Effect of size, tissue parts and location on six biochemical markers in the green-lipped mussel, *Perna viridis*. *Marine Pollution Bulletin*, *46*(12), 1563–1572.

Leung, K. M. Y., & Furness, R. W. (1999). Induction of metallothionein in dogwhelk *nucella Lapillus* during and after exposure to cadmium. *Ecotoxicology and Environmental Safety*,

43(2), 156–164.

Leung, P. T. Y., Park, T. J., Wang, Y., Che, C. M., & Leung, K. M. Y. (2014). Isoform-specific responses of metallothioneins in a marine pollution biomonitor, the green-lipped mussel *Perna viridis*, towards different stress stimulations. *Proteomics*, *14*(15), 1796–1807.

Li, L., Li, Z., Xv, G., Wang, C., & Jiang, M. (2021). Accumulation of PAH in bivalves (*Crassostrea gigas* and *Mytilus coruscus*) from Zhejiang coastal,China , and associtated human health risk assessment. *Research square*.

Li, X. (2009). Glutathione and Glutathione-S-Transferase in Detoxification Mechanisms. *Molecular and Cellular Aspects of Toxicology*.

Li, Z. H., Zlabek, V., Grabic, R., Velisek, J., MacHova, J., & Randak, T. (2010). Enzymatic alterations and RNA/DNA ratio in intestine of rainbow trout, *Oncorhynchus mykiss*, induced by chronic exposure to carbamazepine. *Ecotoxicology*, *19*(5), 872–878.

Lionetto, M. G., Caricato, R., & Giordano, M. E. (2019). Pollution Biomarkers in Environmental and Human Biomonitoring. *The Open Biomarkers Journal*, *9*(1), 1–9.

Liu, C., Chang, V. W. C., Gin, K. Y. H., & Nguyen, V. T. (2014). Genotoxicity of perfluorinated chemicals (PFCs) to the green mussel (*Perna viridis*). *Science of the Total Environment*, *487*(1), 117–122.

Liu, J. H., & Kueh, C. S. W. (2005). Biomonitoring of heavy metals and trace organics using the intertidal mussel *Perna viridis* in Hong Kong coastal waters. *Marine Pollution Bulletin*, *51*(8–12), 857–875.

Lobel, P. B., Bajdik, C. D., Belkhode, S. P., Jackson, S. E., & Longerich, H. P. (1991). Improved protocol for collecting mussel watch specimens taking into account sex, size, condition, shell shape, and chronological age. *Archives of Environmental Contamination and Toxicology*, *21*(3), 409–414.

Lomartire, S., Marques, J. C., & Gonçalves, A. M. M. (2021). Biomarkers based tools to assess environmental and chemical stressors in aquatic systems. *Ecological Indicators*, *122*, 107207.

López-Pedrouso, M., Varela, Z., Franco, D., Fernández, J. A., & Aboal, J. R. (2020). Can proteomics contribute to biomonitoring of aquatic pollution? A critical review. *Environmental Pollution*, *267*, 115473.

Lowe, D. M., Soverchia, C., & Moore, M. N. (1995). Lysosomal membrane responses in the

blood and digestive cells of mussels experimentally exposed to fluoranthene. *Aquatic Toxicology*, *33*(2), 105–112.

Lowe, David M., Moore, M. N., & Clarke, K. R. (1981). Effects of oil on digestive cells in mussels: Quantitative alterations in cellular and lysosomal structure. *Aquatic Toxicology*, *1*(3–4), 213–226.

Luzhna, L., Kathiria, P., & Kovalchuk, O. (2013). Micronuclei in genotoxicity assessment: From genetics to epigenetics and beyond. *Frontiers in Genetics*, *4*(JUL), 131.

Marigómez, I., Soto, M., Cajaraville, M. P., Angulo, E., & Giamberini, L. (2002). Cellular and subcellular distribution of metals in molluscs. *Microscopy Research and Technique*, *56*(5), 358–392.

Mathew, R., & Menon, N. R. (1983). Oxygen consumption in Tropical Bivalves *Perna viridis* (Linn.) & *Meretrix casta* (Chem.) Exposed to Heavy Metals. *Indian Journal of Marine Sciences*, *12*, 57–59.

McCarty, L. S., & Munkittrick, K. R. (1996). Environmental biomarkers in aquatic toxicology: Fiction, fantasy, or functional? *Human and Ecological Risk Assessment (HERA)*, *2*(2), 268–274.

Micklem, J. M., Griffiths, C. L., Ntuli, N., & Mwale, M. (2016). The invasive Asian green mussel *Perna viridis* in South Africa: all that is green is not viridis.

Moore, M. N. (1985). Cellular responses to pollutants. *Marine Pollution Bulletin*, *16*(4), 134–139.

Morton, B. (1989). Pollution of the coastal waters of Hong Kong. *Marine Pollution Bulletin*, *20*(7), 310–318.

Morton, B. S. (1976). The Hong Kong Sea-shore — an Environment in Crisis. *Environmental Conservation*, *3*(4), 243–254.

Morton, B. S. (1987). The functional morphology of the organs of the mantle cavity of *Perna viridis* (Linnaeus, 1758) (Bivalvia: Mytilacea). *American Malacological Bulletin*, *5*(2), 159–164.

Morton, B., & Wu, S. S. (1975). The hydrology of the coastal waters of Hong Kong. *Environmental Research*, *10*(3), 319–347.

Moschino, V., Del Negro, P., De Vittor, C., & Da Ros, L. (2016). Biomonitoring of a polluted coastal area (Bay of Muggia, Northern Adriatic Sea): A five-year study using transplanted

mussels. *Ecotoxicology and Environmental Safety*, *128*, 1–10.

Müller, W. E. G., Koziol, C., Wiens, M., & Schröder, H. C. (2000). Chapter 14 Stress response in marine sponges: Genes and molecules involved and their use as biomarkers. In *Cell and Molecular Response to Stress* (Vol. 1, Issue C, pp. 193–208). Elsevier.

Nabizadeh, R., Mahvi, A., Mardani, G., & Yunesian, M. (2005). Study of heavy metals in urban runoff. *International Journal of Environmental Science & Technology*, *1*(4), 325–333.

Nagarjuna, A., Karthikeyan, P., Marigoudar, S. R., & Sharma, K. V. (2019). Effect of sublethal gradient concentrations of nickel on postlarvae of *Penaeus monodon*, *Perna viridis* and *Terapon jarbua*: Enzyme activities and histopathological changes. *Chemosphere*, *237*, 124428.

Nahrgang, J., Brooks, S. J., Evenset, A., Camus, L., Jonsson, M., Smith, T. J., Lukina, J., Frantzen, M., Giarratano, E., & Renaud, P. E. (2013). Seasonal variation in biomarkers in blue mussel (*Mytilus edulis*), Icelandic scallop (*Chlamys islandica*) and Atlantic cod (*Gadus morhua*)-Implications for environmental monitoring in the Barents Sea. *Aquatic Toxicology*, *127*, 21–35.

Narváez, N., Lodeiros, C., Nusetti, O., Lemus, M., & Maeda-Martínez, A. N. (2005). Uptake, depuration and effect of cadmium on the green mussel *Perna viridis* (L. 1758) (Mollusca: Bivalvia). *Ciencias Marinas*, *31*(1A), 91–102.

National Introduced Marine Pest Information System. (2002). Asian green mussel *Perna viridis*. In *The Online Guide to the Animals of Trinided and Tobago*.

Nicholson, Shaun. (1999a). Cytological and physiological biomarker responses from green mussels, *Perna viridis* (L.) transplanted to contaminated sites in Hong Kong coastal waters. *Marine Pollution Bulletin*, *39*(1–12), 261–268.

Nicholson, Shaun. (1999b). Cardiac and lysosomal responses to periodic copper in the mussel *Perna viridis* (Bivalvia: Mytilidae). *Marine Pollution Bulletin*, *38*(12), 1157–1162.

Nicholson, S. (2001). Ecocytological and toxicological responses to copper in *Perna viridis* (L.) (Bivalvia: Mytilidae) haemocyte lysosomal membranes. *Chemosphere*, *45*(4–5), 399–407.

Nicholson, S. (2002). Ecophysiological aspects of cardiac activity in the subtropical mussel *Perna viridis* (L.) (Bivalvia: Mytilidae). *Journal of Experimental Marine Biology and Ecology*, *267*(2), 207–222.

Nicholson, S. (2003a). Lysosomal membrane stability, phagocytosis and tolerance to emersion in

the mussel *Perna viridis* (Bivalvia: Mytilidae) following exposure to acute, sublethal, copper. *Chemosphere*, *52*(7), 1147–1151.

Nicholson, S. (2003b). Cardiac and branchial physiology associated with copper accumulation and detoxication in the mytilid mussel *Perna viridis* (L.). *Journal of Experimental Marine Biology and Ecology*, *295*(2), 157–171.

Nicholson, S. (2003c). The mytilid mussel *Perna viridis* (Mytilidae: Bivalvia) as a pollution monitor in Hong Kong. *P.K.S. Shin (Ed.), Turning the Tides, Marine Biological Association of Hong Kong*, 201–228.

Nicholson, S., & Lam, P. K. S. (2005). Pollution monitoring in Southeast Asia using biomarkers in the mytilid mussel *Perna viridis* (Mytilidae: Bivalvia). *Environment International*, *31*(1), 121–132.

Nicholson, S., & Szefer, P. (2003). Accumulation of metals in the soft tissues, byssus and shell of the mytilid mussel *Perna viridis* (Bivalvia: Mytilidae) from polluted and uncontaminated locations in Hong Kong coastal waters. *Marine Pollution Bulletin*, *46*(8), 1040–1043.

Nicotera, T. M., & Bardin, S. (1998). Electrochemical detection of 8-hydroxy-2-deoxyguanosine levels in cellular DNA. In *Methods in molecular biology (Clifton, N.J.)* (Vol. 108, pp. 181–190). Humana Press.

Noor, A. R., Shakil, A., Hoque, N. F., Rahman, M. M., Akter, S., Talukder, A., Ahmad-Al-Nahid, S., Wahab, M. A., Nahiduzzaman, M., Rahman, M. J., & Asaduzzaman, M. (2021). Effect of eco-physiological factors on biometric traits of green mussel *Perna viridis* cultured in the south-east coast of the Bay of Bengal, Bangladesh. *Aquaculture Reports*, *19*, 100562.

Pagano, M., Porcino, C., Briglia, M., Fiorino, E., Vazzana, M., Silvestro, S., & Faggio, C. (2017). The Influence of Exposure of Cadmium Chloride and Zinc Chloride on Haemolymph and Digestive Gland Cells from *Mytilus galloprovincialis*. *International Journal of Environmental Research*, *11*(2), 207–216.

Perić, L., Nerlović, V., Žurga, P., Žilić, L., & Ramšak, A. (2017). Variations of biomarkers response in mussels *Mytilus galloprovincialis* to low, moderate and high concentrations of organic chemicals and metals. *Chemosphere*, *174*, 554–562.

Peven, C. S., Uhler, A. D., & Querzoli, F. J. (1996). Caged mussels and semipermeable membrane devices as indicators of organic contaminant uptake in dorchester and duxbury

bays, Massachusetts. *Environmental Toxicology and Chemistry*, *15*(2), 144–149.

Phillips, D. J. H. (1985). Organochlorines and trace metals in green-lipped mussels *Perna viridis* from Hong Kong waters: a test of indicator ability. *Marine Ecology Progress Series*, *21*, 251–258.

Phillips, D. J. H., & Rainbow, P. S. (1988). Barnacles and mussels as biomonitors of trace elements: a comparative study. *Marine Ecology Progress Series*, *49*, 83–93.

Phillips, D., & Yim, W.-S. (1981). A Comparative Evaluation of Oysters, Mussels and Sediments as Indicators of Trace Metals in Hong Kong Waters. *Marine Ecology Progress Series*, *6*, 285–293.

Phillips, David J.H. (1989). Trace metals and organochlorines in the coastal waters of Hong Kong. *Marine Pollution Bulletin*, *20*(7), 319–327.

Prabhudeva, K. N., & Menon, N. R. (1986). Oxygen consumption under copper and zinc stress in *Perna viridis*. *Fishery Technology*, *23*(1), 24-26.

Ramu, K., Kajiwara, N., Tanabe, S., Lam, P. K. S., & Jefferson, T. A. (2005). Polybrominated diphenyl ethers (PBDEs) and organochlorines in small cetaceans from Hong Kong waters: Levels, profiles and distribution. *Marine Pollution Bulletin*, *51*(8–12), 669–676.

Rashid, A., Nawaz, S., Barker, H., Ahmad, I., & Ashraf, M. (2010). Development of a simple extraction and clean-up procedure for determination of organochlorine pesticides in soil using gas chromatography-tandem mass spectrometry. *Journal of Chromatography A*, *1217*(17), 2933–2939.

Reddy, P. M., & Philip, G. H. (1992). Changes in the levels of respiration and ions in the tissues of freshwater fish, *Labeo rohita* under fenvalerate stress. *Chemosphere*, *25*(6), 843–852.

Richardson, B. J., Mak, E., De Luca-Abbott, S. B., Martin, M., McClellan, K., & Lam, P. K. S. (2008). Antioxidant responses to polycyclic aromatic hydrocarbons and organochlorine pesticides in green-lipped mussels (*Perna viridis*): Do mussels "integrate" biomarker responses? *Marine Pollution Bulletin*, *57*(6–12), 503–514.

Richardson, B. J., Zheng, G. J., Tse, E. S. C., & Lam, P. K. S. (2001). A comparison of mussels (*Perna viridis*) and semi-permeable membrane devices (SPMDS) for monitoring chlorinated trace organic contaminants in Hong Kong coastal waters. *Chemosphere*, *45*(8), 1201–1208.

Rickwood, C. J., & Galloway, T. S. (2004). Acetylcholinesterase inhibition as a biomarker of

adverse effect: A study of *Mytilus edulis* exposed to the priority pollutant chlorfenvinphos. *Aquatic Toxicology*, *67*(1), 45–56.

Ringwood, A. H., Hoguet, J., Keppler, C. J., Gielazyn, M. L., Ward, B. P., & A.H. Ringwood, J. Hoguet, C.J. Kappler, M.L. Gielazyn, B.P. Ward, A. R. R. (2003). Cellular Biomarkers (Lysosomal Destabilization , Glutathione & Lipid Peroxidation) in Three Common Estuarine Species : A Methods Handbook. In *Environmental Technology*. Marine Resources Research Institute, South Carloina Department of Natural Resources.

Ringwood, Amy Huffman, Conners, D. E., & Hoguet, J. (1998). Effects of natural and anthropogenic stressors on lysosomal destabilization in oysters *Crassostrea virginica*. *Marine Ecology Progress Series*, *166*, 163–171.

Rola, R. C., Monteiro, M. da C., Reis, S. R. da S., & Sandrini, J. Z. (2012). Molecular and biochemical biomarkers responses in the mussel *Mytilus edulis* collected from Southern Brazil coast. *Marine Pollution Bulletin*, *64*(4), 766–771.

Saavedra, C., & Bachère, E. (2006). Bivalve genomics. *Aquaculture*, *256*(1–4), 1–14.

Sakson, G., Brzezinska, A., & Zawilski, M. (2018). Emission of heavy metals from an urban catchment into receiving water and possibility of its limitation on the example of Lodz city. *Environmental Monitoring and Assessment*, *190*(5).

Sałata, A., Bak, L., & Górski, J. (2019). Ecological risk assessment of chemical contaminants in stormwater sediments. *E3S Web of Conferences*, *86*, 00017.

Schmidt, W., Power, E., & Quinn, B. (2013). Seasonal variations of biomarker responses in the marine blue mussel (*Mytilus* spp.). *Marine Pollution Bulletin*, *74*(1), 50–55.

Schöne, B. R., & Krause, R. A. (2016). Retrospective environmental biomonitoring – Mussel Watch expanded. In *Global and Planetary Change* (Vol. 144, pp. 228–251). Elsevier B.V.

Shanbehzadeh, S., Vahid Dastjerdi, M., Hassanzadeh, A., & Kiyanizadeh, T. (2014). Heavy metals in water and sediment: A case study of Tembi River. *Journal of Environmental and Public Health*, *2014*.

Shewa, W. A., & Dagnew, M. (2020). Revisiting chemically enhanced primary treatment of wastewater: A review. *Sustainability (Switzerland)*, *12*(15), 5928.

Shin, P. K. S., Yau, F. N., Chow, S. H., Tai, K. K., & Cheung, S. G. (2002). Responses of the green-lipped mussel *Perna viridis* (L.) to suspended solids. *Marine Pollution Bulletin*, *45*(1–12), 157–162.

Shugart, L. R. (1998). Structural Damage to DNA in Response to Toxicant Exposure. In *Genetics and Ecotoxicology* (1st ed., pp. 151–168). CRC Press.

Siddall, S. (1980). A Clarification of the Genus *Perna* (Mytilidae). *Bulletin of Marine Science*, *30*(4), 858–870.

Singh, N. P., McCoy, M. T., Tice, R. R., & Schneider, E. L. (1988). A simple technique for quantitation of low levels of DNA damage in individual cells. *Experimental Cell Research*, *175*(1), 184–191.

Singh, S., & Srivastava, A. K. (2015). Variations in Hepatosomatic index (HSI) and Gonadosomatic index (GSI) in fish heteropneustes fossilis exposed to higher sub-lethal concentration to Arsenic and Copper. *Journal of Ecophysiology and Occupational Health*, *15*(3–4), 89–93.

Siu, S. Y. M., Lam, P. K. S., Martin, M., Caldwell, C. W., & Richardson, B. J. (2008). The use of selected genotoxicity assays in green-lipped mussels (*Perna viridis*): A validation study in Hong Kong coastal waters. *Marine Pollution Bulletin*, *57*(6–12), 479–492.

Siu, W. H. L., Cao, J., Jack, R. W., Wu, R. S. S., Richardson, B. J., Xu, L., & Lam, P. K. S. (2004). Application of the comet and micronucleus assays to the detection of B[a]P genotoxicity in haemocytes of the green-lipped mussel (*Perna viridis*). *Aquatic Toxicology*, *66*(4), 381–392.

Sminia, T. (1981). PHAGOCYTIC CELLS IN MOLLUSCS. *Aspects of Developmental and Comparative Immunology*, 125–132.

Świacka, K., Maculewicz, J., Smolarz, K., Szaniawska, A., & Caban, M. (2019). Mytilidae as model organisms in the marine ecotoxicology of pharmaceuticals - A review. *Environmental Pollution*, *254*, 113082.

Tang, C. W. Y., Ip, C. C. M., Zhang, G., Shin, P. K. S., Qian, P. Y., & Li, X. D. (2008). The spatial and temporal distribution of heavy metals in sediments of Victoria Harbour, Hong Kong. *Marine Pollution Bulletin*, *57*(6–12), 816–825.

Tanner, P. A., Leong, L. S., & Pan, S. M. (2000). Contamination of heavy metals in marine sediment cores from Victoria harbour, Hong Kong. *Marine Pollution Bulletin*, *40*(9), 769–779.

Tateda, Y., Sakaguchi, I., & Itani, G. (2015). Scope for growth of *Mytilus galloprovincialis* and *Perna viridis* as a thermal stress index in the coastal waters of Japan: Field studies at the

Uranouchi inlet and Yokohama. *Journal of Experimental Marine Biology and Ecology*, *470*, 55–63.

Tates, A. D., Neuteboom, I., Hofker, M., & den Engelse, L. (1980). A micronucleus technique for detecting clastogenic effects of mutagens/carcinogens (DEN, DMN) in hepatocytes of rat liver in vivo. *Mutation Research/Environmental Mutagenesis and Related Subjects*, *74*(1), 11–20.

Tenuzzo, B. A., Zaccarelli, N., & Dini, L. (2012). The reproductive cycle of the commercial sea urchin *Paracentrotus lividus* (Lamark, 1816) (Echinodermata: Echinoidea) in the Ionian Sea. *Italian Journal of Zoology*, *79*(2), 200–211.

Trevisan, R., Flesch, S., Mattos, J. J., Milani, M. R., Bainy, A. C. D., & Dafre, A. L. (2014). Zinc causes acute impairment of glutathione metabolism followed by coordinated antioxidant defenses amplification in gills of brown mussels *Perna perna*. *Comparative Biochemistry and Physiology Part C: Toxicology & Pharmacology*, *159*(1), 22–30.

Triant, D. A., & Whitehead, A. (2009). Simultaneous extraction of high-quality RNA and DNA from small tissue samples. *Journal of Heredity*, *100*(2), 246–250.

Tsangaris, C., Kormas, K., Strogyloudi, E., Hatzianestis, I., Neofitou, C., Andral, B., & Galgani, F. (2010). Multiple biomarkers of pollution effects in caged mussels on the Greek coastline. *Comparative Biochemistry and Physiology - C Toxicology and Pharmacology*, *151*(3), 369–378.

United Nations. (1982). United Nations convention on the law of the sea. In *Law of the Sea Bulletin* (Vol. 1999, Issue 39).

Vakily, J. M. (1989). The Biology and Culture of Mussels of the Genus *Perna*. In *ICLARM Studies and Reviews* (Vol. 17). ICLARM Studies and Reviews 17. International Center for Living Aquatic Resources Management.

Valavanidis, A., Vlachogianni, T., & Fiotakis, C. (2009). 8-Hydroxy-2′ -deoxyguanosine (8-OHdG): A critical biomarker of oxidative stress and carcinogenesis. *Journal of Environmental Science and Health - Part C Environmental Carcinogenesis and Ecotoxicology Reviews*, *27*(2), 120–139.

Vasanthi, L. A., Revathi, P., Babu Rajendran, R., & Munuswamy, N. (2017). Detection of metal induced cytopathological alterations and DNA damage in the gills and hepatopancreas of green mussel *Perna viridis* from Ennore Estuary, Chennai, India. *Marine Pollution Bulletin*,

117(1–2), 41–49.

Vasanthi, R. L., Arulvasu, C., Kumar, P., & Srinivasan, P. (2021). Ingestion of microplastics and its potential for causing structural alterations and oxidative stress in Indian green mussel *Perna viridis*– A multiple biomarker approach. *Chemosphere*, *283*, 130979.

Vaughn, C. C., & Hoellein, T. J. (2018). Bivalve impacts in freshwater and marine ecosystems. *Annual Review of Ecology, Evolution, and Systematics*, *49*, 183–208.

Verlecar, X. N., Jena, K. B., & Chainy, G. B. N. (2008). Modulation of antioxidant defences in digestive gland of *Perna viridis* (L.), on mercury exposures. *Chemosphere*, *71*(10), 1977–1985.

Verslycke, T., Roast, S. D., Widdows, J., Jones, M. B., & Janssen, C. R. (2004). Cellular energy allocation and scope for growth in the estuarine mysid *Neomysis integer* (Crustacea: Mysidacea) following chlorpyrifos exposure: A method comparison. *Journal of Experimental Marine Biology and Ecology*, *306*(1), 1–16.

Viarengo, A., Arena, N., Canesi, L., Alia, F. A., & Orunesu, M. (1994). Structural and biochemical alterations in the gills of copper-exposed mussels. In A. Renzoni, N. Mattei, L. Lari, & M. Cristina (Eds.), *Contaminants in the Environment: A Multidisciplinary Assessment of Risks to Man and Other Organisms* (pp. 135–144). Lewis Publishers.

Viarengo, A., Lowe, D., Bolognesi, C., Fabbri, E., & Koehler, A. (2007). The use of biomarkers in biomonitoring: A 2-tier approach assessing the level of pollutant-induced stress syndrome in sentinel organisms. In *Comparative Biochemistry and Physiology - C Toxicology and Pharmacology* (Vol. 146, Issue 3, pp. 281–300). Elsevier Inc.

Vijayavel, K., Gopalakrishnan, S., & Balasubramanian, M. P. (2007). Sublethal effect of silver and chromium in the green mussel *Perna viridis* with reference to alterations in oxygen uptake, filtration rate and membrane bound ATPase system as biomarkers. *Chemosphere*, *69*(6), 979–986.

Wang, C., Zhou, X., & Cheng, R. (1993). The effects of pollutants on the filtration rate of *Perna viridis* (Bivalvia: Mytilidae). In B. Morton (Ed.), *The marine biology of the South China Sea* (pp. 253–260). In: Morton B, editor. Hong Kong: Hong Kong University Press.

Wang, S., Hong, H., & Wang, X. (2005). Bioenergetic responses in green lipped mussels (*Perna viridis*) as indicators of pollution stress in Xiamen coastal waters, China. *Marine Pollution Bulletin*, *51*(8–12), 738–743.

Wang, T., Kong, H., Shang, Y., Dupont, S., Peng, J., Wang, X., Deng, Y., Hu, M., & Wang, Y. (2021). Ocean acidification but not hypoxia alters the gonad performance in the thick shell mussel *Mytilus coruscus*. *Marine Pollution Bulletin*, *167*, 112282.

Wang, Y., Hu, M., Li, Q., Li, J., Lin, D., & Lu, W. (2014). Immune toxicity of TiO2 under hypoxia in the green-lipped mussel *Perna viridis* based on flow cytometric analysis of hemocyte parameters. *Science of the Total Environment*, *470–471*, 791–799.

Wang, Y., Hu, M., Shin, P. K. S., & Cheung, S. G. (2011). Immune responses to combined effect of hypoxia and high temperature in the green-lipped mussel *Perna viridis*. *Marine Pollution Bulletin*, *63*(5–12), 201–208.

Wang, Y., Hu, M., Wong, W. H., Shin, P. K. S., & Cheung, S. G. (2011). The combined effects of oxygen availability and salinity on physiological responses and scope for growth in the green-lipped mussel *Perna viridis*. *Marine Pollution Bulletin*, *63*(5–12), 255–261.

Wang, Z., Ren, P., Sun, Y., Ma, X., Liu, X., Na, G., & Yao, Z. (2013). Gas/particle partitioning of polycyclic aromatic hydrocarbons in coastal atmosphere of the north Yellow Sea, China. *Environmental Science and Pollution Research*, *20*(8), 5753–5763.

Watts, J. C. D. (1971). A general review of the oceanography of the northern sector of the South China Sea. *Hong Kong Fisheries Bulletin*, *2*, 41–50.

Wendling, C. C., Huhn, M., Ayu, N., Bachtiar, R., Juterzenka, K. von, & Lenz, M. (2013). Habitat degradation correlates with tolerance to climate-change related stressors in the green mussel *Perna viridis* from West Java, Indonesia. *Marine Pollution Bulletin*, *71*(1–2), 222–229.

Weydert, C. J., & Cullen, J. J. (2010). Measurement of superoxide dismutase, catalase and glutathione peroxidase in cultured cells and tissue. *Nature Protocols*, *5*(1), 51–66.

Widdows, J., Burns, K. A., Menon, N. R., Page, D. S., & Soria, S. (1990). Measurement of physiological energetics (scope for growth) and chemical contaminants in mussels (*Arca zebra*) transplanted along a contamination gradient in Bermuda. *Journal of Experimental Marine Biology and Ecology*, *138*(1–2), 99–117.

Widdows, J., & Johnson, D. (1988). Physiological energetics of *Mytilus edulis*: Scope for Growth. *Marine Ecology Progress Series*, *46*, 113–121.

Wong, C. K. C., Cheung, R. Y. H., & Wong, M. H. (1999). Toxicological assessment of coastal sediments in Hong Kong using a flagellate, *Dunaliella tertiolecta*. *Environmental Pollution*,

105(2), 175–183.

Wong, H. L., Giesy, J. P., & Lam, P. K. S. (2004). Atmospheric deposition and fluxes of organochlorine pesticides and coplanar polychlorinated biphenyls in aquatic environments of Hong Kong, China. *Environmental Science and Technology*, *38*(24), 6513–6521.

Wong, W. H., & Cheung, S. G. (2001). Feeding rates and scope for growth of green mussels, *Perna viridis* (L.) and their relationship with food availability in Kat O, Hong Kong. *Aquaculture*, *193*(1–2), 123–137.

Wong, W. H., & Cheung, S. G. (2003). Seasonal variation in the feeding physiology and scope for growth of green mussels, *Perna viridis* in estuarine Ma Wan, Hong Kong. *Journal of the Marine Biological Association of the United Kingdom*, *83*(3), 543–552.

Wong, Y. S., Tam, N. F. Y., Lau, P. S., & Xue, X. Z. (1995). The toxicity of marine sediments in Victoria Harbour, Hong Kong. *Marine Pollution Bulletin*, *31*(4–12), 464–470.

Wood, A. R., Apte, S., MacAvoy, E. S., & Gardner, J. P. A. (2007). A molecular phylogeny of the marine mussel genus *Perna* (Bivalvia: Mytilidae) based on nuclear (ITS1&2) and mitochondrial (COI) DNA sequences. *Molecular Phylogenetics and Evolution*, *44*(2), 685–698.

Wu, R. S. S., Lau, T. C., Fung, W. K. M., Ko, P. H., & Leung, K. M. Y. (2007). An "artificial mussel" for monitoring heavy metals in marine environments. *Environmental Pollution*, *145*(1), 104–110.

Wu, R. S. S., Siu, W. H. L., & Shin, P. K. S. (2005). Induction, adaptation and recovery of biological responses: Implications for environmental monitoring. *Marine Pollution Bulletin*, *51*(8–12), 623–634.

Xu, P., Junaid, M., Liu, Y., Jiang, X., Chen, Y., Bi, C., Wang, J., & Xu, N. (2021). Nanoplastics influence the perfluorooctane sulfonate (PFOS) mediated toxicity on marine mussel *Perna viridis*: Single and mixture exposure study. *Gondwana Research*.

Yang, H. H., Lee, W. J., Chen, S. J., & Lai, S. O. (1998). PAH emission from various industrial stacks. *Journal of Hazardous Materials*, *60*(2), 159–174.

Yap, C. K., Ismail, A., & Tan, S. G. (2003a). Concentrations of Cd, Cu, Pb and Zn in Different Parts of the Byssus of Green-lipped Mussel *Perna viridis* (Linnaeus). *Pakistan Journal of Biological Sciences*, *6*(8), 789–792.

Yap, C. K., Ismail, A., & Tan, S. G. (2003b). Can the byssus of green-lipped mussel *Perna*

viridis (Linnaeus) from the west coast of Peninsular Malaysia be a biomonitoring organ for Cd, Pb and Zn? Field and laboratory studies. *Environment International*, *29*(4), 521–528.

Yaqin, K., Tresnati, J., Rape, R., & Aslam, M. (2014). The Use of Byssogenesis of Green Mussel, *Perna viridis*, as a Biomarker in Laboratory Study. *Current Nutrition & Food Science*, *10*(2), 100–106.

Yeung, J. W. Y., & Leung, K. M. Y. (2013). Effects of animal size and nutritional status on the RNA/DNA ratio in different tissues of the green-lipped mussel *Perna viridi*s. *Journal of the Marine Biological Association of the United Kingdom*, *93*(1), 217–225.

Yeung, J. W. Y., Zhou, G. J., & Leung, K. M. Y. (2016). Sub-lethal effects of cadmium and copper on RNA/DNA ratio and energy reserves in the green-lipped mussel *Perna viridis*. *Ecotoxicology and Environmental Safety*, *132*, 59–67.

Yeung, J. W. Y., Zhou, G. J., & Leung, K. M. Y. (2017). Spatiotemporal variations in metal accumulation, RNA/DNA ratio and energy reserve in *Perna viridis* transplanted along a marine pollution gradient in Hong Kong. *Marine Pollution Bulletin*, *124*(2), 736–742.

Zhang, G., Parker, A., House, A., Mai, B., Li, X., Kang, Y., & Wang, Z. (2002). Sedimentary records of DDT and HCH in the Pearl River Delta, South China. *Environmental Science and Technology*, *36*(17), 3671–3677.

Zhang, J., Huang, W. W., Liu, S. M., Liu, M. G., Yu, Q., & Wang, J. H. (1992). Transport of particulate heavy metals towards the China Sea: a preliminary study and comparison. *Marine Chemistry*, *40*(3–4), 161–178.

Zhang, M., Sun, X., & Xu, J. (2020). Heavy metal pollution in the East China Sea: A review. *Marine Pollution Bulletin*, *159*, 111473.

Zhao, H., Yin, C., Chen, M., & Wang, W. (2008). Runoff pollution impacts of polycyclic aromatic hydrocarbons in street dusts from a stream network town. *Water Science and Technology*, *58*(11), 2069–2076.

Zhen, Y., Aili, J., & Changhai, W. (2010). Oxygen consumption, ammonia excretion, and filtration rate of the marine bivalve *Mytilus edulis* exposed to methamidophos and omethoate. *Marine and Freshwater Behaviour and Physiology*, *43*(4), 243–255.

Zheng, G. J., & Richardson, B. J. (1999). Petroleum hydrocarbons and polycyclic aromatic hydrocarbons (PAHs) in Hong Kong marine sediments. *Chemosphere*, *38*(11), 2625–2632.

Zhu, L., Lu, H., Chen, S., & Amagai, T. (2009). Pollution level, phase distribution and source

analysis of polycyclic aromatic hydrocarbons in residential air in Hangzhou, China. *Journal of Hazardous Materials*, *162*(2–3), 1165–1170.